

Ruprecht-Karls-Universität Heidelberg  
Geographisches Institut

Master Thesis

**Flood Impact Assessment on  
Road Network and Healthcare Access**

—

**Jakarta, Indonesia**

Isabell Greta Klipper  
Matrikel-Nr. 3536373  
Geography Master of Science  
[isabell.klipper@gmail.com](mailto:isabell.klipper@gmail.com)

Supervisors:  
Dr. Sven Lautenbach  
Prof. Dr. Alexander Zipf

21.10.2020

# Table of Contents

List of Abbreviations.....	iii
Table of Figures.....	iv
Index of Tables.....	vi
Abstract.....	vii
1 Introduction.....	1
2 State of the Art.....	3
2.1 Road Network.....	3
2.1.1 Resilience.....	3
2.1.2 Graph Theory.....	4
2.1.3 Network Centrality.....	6
2.1.3.1 Betweenness Centrality.....	7
2.1.3.2 Closeness Centrality.....	7
2.2 Healthcare Accessibility.....	9
2.2.1 Accessibility.....	9
2.2.2 Isochrones.....	9
2.3 Related Work.....	11
2.3.1 Road Network.....	11
2.3.2 Healthcare Accessibility.....	12
2.4 Research Gaps.....	15
3 Case Study and Datasets.....	16
3.1 Study Area.....	16
3.2 Data.....	20
3.2.1 Administrative City Border of Jakarta, Indonesia.....	21
3.2.2 2013 Flood.....	21
3.2.3 Healthcare Amenities.....	22
3.2.4 Population.....	22
3.3 Tools.....	23
3.3.1 Python 3.....	23
3.3.1.1 OSMnx and NetworkKit.....	23
3.3.1.2 Openrouteservice.....	24
3.3.1.3 Quantum GIS.....	24
4 Methodology.....	25
4.1 Data Preprocessing.....	27
4.2 Road Network.....	28
4.2.1 Graph Download and Preparation.....	28
4.2.2 Centrality Calculation and Network Characteristics.....	29
4.2.3 Network Resilience.....	29
4.3 Healthcare Access.....	31
4.3.1 Healthcare Supply.....	31
4.3.2 Mobility-based Accessibility.....	32

4.3.2.1 Routing Graph Preparation.....	32
4.3.2.2 Calculation of Isochrones and Catchment Areas.....	33
4.3.3 Supply and Demand related Access.....	33
5 Results and Discussion.....	36
5.1 Road Network.....	36
5.1.1 Network Characteristics.....	36
5.1.1.1 Betweenness Centrality: Best roads and junctions for fastest routing.....	37
5.1.1.2 Harmonic Closeness Centrality: Best supply locations to be accessed.....	41
5.1.2 Network Resilience.....	45
5.1.3 Discussion.....	48
5.2 Healthcare Access.....	54
5.2.1 Distribution of Healthcare Supply.....	54
5.2.2 Mobility-based Accessibility.....	57
5.2.3 Supply and Demand related Access.....	61
5.2.4 Discussion.....	65
6 Conclusion.....	70
References.....	72
Acknowledgement.....	79
Affidavit.....	80

## List of Abbreviations

API	Application Programming Interface
BC	Betweenness Centrality
CC	Closeness Centrality
DKI Jakarta	Daerah Khusus Ibukota Jakarta (English: Special Capital Region of Jakarta)
FCA	Floated Catchment Area
GIS	Geographic Information System
HeiGIT	Heidelberg Institute for Geoinformation Technology
HOT	Humanitarian OpenStreetMap Team
HC	Harmonic Closeness Centrality
MCA	Multiple Centrality Assessment
NACH	Normalized Angular Choice (mathematical betweenness)
NAIN	Normalized Angular Integration (mathematical closeness)
NGO	Non-Governmental Organisation
ORS	Openrouteservice
OSM	OpenStreetMap
OSM PBF	OpenStreetMap Protocolbuffer Binary Format (.osm.pbf)
QGIS	Quantum GIS
RQ	Research Question
SR	Sameness Ratio
VGI	Volunteered Geographic Information
WGS	World Geodetic System

## Table of Figures

Figure 1: Simple network graphs; a) connected graph, b) directed graph, c) weighted graph, d) disconnected graph with three components.....	5
Figure 2: Geographical localisation of the study area.....	16
Figure 3: Waterways, water reservoirs and elevation of the Jakarta region.....	18
Figure 4: Spatial extension of the 2013 flood.....	19
Figure 5: Methodology workflow.....	26
Figure 6: Process to generate isochrone fragments to sum up the available bed capacity for each area: (left) healthsite isochrones and isolines, (middle) all available isochrone fragments, (right) attribute value per isochrone fragment and cumulated within the overlapping areas.....	34
Figure 7: Empirical BC value distribution of nodes: (left) cumulative, (right) histogram.....	37
Figure 8: The frequency of crossed road junctions, based on car driving, fastest routing profile on all possible routes: (left) normal scenario, (right) 2013 flooded scenario.....	38
Figure 9: Flood impact on road network regarding BC and node crossing frequency in terms of car driving fastest routing within the entire city.....	40
Figure 10: Empirical HC value distribution of nodes: (left) cumulative, (right) histogram....	41
Figure 11: Spatial distribution of HC valued nodes: (left) normal scenario, (right) 2013 flooded scenario.....	42
Figure 12: Flood impact on road network regarding HC and importance for the most quickly on average accessible locations within the entire city.....	44
Figure 13: Flood impact on the BC related small foreground network and the functionality of the main road structure considering the frequency of crossed locations based on the car fastest routing profile within the city.....	45
Figure 14: Flood impact on the HC related small foreground network and the functionality of the main road structure considering the importance of locations most quickly on average accessible within the city.....	47
Figure 15: Spatial density of health site locations: (left) amount of health sites (HS) per square kilometre in the normal scenario, (right) 2013 flood impact on amount of HS per square kilometre.....	55
Figure 16: Spatial density of available bed capacity: (left) amount of beds per square kilometre in the normal scenario, (right) flood impact on number of beds per square kilometre.....	56
Figure 17: Minimum needed journey time based on car driving shortest routing profile to at least one hospital: (left) within normal scenario, (right) additional needed journey time due to 2013 flood impact.....	57
Figure 18: Minimum needed journey time based on car driving shortest routing profile to at least one clinic: (left) within the normal scenario, (right) additional needed journey time due to 2013 flood impact.....	59

Figure 19: Accessible area size for specific travel time: (left) access to at least one hospital, (right) access to at least one clinic.....	60
Figure 20: Amount of city population with healthcare access within specific time range: (left) access to at least one hospital, (right) access to at least one clinic.....	61
Figure 21: Cumulative amount of available hospital beds, accessible within a 5-minute car drive.....	62
Figure 22: Population density for each 5-minute hospital isochrone fragment.....	63
Figure 23: Cumulative amount of available hospital beds per person per square kilometre accessible within a 5-minute car drive: (left) normal scenario, (right) 2013 flood impact....	64

## **Index of Tables**

Table 1: Graph properties of the normal and the flooded scenario.....	36
Table 2: Sameness ratio for each large foreground graph.....	48
Table 3: Number of health sites distributed by amenity type.....	54

## **Abstract**

In the context of progressive climate change and consequently the increasing number of extreme floods, coastal cities, such as the Indonesian capital Jakarta, experience a growing awareness of possible flood impacts on the urban area with its vulnerable infrastructures. Within this thesis the road network was therefore examined regarding existing characteristics based on fastest routing. By performing a network analysis and using Betweenness Centrality and Harmonic Closeness Centrality, the most frequently used road segments and the locations fastest on average to be accessed were identified. The effects of flooding and, in this context, the resilience to a disturbance were determined by resulting functional changes. The access to healthcare services, with spatially care-based access to available health facilities and beds as well as the existing demand for these, given by the population number, was calculated using location-based isochrones. By determining the urban area accessed as well as the change, insight was gained into the normal condition and the impact of the 2013 flood on this access. The study showed that especially the main roads with the potentially higher speed limit, which run through the entire city, and the city centre, with the advantageous spatial location, are of particular importance for time-efficient routing as well as for easily accessible healthcare. In particular the city centre provided a high resilience against the 2013 flood impacts and maintained its functions to a large extent. In the context of this work, apart from the flood data, only open source data and tools were used.

## 1 Introduction

Extreme natural events create catastrophic situations for cities and their populations. Due to climate change and anthropogenic activities, the number and intensity of these events has steadily increased globally in the past. Floods, in this context, are the most common natural disaster worldwide, which are responsible for economic, social and life losses (Alderman et al., 2012). Low-income countries have a death rate 23 times higher than countries with high financial resources and are therefore much more affected by the impacts (Alderman et al., 2012). The Indonesian capital city Jakarta can be named as an example. The historically grown megacity on the coast of the Java Sea knows how to deal with annual rainy seasons and monsoons, although the number of extreme events has increased significantly in the recent past. The years 1996, 2002, 2007, 2013, 2014 and 2020 (Octavianti and Charles, 2019; Lyons, 2015; AHA Centre, 2020) were marked by intense flooding, with the year 2007 having the worst impact so far. 97 deaths were counted, 500,000 people evacuated, and 60 percent of the city area flooded (Octavianti and Charles, 2019). The rising sea level, land subsidence and the lack of flood protection exacerbate the situation (Baker, 2012).

Cities, including their infrastructures, are vulnerable systems, and the resilience of these systems is important for maintaining their functions. The existing road network as well as the available healthcare system are therefore necessary, among other things, to deal with the event quickly and effectively. The former is needed for spatial mobility but also for the implementation of rapid care. Access to this care and to the related healthcare facilities is essential for the population in their everyday life and even more in such an emergency.

The analysis and evaluation of the various aspects of the road network and healthcare supply are therefore important for understanding and managing the effects of flooding. This work will therefore investigate both subjects, trying to identify the daily state of the existing functions and characteristics and the changes that occur in the event of a flood disaster. The flood of 2013 will be used as an example, where 14 percent of the entire city was flooded, 20 people died, and 50,000 people had to be evacuated (Octavianti and Charles, 2019).

Although aspects of the above-mentioned topics have already been examined in various studies, it is rare to find a combination of both subjects in one study. Consequently, this offers potential for further investigation, whereby this thesis aims to contribute to close existing research gaps. Several methods will be used for the analysis in order to identify different aspects of the subjects. The road network and the existing characteristics in terms of fastest routing within the city will be examined by applying a network analysis and the measurement methods of Betweenness and Closeness Centrality. The spatial availability

as well as the access to existing health services, will be determined by using, *inter alia*, isochrone-based accessibility analyses. Based on that, the demand for and supply of care through mobility-based access will be investigated using an example.

The structure of this work is characterized by the two thematic strings mentioned above. The following chapter will provide an overview of the required theory as well as the current state of the art in order to identify the existing gaps in research. Chapter 3 will present the study area as well as the data and tools used within this thesis, while chapter 4 will deal with the description of the methodology. The results obtained in this work will be presented in chapter 5 and subsequently discussed in order to provide answers to the research questions. Chapter 6 will then conclude the paper and provide ideas for further research.

The application developed in the context of this thesis can be used to answer the research questions for other geographical areas, if the needed input data is provided. The data and tools used are open source, except for the 2013 flood data, and therefore accessible free of charge.

## 2 State of the Art

The following chapter first gives an introduction into the basics of graph theory and network centrality including the needed technical details and further presents research studies where these approaches were applied. Subsequently, subject related terms will be defined and set into context and different concepts will be presented, which try to handle and assess the different aspects of the healthcare accessibility within a city. Furthermore, research studies, considering the impact of changing conditions, for instance external disturbances, will be reviewed. In the last part, the existing research gaps will be defined, which will result in phrased research questions.

### 2.1 Road Network

An urban road network, consisting of streets and road junctions, can be analysed by using the approach of network analysis, which is based on graph theory (Gross et al., 2015). Graph theory has a long tradition and experienced continuing developments on different sections. One main field is represented by the different aspects of network centrality, which can be used to identify significant parts within the network, regarding the desired research question. The following chapter part will first define the term and the subject of '*resilience*' in the context of the given thesis and subsequently gives insights about graph theory as well as network centrality.

#### 2.1.1 Resilience

The definition of '*resilience*' can vary depending on the study field and the research question and can have synonymous like, *inter alia*, '*robustness*', '*reliability*', '*redundancy*' and '*adaptability*' (Abshirini and Koch, 2017; Gauthier et al., 2018; King et al., 2020). The United Nations define resilience as the "ability of a system [...] exposed to hazards to resist, absorb, accommodate to and recover from the effects of a hazard in a timely and efficient manner, including through the preservation and restoration of its essential basic structures and functions" (UNISDR, 2009, p. 24). In the context of network analysis, '*robustness*' can be defined as "the degree to which a networked system continues to function" and the changing network structure after removing or the failure of vertices (Iyer et al., 2013, p. 1). Abshirini and Koch (2017) introduced the terms of '*sameness*' and '*similarity*', which are derived from the resilience definition declared by Holling (1996). '*Sameness*' stands for the ecological resilience, which represents "a system's ability to "bounce back" after a disturbance", whereas '*similarity*' is characterized by "a system's

ability to continue working unaffected by a disturbance" (Abshirini and Koch, 2017, p. 27; Holling, 1996).

The applied approach in this paper will define '*resilience*' as the changing structure of an urban road network affected by an external disturbance as well as the maintenance of its services and the ability to continue to function with the loss of failed and inactive network parts.

### 2.1.2 Graph Theory

The Königsberg bridge problem, considered to be the base of graph theory, was analysed in 1736 by Leonhard Euler (1707-1783), which represents the problem of a circular walk by passing all places in the city of Königsberg and crossing each of the seven bridges exactly once (Euler, 1741). A graph is an abstract representation which can help to understand real-world systems and to reflect and analyse existing problems by describing the structure of it (Boeing, 2017). Urban street patterns and structures can be described by a spatial network graph  $G = (N, E)$ , where  $N$  represents a nonempty, finite set of vertices or nodes and  $E$  a set of links or edges between those nodes. An element  $e = \{i, j\}$  of  $E$  consists of the endnodes  $i$  and  $j$ , where  $e$  is connecting the nodes  $i$  and  $j$  (Bondy and Murty, 1976; Jungnickel, 2008). Depending on the research question and application the graphs edges can be extended with a weighting and is consequently represented by  $G = (N, E, W)$ , where  $W$  is the added edge weight (see figure 1c) (Bondy and Murty, 1976). The weight is used as a function to measure for instance the strength of an edge, where  $w(e) > 0$  for weighted and  $w(e) = 1$ ,  $e \in E$  for unweighted graphs (Brandes, 2001). In case of a road network graph, the weight can hold information about, e.g., the street length or travel cost (Bondy and Murty, 1976).

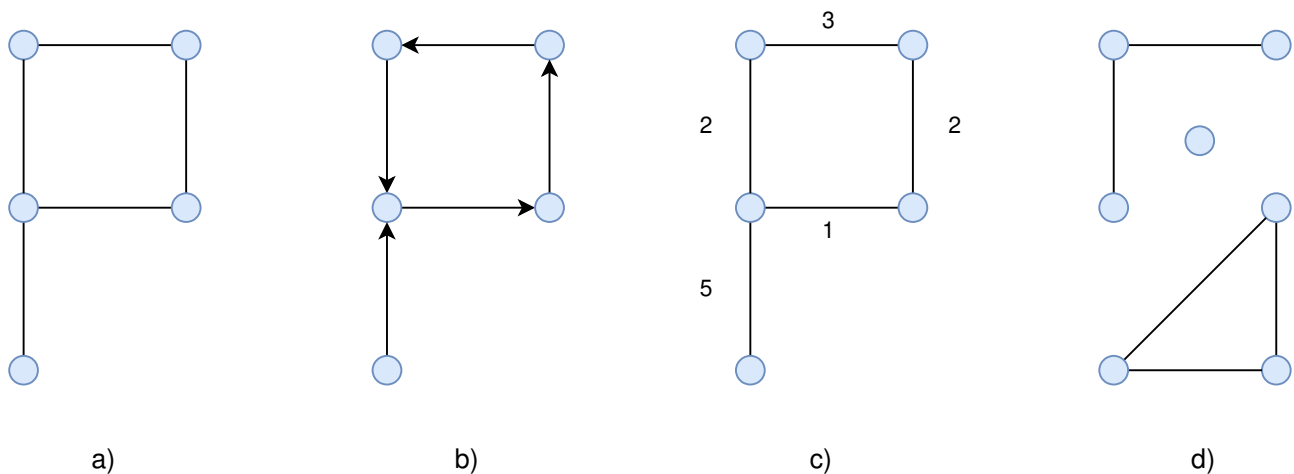


Figure 1: Simple network graphs; a) connected graph, b) directed graph, c) weighted graph, d) disconnected graph with three components (adapted from: Gross et al., 2015)

Two non-adjacent nodes  $i$  and  $j$  of a graph  $G$  are defined as connected, if a path exists between those nodes, respectively called an  $(i, j)$ -path in  $G$ . If one node has no connection to any other node, this one is called isolated. Groups of connected nodes within a graph can be defined as a connected components or subgraphs (see figure 1d). A connected graph (see figure 1a) is given, if all pairs of nodes of  $G$  are connected and if only one component exists. Elsewise  $G$  is called disconnected (Bondy and Murty, 1976; Jungnickel, 2008).

A directed graph  $G = (N, E)$ , also called digraph, consists of  $N$ , a nonempty, finite set of nodes and  $E$ , a set of ordered pairs of  $(i, j)$  where  $i \neq j$  are elements of  $N$ , which can be respectively called as arcs instead of edges within digraphs. In case of a spatial road network concerning information flows of traffic and transportation, the allowed travel direction can be set to the edges of the graph (see figure 1b) and can therefore define for instance the allowed direction of travel, therefore one-way streets (Bondy and Murty, 1976; Jungnickel, 2008). In case of a directed graph, the definition of connectivity can be divided into strongly and weakly connectivity, due to the fact, that a digraph can have a connected spatial topology, but that not every node is accessible. An endnode  $j$  of a digraph  $G$  is accessible from a startnode  $i$  if a directed path exists between  $i$  and  $j$  (Bondy and Murty 1976; Jungnickel, 2008). If not all nodes within a spatial connected digraph are accessible from every other node within the graph,  $G$  is called weakly connected, otherwise strongly connected (Boeing, 2017).

Furthermore, a graph can be characterized by multiple edges, which means that more than one edge is connecting the same two nodes. A loop exists, if an edge holds identical ends (Bondy and Murty, 1976). Urban road networks can be further defined by planarity, which indicates that edges only intersect at nodes (Bondy and Murty, 1976; Barthélemy, 2011), which is not always applied, for instance if tunnels and bridges exist and edges overlap on one point without an actual intersection (Boeing, 2018).

A great distinction in spatial graphs can be made between primal node-based and dual edge-based graphs, where within the first one, street intersections or entire settlements are represented as nodes and the actual roads or relationships as edges. Within an edge-based graph, the allocations are switched (Porta et al., 2006).

### 2.1.3 Network Centrality

One way to inspect and to analyse network graphs, is to calculate the graph centrality. The idea of centrality was developed among others by Freeman (1977; 1978) and has its background in social networks where it can express the actors or in general the nodes importance within a network graph. The idea of centrality is therefore to find the

most important nodes within a graph and to understand the structural properties of the given network. Nodes holding a higher centrality value have a larger impact on other nodes (Demšar et al., 2008). There are several different centrality measurements and algorithm adaptions which result in different ideas of significance. Centrality measurements are holding a major role in evaluating and analysing networks (Ahmadzai et al., 2019).

To determine a nodes centrality, each node will be assigned with an attribute value. This value depends on the node's position within the network and the existing connections to the remaining nodes (Staudt et al., 2015). Two centrality measures are Betweenness and Closeness Centrality, both based on the computation of shortest path between the network nodes. Depending on whether an unweighted or a weighted graph is analysed, the distance is calculated differently. For the first named the breath-first search is applied, where for each node passed one step is counted and therefore the shortest path depending on the least crossed nodes is chosen (Brandes, 2001). For weighted graphs the Dijkstra algorithm is used, which allows assigning distances other than 1 for each step, using for instance the needed duration for each passed road section (Brandes, 2001; Staudt et al., 2015).

Within urban street networks a multiple number of centrality measures are often applied to receive different aspects of the graph structure (Gil and Steinbach, 2008; Caschili and De Montis, 2013; Zhong et al., 2014; Frith et al., 2017). This method can be called Multiple Centrality Assessment (MCA) and is based on primal graphs and distance calculations (Crucitti et al., 2006; Porta et al., 2006; 2008).

### 2.1.3.1 Betweenness Centrality

The Betweenness Centrality (BC) is based on the shortest path between two nodes and was first defined by Freeman in 1977. In case of BC the extent is calculated of which a node  $i$  lies on the path with the least distance among all possible node pairs. A node  $i$  valued with a higher betweenness degree is therefore crossed more frequently and holds a higher importance for the network structure (Freeman, 1977; Wang, 2018).

For more complex graphs including a higher number of nodes and edges, Brandes (2001) extended the algorithm with parallelism to speed up the calculation. It is currently the fastest known betweenness algorithm with a running time of  $O(nm)$  for unweighted and  $O(nm + n^2 \log n)$  for weighted graphs (Brandes, 2001; Staudt et al., 2015). For the node  $i$ , the BC can be defined as:

$$BC(i) = \sum_{i \neq v \neq j \in N} \frac{\sigma_{ij}(v)}{\sigma_{ij}} ,$$

where  $\sigma_{ij}$  defines the number of shortest paths from  $i \in N$  to  $j \in N$  and  $\sigma_{ij}(v)$  the number of shortest paths from  $i$  to  $j$  where  $v \in N$  lies on (Brandes, 2001).

### 2.1.3.2 Closeness Centrality

One of the most used centrality measures is the Closeness Centrality (CC), which indicates how close one node  $i$  is to all other nodes. First considered by Bavelas in 1948, the classic and modern used definition was developed among others by Beauchamp (1965) and Sabidussi (1966). The average distance of the shortest path from the node  $i$  to any other node is calculated, which can be defined as:

$$CC(i) = \frac{N-1}{\sum_{i \neq j \in N} d_{ij}} ,$$

where  $N$  is the total amount of nodes and  $d_{ij}$  the distance between the nodes  $i \in N$  and  $j \in N$  (Sabidussi, 1966; Wang, 2018). The intention for applying the CC on a road network graph can be to identify the nodes which can be reached by others best, due to the reason, that nodes with a higher closeness value are more central and therefore closer to all other nodes (Opsahl et al., 2010).

The algorithm can only be applied on connected graphs since the shortest path is calculated between all existing nodes and therefore nodes from different components do not have a finite distance between them (Boldi and Vigna 2013). To determine the closeness value for nodes within a disconnected graph a variation of the classic algorithm can be used, the so-called Harmonic Closeness Centrality (HC). Developed by Rochat (2009) and studied by Boldi and Vigna (2013) the measurement for the node  $i$  can be defined as:

$$HC(i) = \sum_{i \neq j \in N} \frac{1}{d_{ij}} = \sum_{d_{ij} < \infty, i \neq j \in N} \frac{1}{d_{ij}} ,$$

where  $d_{ij}$  defines the distance between  $i$  and  $j$  and is consequently the distance from node  $i$  to every other node excluding itself (Boldi and Vigna, 2013; Bisenius et al., 2018). If no path exists between two nodes due to two not connected components,  $1/d_{ij} = 0$ , respectively  $\infty^{-1} = 0$  (Boldi and Vigna, 2013).



## 2.2 Healthcare Accessibility

The quality of healthcare can be identified by analysing the access to it including the different aspects of it. Since the subject of '*healthcare access*' is so versatile, the following chapter will give an introduction and define the term for the thesis context. Furthermore, the approach of isochrones will be presented, which can be used to investigate accessibility.

### 2.2.1 Accessibility

Healthcare and its accessibility depend on multiple aspects, why the definition of it can vary from the research's focus. Nevertheless, the two main factors of health access are healthcare supply and population demand (Luo, 2004). A classification can be made by categorising revealed and potential accessibility. The revealed access sets the focus on the actual use of healthcare services, whereas the potential one gives insights on the aggregate supply of medical care resources available in a specific area (Joseph and Phillips, 1984). Furthermore, a definition of accessibility as spatial or geographic and non-spatial or social access to healthcare services can be made, where the former includes factors such as availability and distance and the latter contains attributes like affordability, quality and acceptability (Khan, 1992; Lawal and Anyiam, 2019).

The approach used in this thesis will focus on the definition of the spatial accessibility, which can be further described as "a measure of potential for health care delivery" (Guagliardo, 2004, p. 2), including several different aspects. The measures of '*supply*' in this context of health and healthcare and its measure can be defined as the "amount of care that can be made available" (Blackwood and Currie, 2016), which includes indicators such as staffing, beds, equipment and budget (World Health Organization, 2000). Referred to the transportation context, access to those sites can be defined as "the relative ease by which the locations of activities [...] can be reached from another location" (BTS, 1997, p. 173).

### 2.2.2 Isochrones

The word '*isochrone*' is composed by the two Greek words '*iso*' for '*the same*' and '*chronos*' meaning '*time*' and is used to define "a line on [...] a map connecting points of the same time" (Desai, 2008, p. 26) or of the same distance. Isochrones respectively called isolines can be further defined as an area which can be reached from a given source location within a certain time or which is in range of a certain distance (Desai, 2008; Baum et al., 2015). Having a road network as a base, a routing and graph algorithm, for instance

the Dijkstra algorithm, can be used to calculate the shortest path from the source point to all possible accessible locations (Dijkstra, 1959). The reached and further connected points are representing the border line of the isochrone (Baum et al., 2015; Panig, 2019). Consequently, isochrones can be used for location-based approaches (Geurs and van Wee, 2004).

## 2.3 Related Work

One aspect of healthcare access is mobility-based accessibility based on a road network. Consequently, it is reasonable to analyse both subjects to improve the given situation within a city and to receive insights about potential weak areas, which could be vulnerable for external disturbances, such as flood disasters. Therefore, Albano et al. (2014) estimated the flood consequences on the accessibility and operability of emergency responders by identifying the most critical infrastructures in emergency management. Infrastructures here are not only hospitals and fire stations, but main and secondary roads as well as area connecting bridges. The classification was done by using different indices, based on, inter alia, road closure estimation and a reliability index as well as population at risk and economic impact estimation. Both, the resilience of the city and the accessibility to essential amenities after a flood were also assessed by Abshirini et al. (2017), whose calculations were based on syntactic properties of space syntax methodology and a medium distance of 3 kilometre of the street networks to, inter alia, healthcare centres, schools and commercial centres.

Nevertheless, the multiple aspects of road network graphs and healthcare accessibility were analysed in several research studies, aggregated in the last few years. The applied approaches and the resulting expertise will be viewed in the next chapter parts, to receive an overview about the given context and potential research gaps.

### 2.3.1 Road Network

A road network with the given characteristics as well as its behaviour in case of a disturbance can be analysed by using different approaches, not including network centralities. Singh et al. (2018) developed for instance an index to assess the vulnerability of an urban road network affected by a flood. Meteorological information was linked with land use functions, a hydrodynamic model and a safety speed function to evaluate the relation of flood depth to the reduction in travel speed and consequently the identification of road sections most affected to floods. The significance of highway network links under flood damage were evaluated by Sohn (2006) by developing an accessibility index. Borowska-Stefańska et al. (2019) analysed the flood impact on trips. A mobility-based approach was used with consideration of travel speed change from a normal compared to an one-hundred-year-flood scenario to determine the change on mobility and accessibility.

Using graph theory and the variations of centrality algorithms, different kind of aspects of a road network can be further investigated. Jenelius and Mattsson (2015) performed a spatial vulnerability analysis on a road network graph, containing junctions as

nodes and roads as directed links, to assess potential degradations of the transport system, caused by, e.g., accidents, technical failures or nature. Taking network centrality into account, BC was already widely used in the context of urban, transportation, sustainability and disaster studies to analyse road networks and the importance of the individual streets and places within a city (Demšar et al., 2008; Zhang et al., 2011; Boeing, 2017; Gauthier et al., 2018; Kirkley et al., 2018; Ahmadzai et al., 2019; King et al., 2020). It revealed that BC can be used to identify major roads within a street network (Ahmadzai et al., 2019) and to assess the network resilience as well as the changing network performance in case of a disruption (Gauthier et al., 2018). Boeing (2017) showed that a city is more prone to an internal or external disturbance if nodes with high BC exists within the network and, e.g., due to flood fail. Gil (2014) identified with the results of CC the urban accessibility and consequently the urban form, structure and function indicators. The calculation of both, BC and CC, done by Gil and Steinbach (2008), highlighted the indirect impacts of flooding on urban street networks, by quantifying the extent and the accessibility of town centres in the city of London, UK. Taking additional an edge weighting into account, e.g., the number of trips done, can give insights into the essential elements of urban interactions (Zhong et al., 2014) or the strong effect of specific costs associated with the length of edges on the topological structure of these networks (Barthélemy, 2011). The Multiple Centrality Assessment (MCA) applies a set of different centrality algorithms, including BC and CC, to receive an extended overview of the city structure and to identify the road skeleton of the most central routes and subareas within the urban area (Crucitti et al., 2006; Porta et al., 2008). This approach was used to analyse the potential of urban development by highlighting the importance of the specific streets (Porta et al., 2013). Using BC and CC as a base, Hillier et al. (2012) developed methods to normalize angular choice (mathematical betweenness) (NACH) and angular integration (mathematical closeness) (NAIN) values for a better handling of city comparison with different sizes. Those network methods were further used to investigate the city resilience and spatial structure and the impact of disturbances on it (Abshirini and Koch, 2017). To quantify the city resilience in case of a disaster, Abshirini and Koch (2017) developed two new measures, similarity and sameless ratio, using space syntax and the methods of NACH and NAIN. The space syntax theories by Hillier and Hanson (1984) is an approach to analyse dual edge-based graphs based on the axial map representation in the urban design context.

### 2.3.2 Healthcare Accessibility

To measure the accessibility to existing healthcare, including the different aspects, several different approaches were developed and applied in the past. A proven approach is the use of a gravity model, which takes multiple input factors regarding supply and demand into account, including distance decay (Guagliardo, 2004). A modified form of the gravity

model is the two-step floating catchment area method (2SFCA), first introduced by Radke and Mu (2000), which uses two steps to calculate accessibility by considering demand and supply. Luo and Wang (2003) for example, analysed the spatial accessibility to primary healthcare in Chicago by taking the physician-to-population ratio for each catchment area into account and summing up the results for overlapping areas, where several physician locations can be reached within a certain time. Adding a weighting to the algorithm, to include the influence of travel time zones and distance decay, Luo and Qi (2009) enhanced the method. Kanuganti et al. (2016) applied the method on rural areas. A similar approach was followed by Kim et al. (2018), who developed the Seoul Enhanced 2-Step Floating Catchment Area (SE2SFCA) method for the city of Seoul, which shows characteristics such as a higher population density and a shorter average distance to healthcare-service locations compared to North American or European cities. The algorithm considered the hospital size as well as the capacity and distinguishes between private and public transportation. The locations of healthcare facilities for different settlements in India were moreover evaluated by Rekha et al. (2017) using a spatial accessibility index based on a three-step-floating-catchment-area considering the attractiveness of each health site, the needed travel time or distance, the capacity of each site, defined by available beds and physicians and the actual population demand. The index was furthermore used to identify potential locations for new health facilities. Lawal and Anyiam (2019) pursued a similar study aim with the focus on the spatial accessibility of settlements to the closest existing health site. Open data were combined with an ArcGIS based geospatial analysis using health site locations, terrain attributes, road network distances and a speed model. Considering likewise the distance, travel time and cost, Jalil et al. (2018) tried to determine the shortest path and the optimal healthcare accessibility from residential areas. Alternative routes were calculated and suitable sites for new healthcare facilities were identified. Taking into account variables according availability and community health related expectations, such as healthcare indices, including, *inter alia*, the number of doctors and hospital beds per 10,000 population, dietary consumption indices as well as economic and demographic factors, Cochrane et al. (1978) analysed the differences in mortality between several countries. To receive insights about differences in healthcare resources of high, middle- and low-income countries, the World Health Organization (2000) used a health system input mix, consisting of eight indicators, such as material equipment, financial capacity and human resources.

One aspect of the named approaches is the analysis of spatial, mobility-based accessibility by using the calculation of isochrones, done for instance by O'Sullivan (2000) using a desktop GIS application, who came to the result, that isochrones are an easily understood method for examining accessibility. Arrighi et al. (2019), who applied a flood risk assessment on the city area of Galluzzo in Italy, showed that the town centre in case of a flood cannot be reached by any emergency services and are therefore cut off from those operations. Although they did not use the definition of isochrones, Arrighi et al. (2019) identified the service area by calculating the region accessed within an 8-minute time

frame. A similar modelling of emergency service accessibility was done by Coles et al. (2017), who quantified the spatial coverage of health sites and the response time from those to vulnerable care homes and sheltered accommodations by using the time frame of 8 to 10 minutes. In comparison, Green et al. (2017) defined this accessibility of hospitals and fire-departments within 8 to 10 minutes as isochrones using the Dijkstra's algorithm, weighting the routing network with travel time instead of distance and evaluated the flood resilience of emergency responders.

The density of the available care provision was calculated by Guagliardo (2004), who suggested to create a grid layer covering the study area to receive insights about the existing healthcare supply for each cell. To get information of the healthcare supply in the context of the given population, provider-to-population ratios, also referred to as supply ratios, can be applied, considering the number of physicians, health facilities or hospital beds as an indicator of health service capacity (Guagliardo, 2004; Luo and Wang, 2003).

## 2.4 Research Gaps

The previous sections have shown various ways of dealing with the issues of analysing road networks and the access to healthcare. Each of the named subjects have been researched in several studies, partly including the impact examination of internal or external disturbances. The parallel investigation of both parts in one study has already been recognised, however, is somewhat scarce. Due to the reason, that fast and effective healthcare access depends, *inter alia*, on the given characteristics of the road network, this research reveals its importance. With the increasing amount of natural disasters, the named connection including its functionality maintenance becomes even more important.

To calculate access to health facilities, many studies have chosen fixed travel times or distances, whereas studies that use time and interval-based isochrones are only found in limited numbers. The importance of weighting these access areas with attributes such as care capacity or the ratio of actual demand to existing supply has been recognised in the past. There is a potential to examine the road network including its functions in this context. Individual sections of the network can have considerable effects on healthcare supply, why it is important to identify these. The impact of a disturbance or a flood disaster on the given functionality, has already been analysed in the past. Despite a separate analysis, an investigation within one study, is useful.

Due to the increasing number of extreme floods within the Indonesian city of Jakarta, the region was chosen for investigations in the past. However, a detailed analysis, with the closure of the mentioned gaps, is necessary. The following phrased research questions (RQ) conclude the focus of this work, each addressing one study object.

- **RQ1:** Which sections of Jakarta's road network are most important for the fastest supply and routing behaviour and as the most accessible supply points, and how did this importance change in the event of flooding in 2013?
- **RQ2:** To what extent is healthcare access available for the population of the city of Jakarta and what impact had the 2013 flood on this access?

The work will be based on the use of open source data and tools, avoiding the disadvantage of cost-intensive commercial programs such as ArcGIS. Commercial as well as free applications have already been used by many studies. However, a free application such as the one developed in this study offers opportunities for, *inter alia*, low- and medium-income countries and Non-Governmental Organisations (NGOs).

### 3 Case Study and Datasets

The capital city of Indonesia, Jakarta, was used as the research area for this thesis, why this chapter will first give a short overview about the country and the city. Subsequently, the data and tools used in the thesis' context will be introduced.

#### 3.1 Study Area

Indonesia, respectively Republic of Indonesia is an island country bridging the continents Asia and Oceania, bordered in the south and west by the Indian Ocean and by the Pacific Ocean in the east. The country, consisting of approximately 17,504 islands, is the largest archipelago in the world, including the five main islands Sumatra, Java/Madura, Borneo, Sulawesi and Papua. Java, hosting 58 percent of the Indonesian population, is giving location to the capital city Jakarta (World Health Organization, 2017).

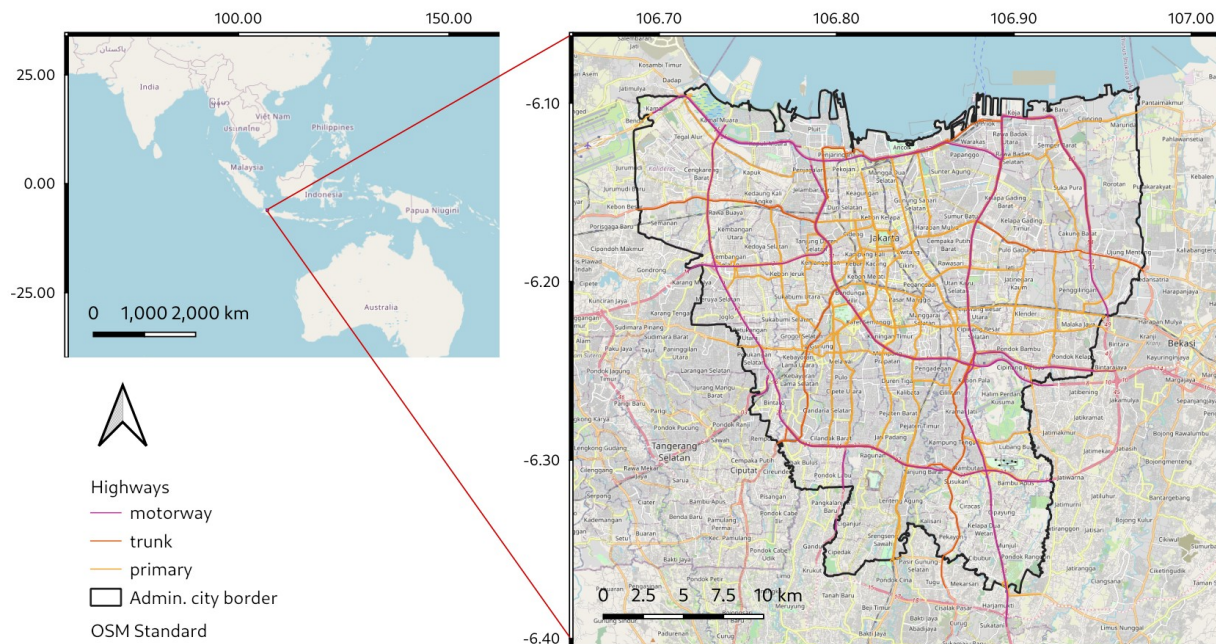


Figure 2: Geographical localisation of the study area (Data source: OpenStreetMap contributors, 2020b)

Note: The area delimited by the administrative city border represents the research area for the thesis. Highways intersect the entire city area and connect the different districts. The maps are projected in WGS 84, EPSG: 4326.

The lower-middle-income country consist of a strong economy, which experienced a strong growth, including a risen Gross Domestic Product (GDP) per capita from US\$464 in

1998 to US\$4,136 in the year 2019 (The World Bank Group, 2020). In terms of purchasing power parity, Indonesia can be counted as the world's 10<sup>th</sup> largest economy and is additionally member of the G-20. Although, the national poverty rate decreased since 1999 by more than a half to 9.4 percent in 2019, more than 25 million inhabitants still live below the poverty line (The World Bank Group, 2020b). Since independency in 1945, the country developed from authoritarianism to democracy and is politically stable. The diversity of the country is characterized by 724 spoken languages and dialects and numerous ethnic and cultural groups. However, Bahasa Indonesia is set as the national language since 1945, and almost 84 percent of the total population are member of the 15 largest ethnic groups. In 2010, more than 87 percent of the inhabitants identified themselves as Muslim (World Health Organization, 2017).

Indonesia is experiencing an increasing urbanization, holding a growing rate of 4.1 percent per year, which results in the expectation that 68 percent of the Indonesian population will be living in urban areas by 2025 (The World Bank Group, 2016). Jakarta, officially called the Special Capital Region of Jakarta or in Indonesian language, Daerah Khusus Ibukota Jakarta (DKI Jakarta), is the largest city of the country, holding a size of 661.5 square kilometre. It is geographical located on the northwest of the island and borders in the north on the Java Sea (World Health Organization, 2017), see figure 2. In 2019, the country counted 270.6 million inhabitants, the world's fourth most populous nation (United Nations, 2020), 10.5 million living in the capital city. The population amount for this megacity for the year 2030 is predicted to rise to 12.6 million (United Nations et al., 2019).

The rapidly growing economic performance and the increasing prosperity within the population, combined with the rapidly growing urban population, create a variety of challenges. In view of the rising number of extreme floods, the responsibility of national and urban disaster management is increasing to find an appropriate way to deal with the vulnerability of the city, including the existing infrastructures.

The northern area of the city is flat alluvial plains and partly below sea level, whereas towards the south the region shows elevation values of up to 94 meters (see figure 3). The terrain is characterized by annual subsidence of 15 cm/year on average up to 20-28 cm/year in some regions (Abidin et al., 2011) and two meters cumulated for the time frame 1960 to 2013 (Erkens et al., 2015). 40 percent of the entire urban area is below sea level (Baker, 2012).

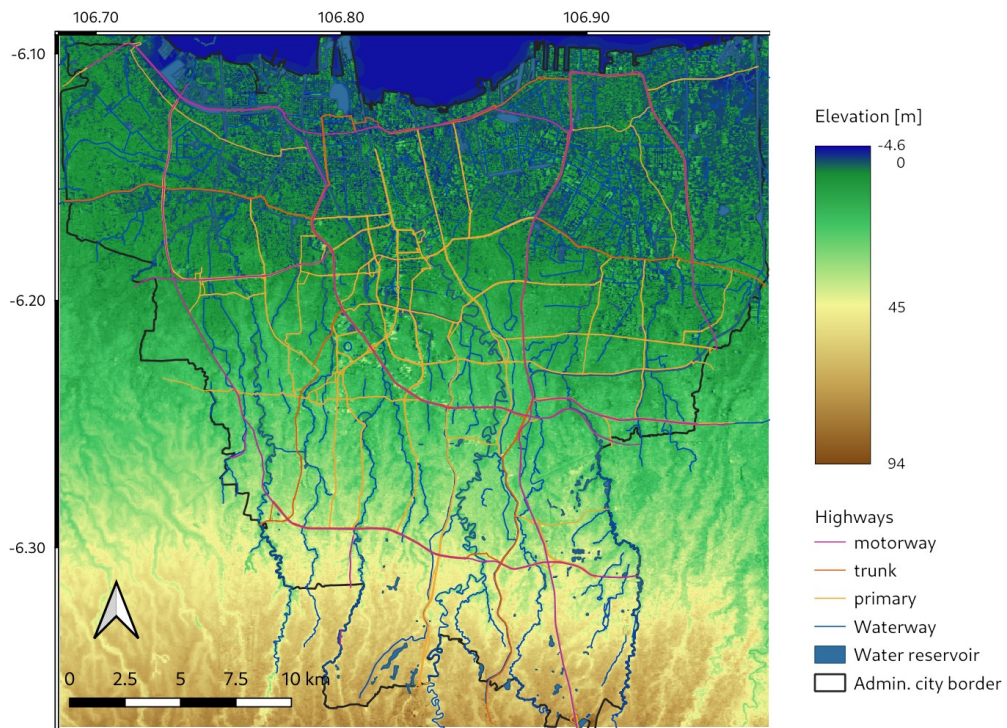


*Figure 3: Waterways, water reservoirs and elevation of the Jakarta region (Data source: HOT Indonesia, received: 16/01/2020; OpenStreetMap contributors, 2020b)*

*Note: A high number of natural rivers and artificial canals exist within the city, with a spatial concentration in the northern region. The city's elevation decreases from south to north and has areas in the north with elevation values below sea level. The map is projected in WGS 84, EPSG: 4326.*

The city's climate is hot and humid and due to its close location to the equator, an annual rain season from October to April exists (Siswanto et al., 2016). Because of the coastal and delta-oriented location and the 13 natural, inner city rivers, artificial canals were built as early as the 5th century to create transport routes and to be able to organise the rising water levels that occur during the rainy season. This development was supported by the Dutch colonial rule. After the extreme floods in the recent past, the canals were further politically encouraged and expanded as a fast and cost-effective way of flood protection (Octavianti and Charles, 2019). 1,400 km of artificial waterways existed in 2012 within the city (Baker, 2012).

The economic development of the city is causing rapid population growth and consequently problems in urban planning and infrastructure construction. People settle in open spaces, especially along waterways, railways and drainage areas, causing slums and informal settlements, which occupies 20 to 30 percent of the total city area (Baker, 2012; Prasetyanti, 2015). Access to hospitals and clinics in Indonesia is mainly private, through

so-called "out-of-pocket" financing. In 2014, the share was 62.2 percent, whereas the state contribution was 27.8 percent (World Health Organization, 2017).

Defined as the administrative city border, the study area for this thesis, is visualized in figure 2, 3 and 4. Although the agglomeration extends spatially beyond this defined administrative region, the research will focus on the named area on the mainland, excluding the northern located small islands, due to better handling.

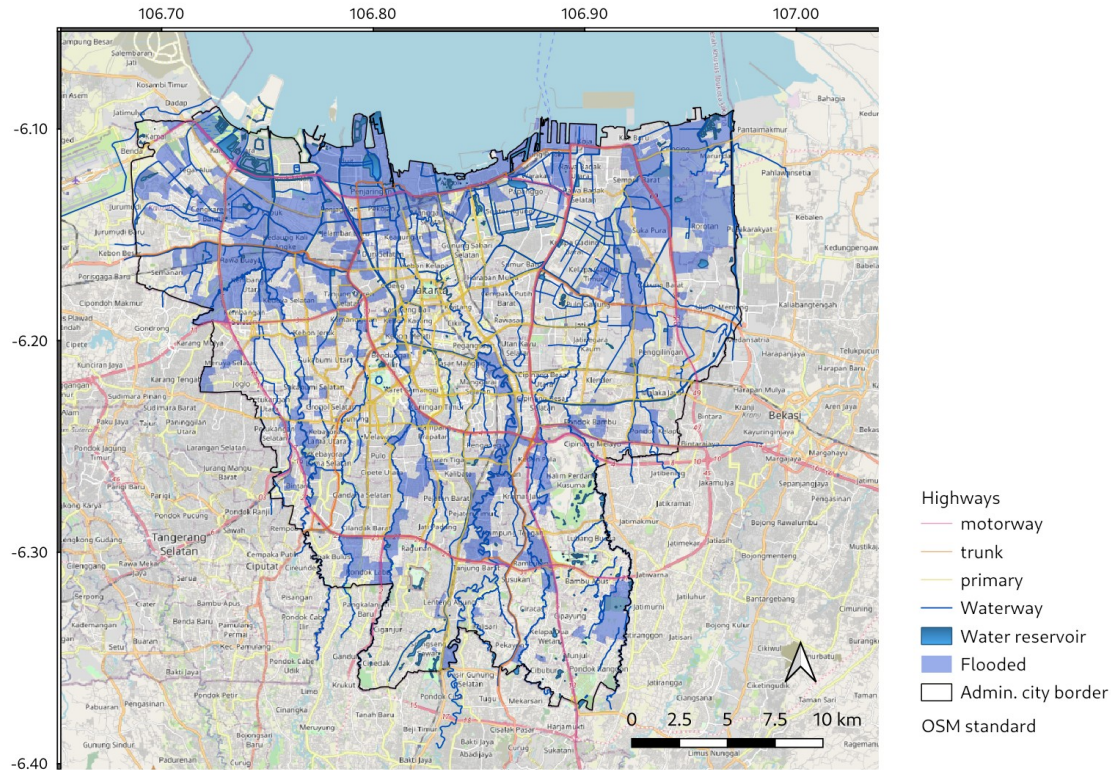


*Figure 4: Spatial extension of the 2013 flood (Data source: HOT Indonesia, received: 16/01/2020; OpenStreetMap contributors, 2020b)*

*Note: The northern city region was particularly affected by the flood, while in the south smaller areas were flooded. The flood data is spatially limited to the defined study area, the city of Jakarta. The map is projected in WGS 84, EPSG: 4326.*

The flood of 2013 will be used in this study as an example for the increasingly frequent extreme floods. As visualized in figure 4, 14 percent of the entire city was flooded during the disaster, 20 people died, and 50,000 people had to be evacuated (Octavianti and Charles 2019).

### 3.2 Data

The input data for the analysis consisted of four files. Except of the 2013 flood related data, all files were open and free accessible. The data base, including its characteristics and the intended use will be described below.

The OpenStreetMap (OSM)<sup>1</sup> project was founded in 2004 with the aim to collect spatial data with a global coverage and to provide it open and freely accessible for everyone. With a focus on spatial objects, regarding, *inter alia*, traffic infrastructures, points of interests, buildings, space utilization and administrative borders, the OSM community contributes via mapping activity mainly without being employed and payed (OpenStreetMap contributors, n.d.). Although OSM is called “the world’s largest Volunteered Geographic Information (VGI) platform” (Anderson et al., 2019, p.1), paid cooperate mappers sometimes exist, for different kind of projects (Anderson et al., 2019). Completeness and quality may vary significantly between regions, with urban areas having a more frequent and higher data input compared to rural areas (Neis and Zielstra, 2014). Personal interest of the contributor may influence the mapping activity, with a focus on areas of interest (Bégin et al., 2013). The mentioned points are only a few existing challenges compared to the number of opportunities. The local knowledge may increase the amount and quality of the content (Bégin et al., 2013). Furthermore, VGI, including OSM, offers new data sets, which provide fast and up-to-date content, for example in disaster situations (Mirbabaie et al., 2016). OSM is handled as a viable alternative to authoritative map services and is already used in different kinds of applications (Senaratne et al., 2017). OSM data is provided as ‘*nodes*’, ‘*ways*’ and ‘*relations*’ elements, representing points in space, linear features and geographic relationships between objects. Elements are associated with several tags, describing the respective attributes (OpenStreetMap contributors, 2020).

The Humanitarian OpenStreetMap Team (HOT) “is an international team dedicated to humanitarian action and community development through open mapping” (HOT, n.d.) and has therefore high impact on the quality as well as on the quantity of OSM data (HOT, n.d.). Within the framework of the “PDC InWARE Indonesia Mapping Project” disaster management tools and data were for instance further developed. Between March and August 2017 data regarding the administrative boundary, critical infrastructures and road network objects within the city district of Jakarta, were mapped and added to the OSM database (HOT, 2018). Only in this project, HOT Indonesia<sup>2</sup> collected almost 25,000 objects regarding the city infrastructure (OpenStreetMap contributors, 2018).

---

1 <https://www.openstreetmap.org/> (accessed: 29/09/2020)

2 <https://openstreetmap.id/en/data-dki-jakarta/> (accessed: 29/09/2020)

### 3.2.1 Administrative City Border of Jakarta, Indonesia

The study area, introduced in 3.1, covers the city area of Jakarta, Indonesia. For a spatial partition of the further data sources, a layer specifying the administrative city boundary of Jakarta, was received, by using the web-based data mining tool overpass turbo<sup>3</sup>. Data can be extracted from the OSM database using a key-value request (Raifer, 2014). The for this study needed data was requested, using the command (requested 9/6/2020):

*(boundary=administrative and admin\_level=5 and name!="Kepulauan Seribu") in Jakarta*

, where only the relation data was used. The areas holding the name ‘*Kepulauan Seribu*’ were ignored, due to the research focus on the mainland instead of the complete administrative area including the northern islands. The output received consisted of several polygons, representing the city districts. The spatial coverage of the administrative city border is illustrated in figure 2.

### 3.2.2 2013 Flood

The flood related data, were provided by HOT Indonesia<sup>4</sup> in the format of 16 polygon shapefiles, containing information about the 2013 flood disaster affecting the city area of Jakarta. One day and a specific timestamp during the flood was featured by one data file. Together the files represented a time frame including successive days during January and February 2013, including information regarding the location and geometry of the affected areas. The areas were not defined by the city district borders nor the individual affected streets, but by individual area boundaries, defined by HOT Indonesia. Although all files were holding the same geometry structure, including unique identification number, the files were very heterogeneous in comparison to each other, some representing only the flood affected areas, some the complete city area with only flood related attribute information. Furthermore, the polygon data were just giving insights about the fact, if an area was temporarily or continuously flooded and not about the actual water depth.

In the context of the flood data, it must be borne in mind that the level of the respective flood can have a decisive influence on local access to areas. Roads that are only affected by a low altitude may for instance be crossed either on foot or by appropriate means of transport. This height of flooding was not considered here. Since the water level cannot be identified with certainty in every case, but cause problems if determined

---

3 <https://overpass-turbo.eu/> (accessed: 29/09/2020)

4 Data received: 16/01/2020

incorrectly, it was specified in this context that an area affected by the flood is not passable, regardless the actual flood level.

### 3.2.3 Healthcare Amenities

In the context of mapping projects, HOT Indonesia has a high impact on OSM health related data acquisition. Therefore, and due to the usage of HOT Indonesia collected flood data, see chapter 3.2.2, the database including information of healthcare amenities was used for this approach. The input data<sup>5</sup> represented the spatial location of hospitals and clinics, open available via the HOT Indonesia website<sup>2</sup> and based on the OSM database. The extracted data for each healthcare type consisted of one point and one polygon shapefile layer. These layers contained the corresponding OSM tags, including information regarding, inter alia, name, address, opening hours, operator type and bed capacity (OpenStreetMap Indonesia, 2020).

### 3.2.4 Population

The initiative WorldPop offers spatial demographic datasets provided with a full open access with the aim to “support development, disaster response and health applications” (WorldPop, 2020). The downloaded population data<sup>6</sup> was received as a raster file covering the complete country Indonesia and is provided by the University of Southampton, UK to the WorldPop project. The data source is updated every year, why the raster file for the year 2020 was used. The estimated total amount of inhabitants was given per grid cell, therefore the people per pixel were representing the file’s unit. The file was provided in GeoTIFF format with a resolution of 3 arc, which is approximately 100 meters at the equator and was projected in Geographic Coordinate System, WGS84. The approach of random forest-based dasymetric redistribution was used to map the data (OCHA and WorldPop, 2020).

---

5 <https://drive.google.com/drive/folders/1azUAetAfVKHmkh8MdBnZv6owD-jzvBkd> (downloaded: 22/05/2020)

6 <https://data.humdata.org/dataset/worldpop-indonesia-population> (downloaded: 10/06/2020)

### 3.3 Tools

The main analysis was written in Python 3, whereas the visualisation was done using Quantum GIS. The named tools, including the main Python packages will be introduced shortly. All used tools are free and open-source software (FOSS) and are consequently free of costs and open accessible for everyone. However, disadvantages of FOSS can be faulty components which can lead to problems in the execution. Incomplete and outdated documentation as well as no official support are further possible points in this context (Heron et al., 2013).

#### 3.3.1 Python 3

The Python scripting language<sup>7</sup> offers the opportunity to import different kind of external modules to extend the functionality regarding the given research question (Python Software Foundation, 2020). The version of Python 3.7.7 was used for the analysis of this thesis.

##### 3.3.1.1 OSMnx and NetworKit

The Python module OSMnx<sup>8</sup> is designed to handle and work with street networks based on OSM data from the perspective of graph theory, transportation and urban design. The package provides the user with the opportunity to download spatial geometries, based on a selected network profile, e.g., ‘drive’ or ‘pedestrian’, and to convert it into an algorithmic corrected network topology. Furthermore, the user can analyse the road graph, calculating for instance desire routes, and visualize the results (Boeing, 2017). In the framework of this thesis OSMnx was used to download the road network OSM data and to receive a simplified and corrected topology of it as a base for further calculations.

NetworKit<sup>9</sup> is a toolkit to analyse large and complex network graphs. It is C++ based and provides a Python interface, which offers tools for networks with up to billions of edges. To run such complex graphs efficiently, many algorithms use shared-memory parallelism and multicore architectures. NetworKit is not primary designed for urban transport research questions, but due to the named advantages, it will be applied for the in this study investigated network graph. It can be used to weight a graph with specific attributes and offers moreover a variation of methods to analyse the graph (Staudt et al.,

---

7 <https://www.python.org/downloads/> (accessed: 10/06/2020)

8 <https://github.com/gboeing/osmnx> (accessed: 29/09/2020)

9 <https://networkit.github.io/> (accessed: 29/09/2020)

n.d.; 2014b; 2015). The module was mainly used to weight the graph and to calculate the BC as well as the HC to analyse the networks structure and its behaviour, including its resilience, in case of a flood.

### 3.3.1.2 Openrouteservice

The openrouteservice API<sup>10</sup> is developed by the Heidelberg Institute for Geoinformation Technology (HeiGIT) in cooperation with the University of Heidelberg and offers an “open source route planner api with plenty of features” (HeiGIT gGmbH, [2017] 2020). The openrouteservice API version 6.0.0 used within this thesis, uses a forked and edited version of GraphHopper version 0.12 and is written in Java. For the usage of the API, a registration is needed, which is free of costs and offers over 7000 requests per day. The data is based on OSM data with a global coverage and can also be accessed via a Python interface (HeiGIT gGmbH, [2018] 2020). Openrouteservice offers spatial services such as routing, the calculation of isochrones and distance-time matrices, which uses the user-generated tags and values of the OSM database related to the road infrastructure. For the case that needed information is not available, default values are provided by the server (HeiGIT gGmbH, [2017] 2020). For the purpose of the research question, two local openrouteservice instances were built on base of the OSMnx downloaded and, depending on the scenario, flood modified, road network graph. Using these instances, isochrones were requested to analyse healthcare accessibility.

### 3.3.1.3 Quantum GIS

Quantum GIS (QGIS)<sup>11</sup> is an open-source Geographic Information System (GIS) and calls itself “The Leading Open Source Desktop GIS” (QGIS Development Team, 2020). It represents a GIS application that can be identified as FOSS, which can be consequently downloaded and used free of costs. Although QGIS can be used to create, edit, analyse and publish geospatial information the software was mainly used for data visualization and map creation in the context of this research study. Within this study the QGIS version 3.14.0-Pi was used.

---

10 <https://openrouteservice.org/> (accessed: 29/09/2020)

11 <https://qgis.org/en/site/> (accessed: 29/09/2020)

## **4 Methodology**

For this thesis and for the specific data analysis, an application programming interface (API) was written in Python 3 to receive results for the examined research questions. Having the API<sup>12</sup> locally installed and the input data, described in chapter 3.2, provided, the data analysis can be executed by running the commands within the terminal. The following chapter describes the methodology followed within this approach and illustrated in figure 5, where a command exists for each part, regarding data preprocessing, road network examination and healthcare access investigation.

---

<sup>12</sup> [https://github.com/GIScience/Jakarta\\_Thesis\\_Klipper](https://github.com/GIScience/Jakarta_Thesis_Klipper) (accessed: 13/10/2020)

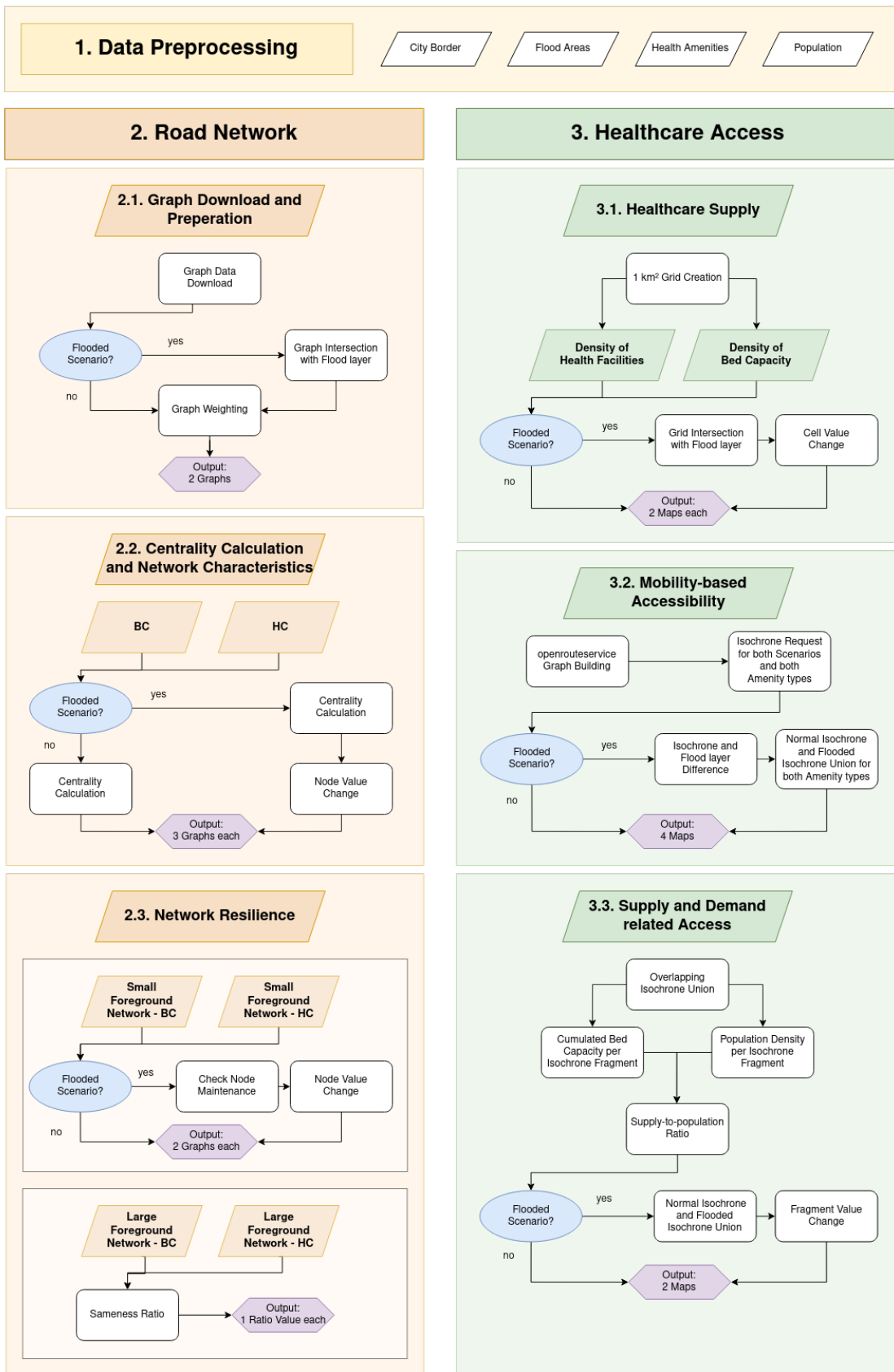


Figure 5: Methodology workflow

Note: BC = Betweenness Centrality, HC = Harmonic Closeness Centrality. The numbers are referring to the subchapters of the following section 4.

## 4.1 Data Preprocessing

Within the first part of the application execution the input data were preprocessed for the subsequent analysis. The four user provided files, were containing the needed information regarding the administrative city border, the flood disaster, the healthcare facilities as well as the spatial distribution of the population.

The data used for the administrative city border were received as several single polygon shapefiles, representing the city districts of Jakarta. Within the preprocessing step these polygons were merged<sup>13</sup> into one polygon shapefile, covering the entire administrative city area.

Due to the strongly heterogeneous structure of the flood data, the preprocessing for this layer was done manually in QGIS. Like already mentioned in 3.2.2. the data consisted of 16 single layers, each representing one time stamp during the 2013 flood. All layers consisted of individual polygons. Some of these layers covered the entire city area and contained flood related attributes, while others represented only the flooded areas. All flood related sub-polygons were selected and merged<sup>13</sup> into one '*flooded*'-layer, which consequently featured the flooded area during the complete flood time frame, regardless if it was only shortly or throughout the time affected.

The healthcare amenity data was provided as a point and polygon layer structure, for the amenity types '*hospital*' and '*clinic*', consisting of individual health locations. For the amenities within the polygon layers, the centroids were calculated, to determine the geographic location of each site as a point structure. The received shapefiles were merged<sup>13</sup> with the already given point files to one single layer, including the locations and information of all given hospitals and clinics. Amenities beyond the administrative border were also provided, why the amenity point layer was intersected<sup>13</sup> with the city border to receive only the health sites located within the city district. To further investigate the flood impact on the healthcare access, the still accessible and not flooded health sites were selected from the flood affected ones. Therefore, an additional point layer was created, consisting of still intact health amenities during the 2013 flood.

A raster file regarding the population information were received for the complete country of Indonesia. For a better and more efficient handling, the layer was cropped<sup>14</sup> by the area of the city border.

---

13 Merge and intersects are methods of the Python package Shapely:  
<https://shapely.readthedocs.io/en/stable/> (accessed: 30/09/2020)

14 Crop is a method of the Python package Rasterio: <https://rasterio.readthedocs.io/en/latest/> (accessed: 30/09/2020)

## 4.2 Road Network

To analyse the characteristics of the urban road network, including its resilience, as well as the flood impacts, the network was represented as a spatial road graph and different network analysis methods were applied. The following chapter part will describe the applied approach, consisting of the graph download and preparation, the examination of the network characteristics and the network resilience to the flood disaster.

### 4.2.1 Graph Download and Preparation

The Python module OSMnx was used to request and download the spatial street network graph for the in 4.1 preprocessed city area. All drivable public roads including service streets were received, by setting the network profile as ‘*drive\_service*’, and were used as data base for the network graph. The request resulted in two shapefiles, one including the ‘*nodes*’, representing the points respectively street junctions and a second file, containing the ‘*edges*’, describing the roads themselves. Both files were holding OSM tags related attributes, providing information regarding the street network. The graph received via OSMnx was directed, unweighted and node based. Depending on the chosen scenario, ‘*normal*’ or ‘*flooded*’, the network graph was modified with the flood related polygon shapefile. Analysing the flooded scenario, the graph was intersected<sup>13</sup> with the flooded areas, removing all affected nodes and edges from the graph. The graph of the normal scenario was not changed.

Within the next step, the graph’s edges were weighted with the fastest allowed and needed duration for each road segment, to prevent an equally treatment of all links. The present graph was firstly converted into a format, which can be handled by the Python module NetworkKit. The specific road duration was calculated by using the algorithm:

$$\text{duration} = \frac{\text{road length}}{\text{speed limit}} ,$$

where the road length, in meters, was received with the edge attributes. The allowed speed limit depends on the specific road type, which was also provided by the edge attributes. A file containing information regarding the speed limit per road type was created by the openrouteservice team<sup>15</sup>. The format of the calculated duration for each road segment was minutes.

---

<sup>15</sup> <https://github.com/GIScience/openrouteservice/blob/e4edb0fc1199612abec35ef86c1f58751cdbe51/openrouteservice/src/main/java/org/heigit/ors/routing/graphhopper/extensions/flagencoders/VehicleFlagEncoder.java> (accessed: 30/09/2020)

#### 4.2.2 Centrality Calculation and Network Characteristics

Centrality calculations were used to analyse various aspects of the routing network, with each centrality algorithm providing different insights into the importance of the nodes for the characteristics of the network. The BC were applied to calculate the frequency with which the respective nodes are approached or crossed on the fastest routes between all nodes. Nodes with a high betweenness value are crossed more frequently and are in this context important for a fast routing and traffic flow. An even spatial distribution of betweenness values indicates, furthermore, a resilient road network, since the maintenance of traffic does not depend on individual nodes and is therefore not affected by the failure of individual sections. In contrast to the BC, the results of the CC, here respectively HC, indicates which nodes can be reached most quickly on average for all existing nodes. Nodes with a higher closeness rating can therefore be regarded as important supply points as well as locations which can be reached quickly by all other nodes in comparison.

The BC and the HC were received for each node, by using the provided NetworKit functions. The calculation was executed for the normal as well as for the flooded scenario to get insights about the current and the disaster network behaviour. The results were added as new attributes to each node file. The received BC data was normalized for a better result classification, whereas a normalisation in case of HC for weighted graphs was not applicable. Consequently, the HC results were provided in absolute numbers. The output for each scenario consisted of one map for each centrality algorithm. The centrality values, BC and HC, for each node were additionally used for the following analysis steps.

To examine the indirect flood impact on the road network, including its fastest routing behaviour, the value change of each graph node was calculated by taking the value difference of the normal and the flooded scenario. The analysis resulted in one map for each centrality algorithm. This approach was also applied by Gil and Steinbach (2008) to evaluate, *inter alia*, the extent to which flooding affects the performance of the transport network.

#### 4.2.3 Network Resilience

Based on the idea of Cutini (2013), that the foreground network respectively the main urban road structure can be defined by the nodes with the highest centrality value, Abshirini and Koch (2017) developed a method to determine the resilience of road networks under the influence of internal or external disturbances and its ability to maintain its functionality after this disturbance. Under the definition of '*sameness*' Abshirini and Koch (2017) examined how much of the existing foreground network remains the same

after a disruption and follows the idea that a network is less resilient if the high centrality values do not remain with the existing nodes but are transferred to others. For the chosen centrality algorithm, the foreground network was represented by the nodes that were found in the top ten percent of the calculated centrality values. The ten percent were therefore not defined according to the number of nodes, whereby ten percent of the total number of nodes were not used per se, but according to the distribution of the centrality values. The nodes were sorted in ascending order according to their calculated value, whereby the data were subsequently selected which are within the top ten percent of the centrality value range. Since the data used in this thesis had a very strong left-skewed distribution, only a very small number of nodes were present in the top ten percent of the respective centrality value range. Consequently, an investigation of these nodes does not lead to any meaningful and representative results. Therefore, based on this approach two adjusted calculations were executed.

Due to the high number of nodes within the study graph, the one percent of the total number of nodes with the best centrality rating, defined in the workflow graph as '*small foreground network*', see figure 5, were firstly examined regarding the maintenance of its importance. It was identified if those nodes were component of the best valued one percent nodes of the flood scenario graph and investigated how the centrality value of these nodes changed. The calculation resulted in two maps, one for each centrality algorithm.

Furthermore, a modified Sameness Ratio (SR), based on the idea of Abshirini and Koch (2017), was calculated using a '*large foreground network*' consisting of ten percent of the total number of nodes, using the nodes with the highest centrality values. Using the adapted definition of the foreground network, the quantified ratio value was calculated for both centrality algorithms to investigate how much of the foreground network remained during a disturbance. The SR was calculated as follows:

$$\Delta x = \frac{\frac{100}{\text{foreground normal}} * \text{foreground disaster}}{100} ,$$

where  $\Delta x$  is the ratio value and the parameter '*foreground normal*' and '*foreground disaster*' indicate the number of nodes selected. The '*foreground disaster*' represents only the number of nodes which were already part of the '*foreground normal*'. The calculated ratio can have a value between 0 and 1, where a higher value expresses that a city and its road network can maintain its functionality better and that a greater resilience against the named disruption exists.

## 4.3 Healthcare Access

To investigate the existing healthcare access and the flood impacts on it, the analysis was subdivided into three main calculations. First, the spatial distribution and potential agglomeration of the health sites were determined to get information about the spatial supply. Because access also depends on the given capacity, the number of beds per health site was additional analysed within this step. Further, the mobility-based spatial accessibility to the existing sites for the resident population was analysed by calculating isochrones based on the needed travel time. To take additionally the population demand into account, the relation of health demand to the spatial supply of hospital beds in case of a 5-minute car drive were calculated. The health sites were defined as hospitals and clinics, as explained in chapter 3.2.3.

### 4.3.1 Healthcare Supply

Inspired by the approach of Guagliardo (2004), the density of the available care provision was calculated, by first creating a grid layer with a cell size of 1 x 1 kilometre respectively 0.009039 degree covering the study area, to receive insights about the existing healthcare supply for each cell. Using this grid layer, the spatial distribution of the located health sites and the available bed capacity were analysed. For the first named, the number of the existing hospitals and clinics per cell was summed up. An effective healthcare access depends not only on the existence and the location of health sites, but on the available capacity of each amenity. In addition to the location of the facility, the data of the health station used in this work partly consisted of additional information on the bed capacity. For the health site features with no given capacity data the average bed amount of the sites with existing data was used for the second analysis. The bed capacity per health site located within one cell was summed up to obtain results on the spatial distribution of available bed capacity per square kilometre. The named calculations were performed for the normal as well as for the flooded scenario, to receive results for each situation.

To examine the actual flood impact on the available supply, the change in the health site distribution and bed capacity was calculated by determining the difference between the results of the normal and the flooded scenario of each cell. The outcome was presented in two maps, one for each aspect of healthcare supply.

### 4.3.2 Mobility-based Accessibility

The mobility-based healthcare accessibility was calculated following the approach of time-based isochrones using the Python module openrouteservice. The idea of isochrones in this framework was that an area that can be reached within a certain time from a health sites location provides healthcare access for the people living in that area. Based on that, a routing graph were prepared in the first step, following by multiple requests for isochrones with different time ranges for each health location to assess the access as well as the flood impact.

#### 4.3.2.1 Routing Graph Preparation

For the isochrone analysis a street network graph is needed as a base for routing calculations. Openrouteservice offers the opportunity to perform such calculations on a user provided modified database, by creating an individual instance or local set up of the application. Although the network graph used for the resilience analysis is based on OSM data, the graph was simplified and topological corrected by OSMnx. To be sure, to have the same database for the analysis calculation of the resilience as well as of the healthcare access, the local modified road network graph was used as base for the isochrone calculation. An additional reason for this procedure was the restricted network graph in case of the flood scenario. Streets and areas which were impacted by the flood could not be accessed and had consequently no access to healthcare supply, why these parts were not considered within the routing. Consequently, for each scenario a separate local openrouteservice instance was built based on the specific network graph data. For this purpose, the data had to be provided in OSM PBF (OpenStreetMap Protocolbuffer Binary Format = .osm.pbf) format. The existing edge shapefile, holding the road related geometry including OSM tags, like road length and highway type, was converted in a three-step process. First, the modified shapefile was converted into the OSM .osm format using the open-source Python module ogr2osm<sup>16</sup>. Due to the reason, that the received output consisted of, inter alia, negative valued OSM ids, the attribute elements were converted into positive values within the next step. Lastly, the open-source program osmconvert<sup>17</sup> was used to convert the received .osm file into an OSM PBF file, for the advantage of a more flexible and faster processing (OpenStreetMap contributors, 2020b). This preparation step and subsequently the building of the openrouteservice routing graph in docker had to be applied on each scenario graph. The received routing environments were used for the following scenario-based analyses.

---

16 <https://github.com/pnorman/ogr2osm> (downloaded: 05/02/2020)

17 <https://wiki.openstreetmap.org/wiki/Osmconvert#Linux> (downloaded: 05/02/2020)

#### 4.3.2.2 Calculation of Isochrones and Catchment Areas

The isochrones were created by using an openrouteservice HTTP POST request and by providing several parameters. For each healthcare location, given in coordinates, six isochrones were requested based on a ‘driving-car’ profile. A request for an isochrone with the time range of 1800 seconds respectively 30 minutes was sent, which was additionally subdivided by an interval size of 300 seconds or five minutes. This resulted in six isochrones for each health site from the time range of five to 30 minutes. The reachability type was consequently defined as ‘*time*’ instead of ‘*distance*’. Within this thesis the definition was set, that the shorter the needed duration to a health site, the better the healthcare access and supply. Openrouteservice offers furthermore several additional parameters to either receive extended information or to further specify the output. In the used study methodology, the default isochrones without any add-on’s modifications were requested for the health facilities available within the normal and the flooded scenario. The request was divided according the amenity type, i.e., hospital and clinic.

In the case of the flood scenario, not all streets were passable and areas accessible. Using the isochrone algorithm only the isoline border was calculated, wherefore small flooded areas within the isochrones were counted as part of the output. For the reason, that flooded areas within the isochrones were consequently ignored, the geometry difference<sup>18</sup> of the requested output and the flood related polygon shapefile was calculated to receive only the area, which was still accessible and not flooded.

To receive insights about the flood impact on the access and supply areas of the given amenity locations, the calculated isochrones of the normal and the flooded scenario were compared, and the difference determined. If an area had access to the same or another facility within the same time frame, the mobility-based accessibility was defined as not changed. On the other hand, the access time could increase if alternative routes or health sites had to be chosen. For each amenity type such an impact map was generated. Furthermore, histograms were created, containing additional information regarding the changing area size and the accessed population number for each health site type and isochrone time frame interval.

#### 4.3.3 Supply and Demand related Access

To further elaborate the access analysis to healthcare, not only the health supply, but the population demand is worth to be considered. Therefore, one additional analysis was performed, which was taking into account healthcare supply, calculated by the spatial

---

<sup>18</sup> Difference is a method of the Python package Shapely, used within the Geopandas framework:  
[https://geopandas.org/set\\_operations.html](https://geopandas.org/set_operations.html) (accessed: 30/09/2020)

distribution of the health site locations, the available bed capacity and the mobility-based accessibility, as well as the population demand, here defined by the spatial density of the city inhabitants. This approach's idea is similar to the calculation of floating catchment areas (FCA) (Luo and Wang, 2003; Luo and Qi, 2009; Kim et al., 2018), with the difference of the chosen input parameter and the usage of isochrones as catchment areas. The access in this context was defined as better if a person had a greater choice of health locations and a higher bed capacity available within the same travel time.

For illustration purposes and since differences in local accessibility can be better identified on a small scale, the calculation was done only for the hospital isochrones, which represent the access available within a maximum 5-minute car drive. The isochrones contained information about the available bed capacity within this area. The boundaries of the selected isochrones (see figure 6, left) were unioned<sup>19</sup> and polygonized<sup>19</sup> to generate the geometries of each isochrone fragment (see figure 6, middle). These polygons were intersected<sup>19</sup> with the original isochrone layer to count the number of available hospital care beds within each area, overlapping and non-overlapping (see figure 6, right), to receive insights about regional variations. Multiple health sites and a larger amount of available beds accessible within the same time frame results in better access.

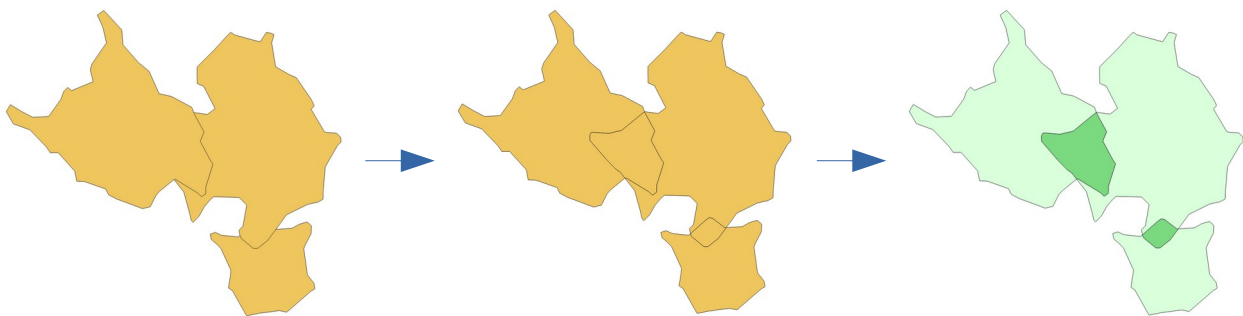


*Figure 6: Process to generate isochrone fragments to sum up the available bed capacity for each area: (left) healthsite isochrones and isolines, (middle) all available isochrone fragments, (right) attribute value per isochrone fragment and cumulated within the overlapping areas*

*Note: Isochrone fragments were generated by unioning and polygonizing the given isochrone boundaries. To receive the summed number of available hospital beds for each spatial fragment, the polygon fragments were intersected with the original isochrone layer.*

In addition, the population per isochrone fragment was calculated in relation to the area size to obtain information about the living population density. To receive insights about the actual supply available per inhabitant, the supply-to-population ratio was calculated, by using the following formula:

---

<sup>19</sup> Union, polygonize and intersects are methods of the Python package Shapely:  
<https://shapely.readthedocs.io/en/stable/> (accessed: 30/09/2020)

$$\Delta sp = \frac{\text{amount of beds}}{\frac{\text{population}}{\text{area}}} ,$$

where  $\Delta sp$  is the ratio value per isochrone fragment. The parameter ‘*amount of beds*’ indicates the available cumulated bed capacity for each area (see figure 6, right) which is set into relation to the population density for each spatial fragment, calculated by using the ‘*population*’ size and the ‘*area*’ size. A similar ratio, the physician-to-population ratio, was already applied by Luo and Wang (2003) considering the physician’s location.

Furthermore, the flood impact was identified by examining the access for the normal and the flooded scenario and by comparing the results within the next step. The isochrones received for both scenarios were unioned<sup>19</sup> and the change in ratio for each fragment was determined.

## 5 Results and Discussion

Within this chapter the results of the two stringed analysis will be presented. The research questions, phrased in chapter 2.4, regarding the road network (RQ1) and healthcare access (RQ2) as well as the flood impact on both subjects will be answered and discussed.

### 5.1 Road Network

Within the normal scenario, the road network was represented by a weakly connected graph, which broke apart due to the direct flood impacts. As shown in table 1, nearly a quarter of all nodes and 25 percent of the edges were affected by the failure, which split the network into one main graph and several subgraphs. The direct flood impacts can be identified by the decrease in the number of nodes and edges, whereas the indirect effects were characterized, among other things, through the reduction in centrality values.

*Table 1: Graph properties of the normal and the flooded scenario*

Note: BC = Betweenness Centrality, HC = Harmonic Closeness Centrality

	<b>Normal scenario</b>	<b>Flooded scenario</b>
<b>Number of nodes</b>	145,406	111,379
<b>Number of edges</b>	195,385	145,986
<b>Weakly/strongly connected</b>	yes/no	no/no
<b>Min/max BC</b>	0/0.0038	0/0.0043
<b>Mean BC</b>	0.000039	0.000022
<b>Min/max HC</b>	0/2.74	0/2.59
<b>Mean HC</b>	0.24	0.13

#### 5.1.1 Network Characteristics

The network characteristics were examined by the approach of the network and node centrality. Therefore, BC and HC were calculated for each node within the graph.

Each node received a value representing its importance for the functionality of the graph, depending on the definition of the applied centrality algorithm. The most significant nodes as well as urban road structures and the fundamental street skeleton of the city were identified. Furthermore, the flood impact was examined by analysing the change of the node's centrality value.

### 5.1.1.1 Betweenness Centrality: Best roads and junctions for fastest routing

The BC application to the road network revealed a strong left-skewed distribution of centrality values within the normal as well as the flooded scenario. Although, the BC results were normalized and were able to represent values between 0 and 1, the results contain only scores between 0 and 0.0038 respectively 0.0043 for the normal respectively the flooded scenario. Figure 7 shows the nodes value distribution, on the left in cumulative modality and on the right in a histogram. The selected bar thresholds for the normal scenario were divided into ten equal intervals that were aligned with the existing minimum and maximum values and therefore represented the threshold basis for the bars of the flooded scenario. Due to changing conditions, the flooded scenario revealed higher betweenness values, why two additional bars with equal value intervals emerged. The extended range did not exist within the normal scenario; therefore, no value number is specified.

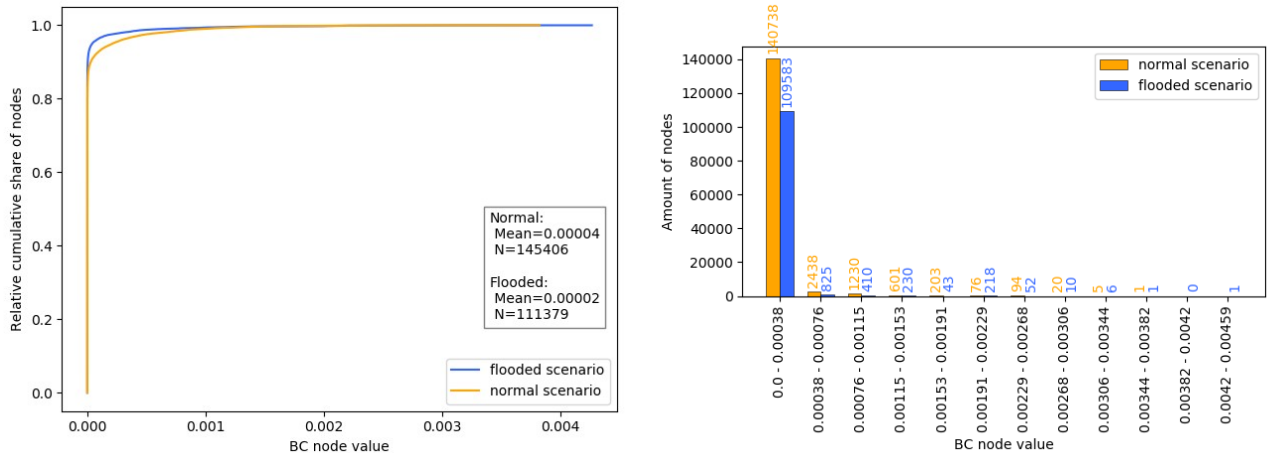
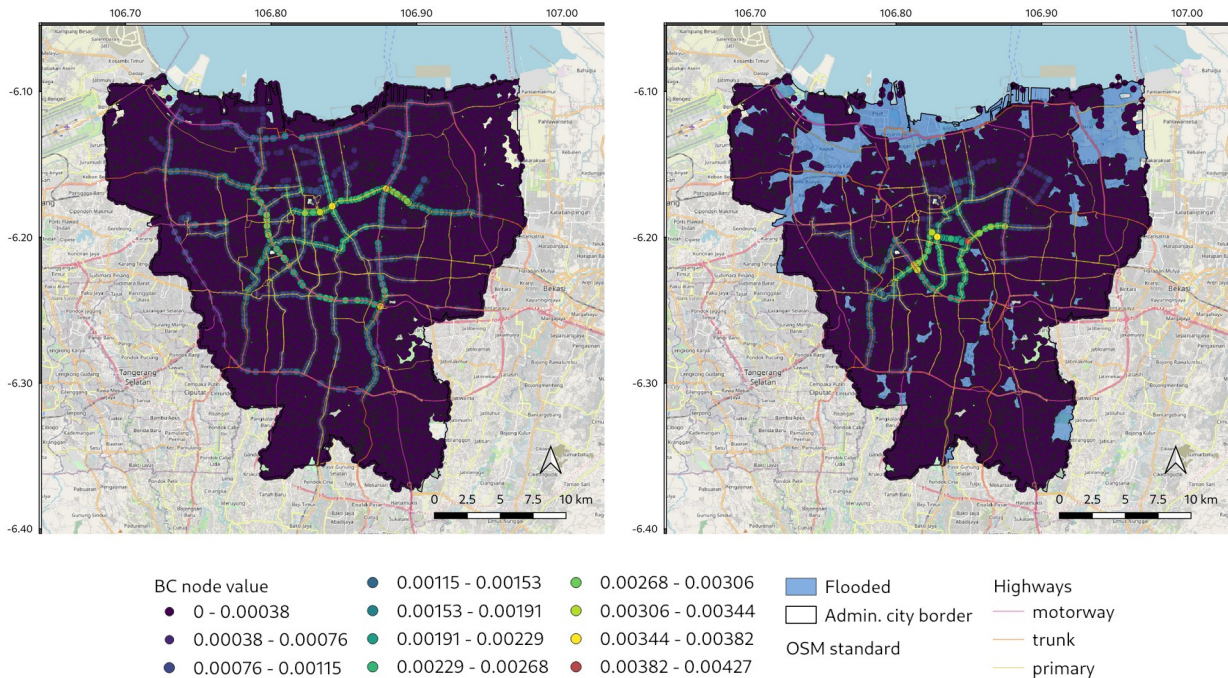


Figure 7: Empirical BC value distribution of nodes: (left) cumulative, (right) histogram

Note: BC indicates the frequency of crossed nodes, based on car driving, fastest routing profile on all possible routes. Most of the traffic is distributed among most of the nodes, whereas a small number of nodes serve as main traffic points. Values of the normal scenario were divided into ten equal intervals for the presentation of the histogram. Due to extended node values within the flooded scenario, the two additional value bars appear.

The nodes distribution of the normal and the flooded scenario are quite similar, strong left-skewed with a node concentration within the value interval of 0 and 0.00038.

Due to the flood disaster, the number of nodes within this graph decreased, from 145,406 to 111,379, see table 1, which reinforced this characteristic. This value interval contains 96.8 percent of the normal scenario nodes and 98.4 percent of the flooded scenario nodes, spatially distributed over the entire study area, see figure 8. The results for both scenarios are illustrated within this figure. The value intervals used within the histogram in figure 7 are equal to those of the maps in figure 8. Excluded are the two additional value bars, which were combined to one value group within figure 8. This 11<sup>th</sup> and last interval of 0.00382 to 0.00427 is the already mentioned interval, valid for the flooded scenario holding an increased centrality value, which did not emerge within the normal scenario.



*Figure 8: The frequency of crossed road junctions, based on car driving, fastest routing profile on all possible routes: (left) normal scenario, (right) 2013 flooded scenario*

*Note: High BC values indicate nodes, crossed more frequently based on the named routing profile. A node holding a BC value of, e.g., 0.00382, indicates that 0.38% of all possible routes between all nodes, are passing this node. A doubling in value indicates that the specific node is passed twice as often. It is noticeable, that in particular nodes of main roads are rated high within the normal scenario. Impacted by the flood a spatial shifting of high valued nodes to a concentration within the city centre occurred. The maps are projected in WGS 84, EPSG: 4326.*

Conspicuous in both scenarios is the concentration of high rated nodes along the main roads within the city, marked as highways within the maps in figure 8. These motorways, trunks and primary roads have characteristically higher speed limits and connect the different districts of the city with each other. They represent a basic framework of the road network, consisting of roads and road sections most used for the fastest routing. The nodes, which are part of large road junctions, connecting such main roads, were also rated high, sometimes even higher. In addition, it can generally be noted that

nodes that are located more central tend to be valued higher than nodes that are closer to the border of the city.

Within the normal scenario, the street basic framework is clearly identifiable, spread across the entire city and connecting the areas. Ring sections exists, recognizable especially in the western and northern part, around the city centre and parallel to the city border. Furthermore, connecting segments from the centre to the border, in all directions are present. The most highly rated nodes, partly used for 0.38 percent of all possible routes, are in places that connect such streets. They are located in the centre and at the western edge of the city centre.

The above-mentioned road structure partially exists within the flooded scenario, with the main connection from the centre to the areas located in the west and northeast. Due to the extensive flooding, especially in the northern part of the city, the nodes along the main roads to the north and in particular to the northwest lost in importance. This effect can also be found in the south-eastern region, despite the small-scale flooding, but greater network fragmentation. The city centre is conspicuous, as in the normal scenario, with a shift in road preference in terms of the fastest route. The roads and junctions in this area gained in importance. The most important nodes, regarding the betweenness definition, are located in this area and partly represent the main traffic junctions. It is noticeable that one point has a value of 0.0043, which is located above the range of values of the normal scenario, maximum value of 0.0038. The named node is used for 0.43 percent of all possible fastest routes, representing the most frequented place within the flooded scenario.

Figure 9 shows the flood impact on the road network, showing which nodes lost and gained in BC value and consequently in their importance for the car driving fastest routing behaviour within the entire city compared to the normal scenario.

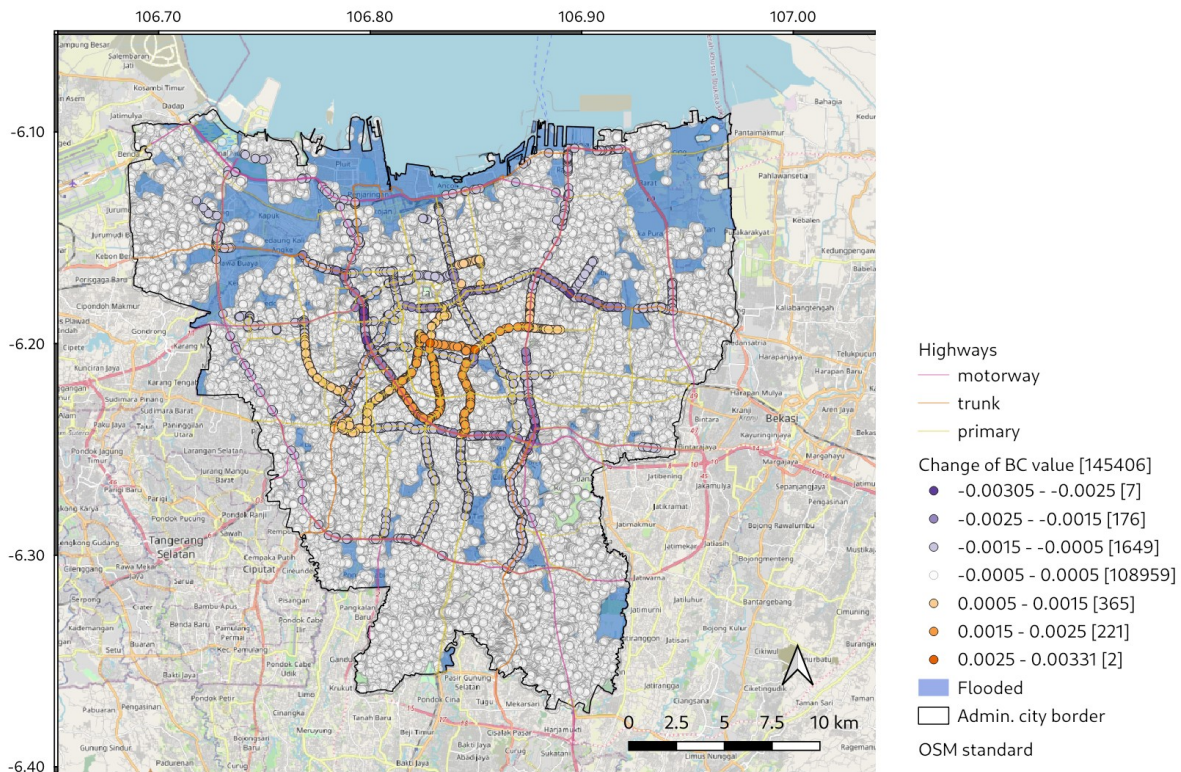


Figure 9: Flood impact on road network regarding BC and node crossing frequency in terms of car driving fastest routing within the entire city

Note: The results were received by taking the value difference of each node between the flooded and the normal scenario. The nodes, which lost in value due to the flood, are used and crossed less frequently when preferring the car profiled fastest route within the city, which may cause in traffic reduction. In comparison, the nodes with positive scores experienced an increase in the above characteristics. The map is projected in WGS 84, EPSG: 4326.

The flood had direct impact on 34,027 nodes, which were flooded and therefore no longer passable. Most of the nodes (~75 percent) did not change in value or only change to a small amount (-/+0.0005), which means that these nodes had an increasing or decreasing traffic volume of up to 0.05 percent. Furthermore, it is not possible to speak exclusively of a deterioration or improvement of the BC functionality within the road network, as different changes are present in the respective areas. As already mentioned, especially the nodes, which are located on the connecting lines from the centre to the outskirts of the city, or vice versa, lost relevance; a decreasing traffic volume of minus 0.3 percent occurred, compared to the normal scenario. The increased focus on the inner-city area and the resulting value orientation is noticeable, with a rising traffic volume of up to 0.33 percent. The flood caused a shift in the traffic flow based on car driving fastest routing profile.

### 5.1.1.2 Harmonic Closeness Centrality: Best supply locations to be accessed

Since in the context of this work the variant HC was used instead of the classical CC algorithm, the results are not available in normalized form. The values range between 0 and 2.74 respectively 2.59 for the normal respectively the flooded graph are left-skewed distributed, illustrated in figure 9 in a cumulative modality (left) and in a threshold framed histogram with ten bars, each with a value range of 0.27 (right). The value intervals within the histogram were rounded.

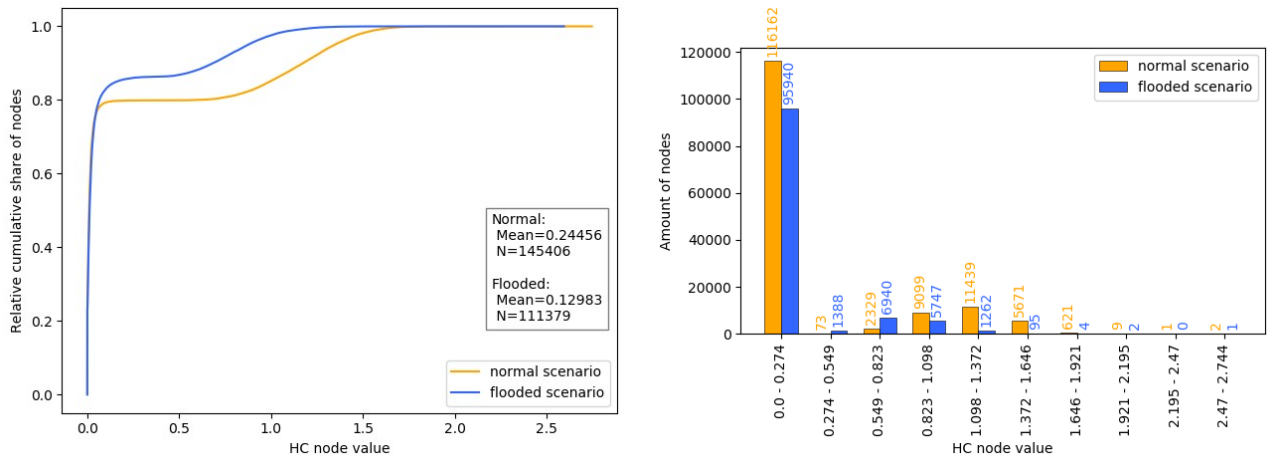


Figure 10: Empirical HC value distribution of nodes: (left) cumulative, (right) histogram

Note: High HC values indicate nodes, accessed most quickly on average for all other nodes based on car driving fastest routing profile. A strong left-skewed distribution with high concentration in low HC values can be seen. Consequently, only a few locations within the city can be accessed faster on average. Values of the normal scenario were divided into ten equal intervals for the presentation of the histogram.

Most of the nodes, almost 80 percent in the normal scenario and 86 percent in the flooded scenario, are at the lower end of the value scale, between 0 and 0.274, representing the strong left-skewed distribution. The maximum value of 2.74 in the normal graph was reduced by 0.15 to 2.59 within the flooded scenario. It can be noticed that the number of nodes decreased almost over the entire given range of values. However, an exception is an increase in the number of nodes between 0.274 and 0.823. Consequently, a very slight approximation of the node distribution within the lower range can be observed.

Compared to the BC results, a visually similar empirical value distribution is noticeable, including a node concentration within the lowest value interval. The HC results show, in contrast to the BC values, an additional increased node accumulation in the middle value range, in the normal as well as in the flood scenario.

Added with the spatial component, the HC nodes distribution are visualized in figure 11, on the left for the normal and on the right for the flooded scenario. The value ranges

identified within the histogram were likewise used for the maps. In both graphs the low-valued nodes, which make up most of the nodes, are distributed over the entire space. Furthermore, the most conspicuous features are the highly rated nodes located in the city centre and along the main roads.

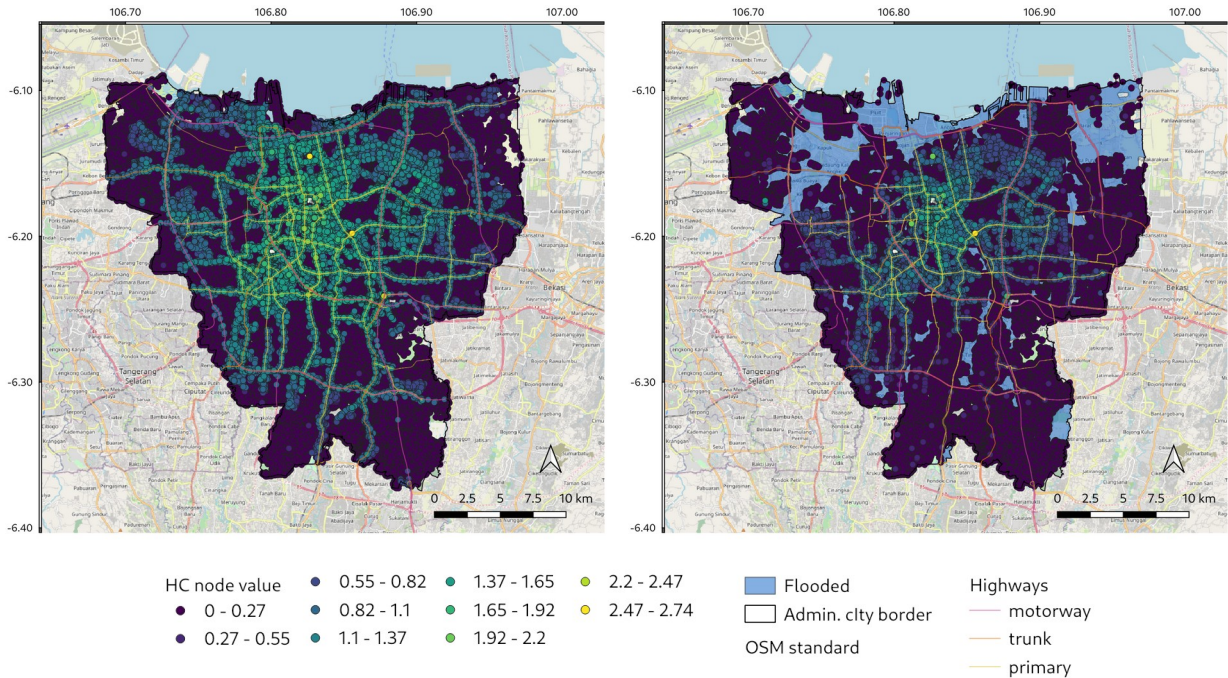


Figure 11: Spatial distribution of HC valued nodes: (left) normal scenario, (right) 2013 flooded scenario

Note: High HC values indicate nodes, accessed most quickly on average for all other nodes based on car driving fastest routing profile. It is noticeable, that within the normal scenario in particular nodes within the city centre and on connecting main roads are rated high. Impacted by the flood, nodes and roads in the outskirts are decreasing in value, whereas the city centre remains important. The maps are projected in WGS 84, EPSG: 4326.

In case of the normal scenario, in addition to the main roads connecting the districts with each other and the city centre with the outside areas, nodes, which are component of access roads to such main roads, were also rated higher. Through this visualization, the local, district-internal traffic characteristics can be partially recognized. In addition, a trend of decreasing values from the city centre to the outskirts of the city can be observed. The number of main roads with the highest speed limits, i.e., motorways, decreased in the city centre, but the spatial location promoted a higher density of nodes with higher closeness values. Two out of three nodes, which are valued between 2.2 to 2.74, are part of main roads or representing access and connection points for such roads.

The number of nodes of the flooded graph decreased in all value classes, whereby the left-skewed distribution became even more pronounced and instead of 80 percent, 86 percent of the nodes are found in the lowest value class. The resulting reduction in the

upper ranges is also evident in the investigation of the highest valued nodes. The node with the maximum closeness value of 2.59 is located at the eastern edge of the city centre at a location where the traffic of three primary roads flows into each other. In addition, the nodes located near the city border lost a lot of their HC importance. This is particularly noticeable in the southern and south-eastern as well as in the north-western region. The intactness of the network in the spatial strip, between the south-western and north-eastern area, becomes clear, whereby a higher concentration of values in the area close to the centre is also visible.

The suburbs as well as the local districts are characterized by low BC and HC values, whereas the main roads tend to have higher values. The low number of nodes with medium and high BC values are concentrated on single streets, while the entire city centre, the district centres as well as the main streets are holding medium to high HC values. These BC and HC values decreased within the flood scenario in the outer areas.

The flood impact and the resulting changes on the road network in terms of HC and therefore on the importance of the most quickly on average accessible locations within the entire city are shown in figure 12. The value difference of each node between the flooded and the normal scenario, resulted in value-losing nodes, which lost importance due to the flood in terms of fast access for all areas within the city. More time is needed to access the location, whereas the nodes that gained in value can be accessed faster on average within the flooded scenario. Almost a quarter of the nodes (34,027) were affected by the direct impact and were consequently flooded. No or only a marginal change of -/+0.2 HC, experienced more than 60 percent of the nodes (88,765) of the remaining 111,379 nodes, which indicates that most of the nodes and the major part of the network, respectively, maintained its functionality regarding fast access.

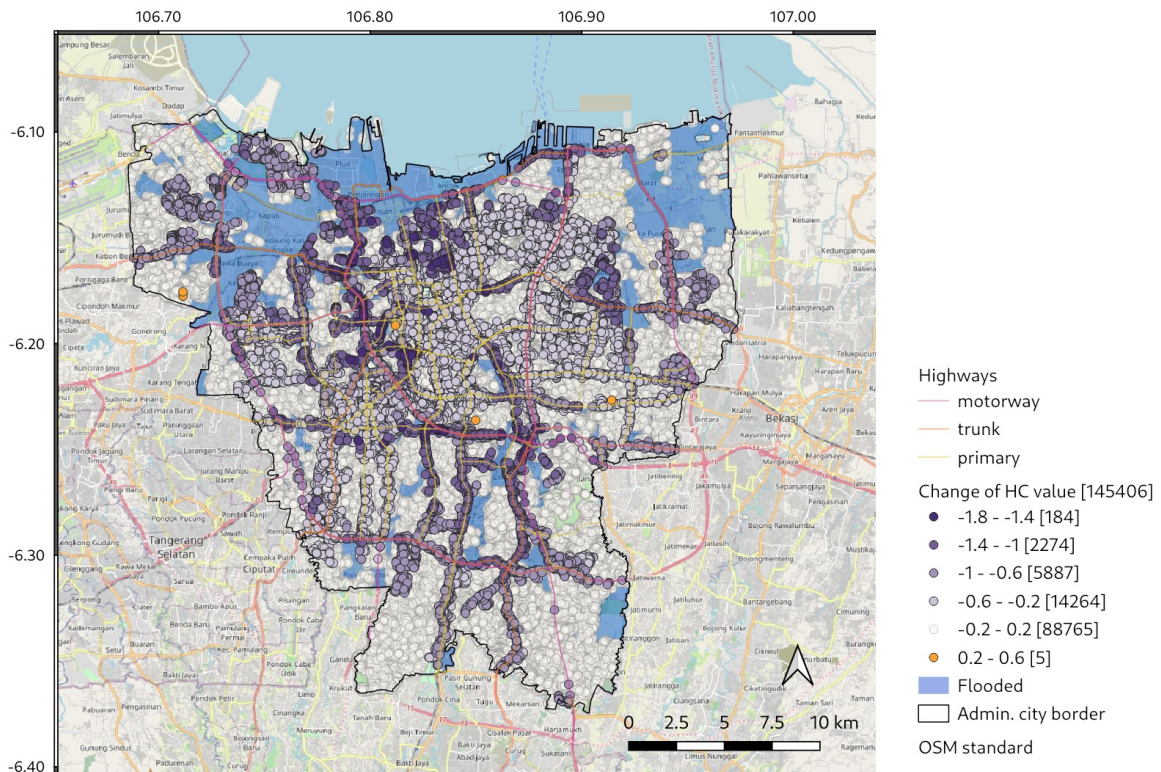


Figure 12: Flood impact on road network regarding HC and importance for the most quickly on average accessible locations within the entire city

Note: The results were received by taking the value difference of each node between the flooded and the normal scenario. In order to access the nodes that have lost in value, a longer journey time on average is required. In comparison, the nodes with positive scores gained in importance. The map is projected in WGS 84, EPSG: 4326.

There is mainly a value deterioration of the nodes, spatially distributed over the entire area, maximum reduction of 1.67. However, the nodes that make up the main roads, which are located in the space between the city centre and city border are conspicuous. Affected were, in particular, those points spatially adjacent to a flooded area and rather close to the centre. Furthermore, the centre of the city experienced only a very slight deterioration of values. In comparison to the mentioned loss of importance, an increase of the HC value can be recorded for five nodes. Three of the mentioned nodes are in the main graph respectively in the largest existing subgraph, whereas they are not part of large main streets. The other two nodes are located in the north-western subgraph, which was cut off from the city centre by the flood.

In contrast to the BC results, hardly any nodes were affected by an increase in HC value. Connecting streets, which especially connect the city centre with the outside areas, decreased in value within both sets of results and therefore lost in importance. This

characteristic is much more pronounced within the HC results. However, most of the nodes, BC and HC respectively, were not or hardly changed by the flood.

### 5.1.2 Network Resilience

Maintaining the foreground structure of the road network is important for an efficient traffic behaviour and for the various functions of the city. Analysing the small foreground network, consisting of the one percent of nodes with the highest BC values, shown in figure 13, revealed again the main structure of the road network in the normal scenario, which, in relation to a time-efficient routing, experienced the highest utilisation.

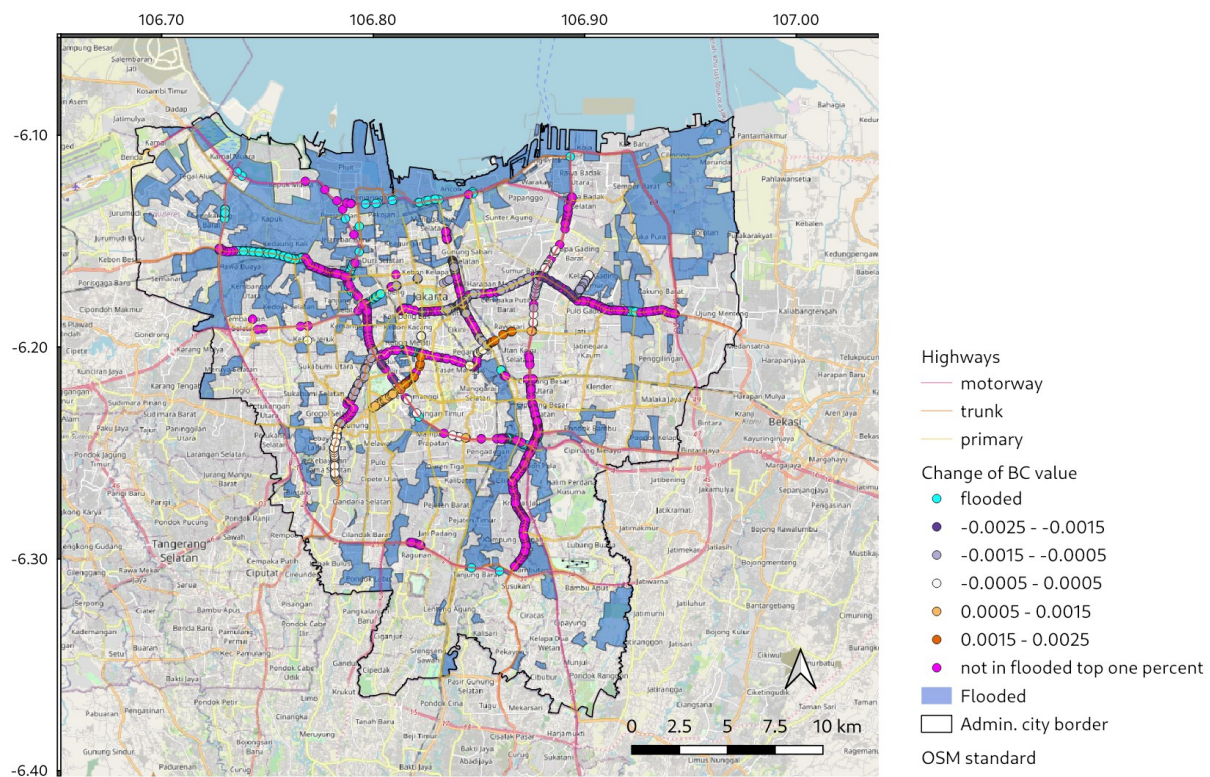
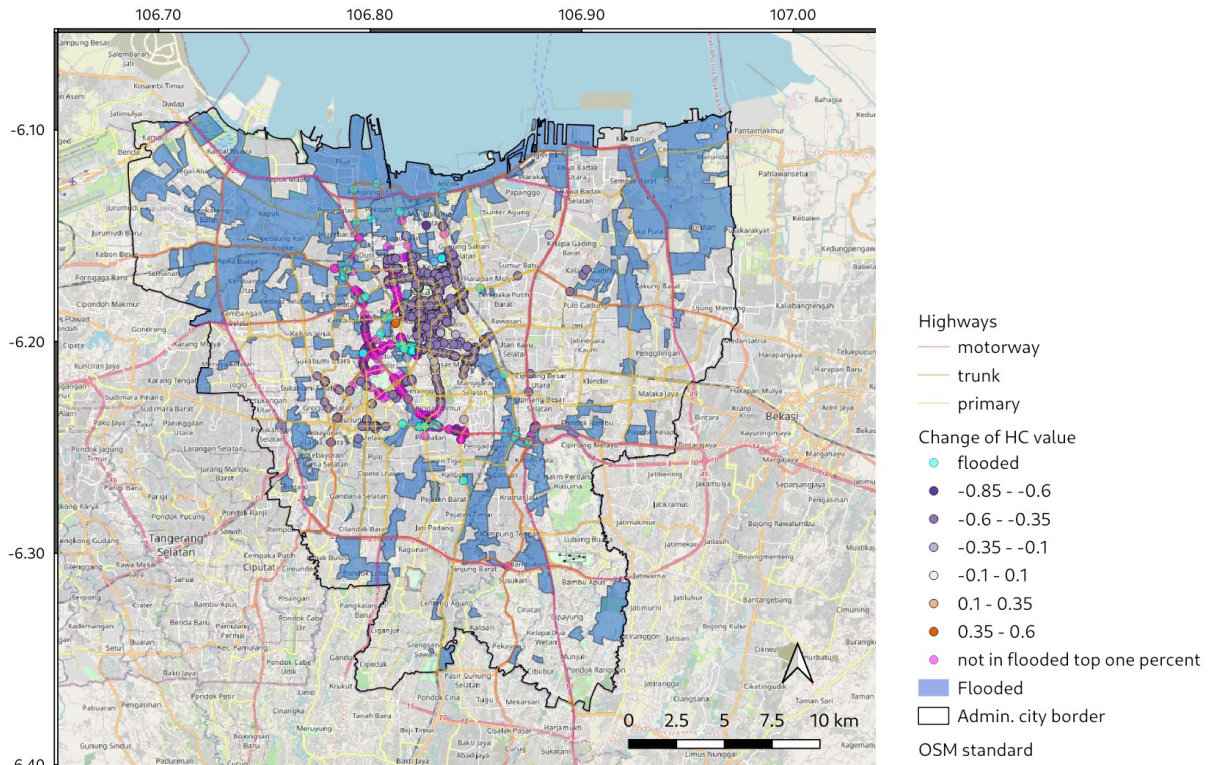


Figure 13: Flood impact on the BC related small foreground network and the functionality of the main road structure considering the frequency of crossed locations based on the car fastest routing profile within the city

Note: The flood effect on the small foreground network respectively the one percent of nodes with the highest BC values. The main roads connecting the city centre and the outskirt areas become clear. Particularly affected by the flood as well as by the loss of importance, are the connecting roads to the north-west and to the south. The city centre area, on the other hand, even gained in importance in some cases and is consequently used more intensively. The map is projected in WGS 84, EPSG: 4326.

The spatial distribution of the most important nodes was determined, holding a BC value between 0.00097 and 0.0038. In addition, the results give insights about whether these nodes are also located in the upper one percent of the most important nodes of the flood scenario due to the flood impact. It becomes clear that the value of about 50 percent of the nodes decreased to a degree that the high importance within the road framework could not be maintained. As already shown in figure 9, this affected, among other things, the north-south connection to the southeast, the connection from the centre to the northwest and to the east, and road sections in the city centre. These nodes were particularly affected by the active flooding of other top-valued nodes (22 percent), which are no longer accessible and are therefore incompatible. Only marginally affected by the flood and therefore robust against the effects, individual nodes exist along the main roads throughout the entire area, such as those along main roads running southwest. In addition, 69 nodes (4.7 percent), which experienced an increase in BC value (0.0005 - 0.0025) and an increase in traffic or additional load of 0.05 to 0.25 percent, are conspicuous. The nodes are located particularly in the area close to the city centre on the east-west connection. These road sections are spatially parallel to those which lost importance.

Compared to the small foreground network regarding the fastest routing functionality within the entire city, the one considering the HC importance and consequently the most quickly on average accessible locations are shown in figure 14. The main road structure is characterized by a spatial node concentration in the city centre as well as a deterioration in the values of almost all nodes.



*Figure 14: Flood impact on the HC related small foreground network and the functionality of the main road structure considering the importance of locations most quickly on average accessible within the city*

*Note: The flood effect on the small foreground network respectively the one percent of nodes with the highest HC values. The city centre plays an important role in the context of fast supply. Although there is a loss of importance due to the flood, the functions can largely be maintained. The map is projected in WGS 84, EPSG: 4326.*

It is noticeable that the node concentration is mainly limited to the western inner-city area. Almost 30 percent of the nodes experienced such a strong importance decrease that the respective nodes could not be assigned to the top one percent of the flood scenario graph. The nodes located in the centre of the city were decreasing in value, too, but the resulting HC values are still part of the flooded small foreground network and therefore still of high importance for a fast supply within the city. This testifies to a core maintenance and resilience of the road network. In addition, there is one node that gained in importance, from 0.51 to 2.18, which is located centrally among the nodes studied. 12 percent of the nodes were directly affected by the flood and consequently not part of the flood graph.

The quantification of the road network resilience was calculated by applying the sameness ratio on the changing size of the large foreground network respectively for each centrality algorithm. Table 2 shows the results for the named ratio, whereas an average to above-average value, independent of the centrality, for the street network appears.

*Table 2: Sameness ratio for each large foreground graph*

*Note: BC = Betweenness Centrality, HC = Harmonic Closeness Centrality*

	Number of nodes		<b>Sameness ratio</b>
	<b>Normal scenario</b>	<b>Flooded Scenario</b>	
<b>BC</b>	14,540	9,004	0.619
<b>HC</b>	14,540	9,977	0.686

### 5.1.3 Discussion

RQ1, phrased at the beginning of this work, was examined in the previous chapter. The results obtained are in the following section to be analysed and interpreted. The investigation was limited to the case of the study area Jakarta in Indonesia, described in chapter 3.1, and the flooding that took place in 2013. Since the impact analysis of the road network resilience depends on the given flood situation respectively the occurring internal and external disturbances, the calculated results may differ. The damaged area extent of the network and the individual node characteristics have an impact. This experience has already been made by Berche et al. (2009), investigating fourteen cities. In this context resilience can be phrased as “a multifaceted and fuzzy concept”, whereas the city “show[s] complex reactions to disturbances in their structure” (Abshirini et al., 2017, p.39). Although, the calculated results of this thesis are related to the 2013 flood, the identified dependencies on specific road segments may also be valid for other flood scenarios, as the occurring floods are possible to have similar recurring spatial expansions.

Within the calculation of BC and HC, strong left-skewed distributions of the result values were observed, which revealed most nodes with a very low centrality value and some nodes with a higher value. As in this case, most of the existing nodes, distributed over the area, showed similar centrality values, it can be generally concluded that a relatively robust road network is present. The maintenance of the respective basic functions is distributed over this main component of the nodes and can, if disturbances occur, switch to alternative roads and routes without losing much performance.

Due to the direct and indirect impact of the 2013 flood, the road network broke up into subgraphs. However, the major part of the network remained as a main graph. The network experienced inevitably a reduction of the given functions, as road segments actively failed and became impassable. A few areas were cut off from the main part of the city and from the main supply. Consequently, the road network became more fragile and

the sensitivity to the effects of the disruption increased. Such a network condition has already been identified by Green et al. (2017), who examined the impact of flood events on the accessibility of emergency responders in Leicester, England.

### **Betweenness Centrality: Best roads and junctions for fastest routing:**

The calculation of BC revealed the behaviour and characteristics of the road network regarding efficient and fastest possible routing between all places within the city, based on a car driving fastest routing profile. By investigating the flood-related change results, insights into dependencies on specific roads were provided.

As most of the nodes have a low BC value, which are spread almost equally over the entire urban area within the normal and the 2013 flood scenario (see figure 7 and 8), it can be stated that most of the traffic is distributed over these nodes. In contrast, a small number of nodes with a medium to high BC value serve as main traffic hubs within the city and are therefore much more frequently crossed and used.

Some basic characteristics of the network condition within the normal scenario were identified by the results highlighted in figure 8. The main roads running close to the outskirts of the city are mainly used by the local population, as these roads were not as highly valued as the inner-city main roads. Compared to the immediate surroundings, however, the nodes in question were rated higher, as these are used as access and connection roads between the local districts and to the city centre. In the city centre a high volume of traffic and a short driving time are combined. Crossroads of main roads are particularly important, since this is where main roads with the above-mentioned traffic beneficial characteristics connect spatially. This differentiation of meaning between road types and spatial location was emphasised by the given value distribution (see figure 7).

The importance of the city centre increased in case of the 2013 flooding, which became clear in figure 9. In case of the BC results, the flood caused a shift of the highest centrality values, which means that the usual, previously used routes were no longer the fastest connections and the traffic flow shifted to other roads and paths. Considering the choice of the fastest route, the traffic was concentrated on the main roads close to the city centre, covering a much smaller area, since the highest centrality values were spatially much closer and more compact during this flood. Such a transformation can lead to a concentration of traffic and consequently to congestion.

These change results were reinforced by the output of figure 13 and by the change of the small foreground network. Half of the roadway main structure did not withstand the effects of the flood and consequently did not maintain the provision of its functions. This applied in particular to the connecting roads between the city centre and the outskirts. Due to larger but also smaller impassable roads, alternative routes were chosen to reach the

desired destination within the city as quickly as possible. Main roads as well as large traffic junctions running from southeast to northwest were increasingly used during the 2013 flood. This was also because this area was relatively little affected by the flood.

The average BC value decreased from 0.0004 to 0.0002, while the maximum value changed from 0.0038 to 0.0043. This led to a stronger left-skewed distribution and traffic dispersion over the majority of the road network as well as to an increase in the importance of individual nodes and network segments.

### **Harmonic Closeness Centrality: Best supply locations to be reached:**

In comparison, HC can be used to identify the places that are the quickest on average for everyone to reach and can therefore serve as good supply locations within the city. These places can be used to provide contact points for people seeking help, but also to better coordinate the supply of the affected areas.

The high proportion of nodes with a very low HC value (see figure 10), spatially located in the local districts in the outskirts (see figure 11), revealed that access to them, in conjunction with the existing speed-limited roads, is more time-consuming. Furthermore, nodes with a medium HC value between 0.0549 and 1.646 (see figure 10), revealed local district centres, which serve as important regional supply points. Access to these locations is strengthened by the higher speed limit on the surrounding main roads (see figure 11). Overall supply points, which are the quickest on average to access for everyone, are only present in a small number in the normal scenario and decreased slightly in the 2013 flood scenario (see figure 10). The city centre and the main traffic junctions within the centre occupy this importance and act as traffic hubs within the city. Its spatial location and the high speed limit at the mentioned junctions make them easily accessible for all surrounding areas (see figure 11). The slight temporal deterioration in access to the city centre was caused by the decrease in HC value of the nodes along the main roads, which were particularly affected by the indirect flood effects (see figure 12). Some parts of the main roads were no longer passable and were not able to maintain their function of providing fast supply. However, due to the large number of routing possibilities between the outer areas and the city centre, the city centre was still able to provide its main supply functions for the entire city (see figure 14). In this context, one node experienced an increase in value (see figure 14) and adapted to the node values localized in the centre. If this were to happen on a larger scale, one could speak of a spatial expansion and consequently a stabilization of the centre and the supply line. With only one node, however, this effect is hardly or not at all to speak of.

The left-skewed distribution of the nodes, which is already present in the normal state, and therefore the large-area distribution of the general HC assessment, was further intensified in the flooded scenario, whereby the number of important nodes within the

network was reduced. This becomes clear when looking at the decreasing average HC value from 0.24 to 0.13. Since higher centrality values represent a better functionality of the road network, this reduction of the average HC value shows a limitation of the overall performance.

### **Sameness ratio: Road segments for main functionality:**

It must be mentioned that the SR cannot be used to determine the quality of the networks condition and the respective partial importance regarding the respective centrality, but the degree of change during the disaster. The SR gives insights about how resilient the street framework, here large foreground network, and therefore the city is to a disturbance. The BC SR examined the nodes that were most important for fast routing and its maintenance. The SR of 0.619 therefore resulted in a slightly above average value, which indicates that the mentioned road framework was able to withstand the flood to a certain degree and that most of the corresponding nodes held the position for maintaining fast routing. However, some areas were affected by the flood, either directly or indirectly, which means that the BC importance was transferred to other nodes and therefore was not able to withstand the external disturbance. Using the HC SR, however, the base framework was examined, which consisted of the nodes that were of high importance for efficient and fast supply and were therefore the fastest on average to reach for all urban areas. The SR value of 0.686 resulted in a similar value as the BC SR. Much of the functionality of the scaffolding was maintained, ensuring rapid access and supply in such a disaster situation. As with the BC SR, however, there were also nodes which lost in importance as essential access points due to the 2013 flood and consequently experienced an unaccustomed lack of supply.

Although both calculations of the SR show similar results, see table 2, the values cannot be compared directly, as the large foreground networks consist of different nodes, see figure 13 and 14. However, the respective node groups were affected directly and indirectly by the same flood and are therefore able to emphasise the previously formulated results. Consequently, it can be said that the main and access roads as well as the city centre are of utmost importance for fast supply within the city. This is partly since these areas are the most time-efficient for everyone to access, and partly to the fact that they are passed most frequently if the fastest route is chosen. However, this can also have the disadvantage that those seeking help and those providing it, must also meet with normal traffic and may consequently lead to congestion on the road network. In addition, a concentration may lead to local traffic jams with an increased risk of accidents and aggravated emergency care. This increased traffic volume is possible to occur especially when single nodes and places exist, which are highly valued and therefore experience a high usage.

It can be stated that main roads ensure time-efficient routing as well as a fast and effective supply of the city, as districts are directly connected, larger traffic volumes can be handled and in addition a higher speed limit can be used. The flood of the year 2013 had a negative impact on these main transport axes, resulting in a reduction in functionality. In order to maintain traffic and healthcare, these streets should be more stabilised and protected from flood impacts in the future.

### **Limitations and Improvements:**

A range of different centrality measurements can be advantageous to analyse a city and the road network with its different aspects and characteristics and to obtain more robust results. Two classical and proven measurements, BC and HC, have been applied in this study to receive information on the basic framework and basic traffic characteristics. Information Centrality, as a further method, could be useful to investigate another aspect of the meaning of the individual nodes. Here, the change in network functionality, when the individual nodes are deactivated, is examined in order to provide information about the influence of the respective nodes on them (Porta et al., 2006; Crucitti et al., 2006).

In addition, it must be noted that the chosen study area is only a section of reality and that the influence of surrounding areas was not included in the analysis. Consequently, the surrounding road network and existing healthcare facilities were not considered. The 2013 flood and the spatially limited investigation area caused an interruption of the spatial connections between the city centre and the north-western urban area. If the surrounding areas were to be included, alternative routes could exist which would enhance the local supply of services. When considering the calculated centrality values of the entire urban region, it can be assumed that the choice of a spatially larger study area would lead to different results. The basic structure of the results would probably remain the same, with a concentration of high values in the city centre and along the main roads. However, it is likely that the urban border areas, with a focus on the main transport axes, would show higher values than in the currently chosen context, since, among other things, the needs of the population groups living in the surrounding area would have an influence. However, the surrounding areas may also be affected by the flood, which may reduce the impact of additional roads and health facilities.

Within the chosen approach the graph was weighted with the required driving time per road segment. This leads to the assumption that people know and use the fastest routes. Subjectively chosen routes were therefore not recorded and considered. Furthermore, the actual traffic volume was not included in the study calculations. As a result, in case of traffic jams, the importance of associated faster alternative routes and individual route changes was not identified. In the case of emergency services, in particular supply vehicles, such as rescue and police forces, may exceed the maximum permitted speed limits. The road sections that are important in this context can not be

identified with the graph weighting selected here. Instead of the permitted fastest route, the shortest routes are chosen. The importance of these network characteristics may be investigated by weighting the graph with the road length. Due to the selected data basis for the road network, only roads and components that are accessible to all road users were included in the study. Private areas as well as sections that are only available for emergency services were therefore not examined for their routing and access importance.

Analysing the importance of the road network based solely on car use leads to a one-sided view. The analysed characteristics can also be caused by other influences and can be advantageous in the context of an overall consideration of all needs. Main roads are important for a time-efficient supply, but a city with an oversupply of main roads would not be feasible. Traffic-calmed districts are equally important for urban planning that satisfies all interests.

## 5.2 Healthcare Access

The quality of healthcare access depends on the existing health sites with the specific and individual characteristics. The flood can have different rated impacts on various aspects of the health access, affecting the complete health site or the spatial accessibility to the available supply. Table 3 shows, *inter alia*, the number of flood-affected hospitals and clinics, which were inactive for the emergency supply, in case of the 2013 flood. 24 percent of all available health sites were flooded, which resulted in 1,196 of 1,575 active and accessible health facilities.

*Table 3: Number of health sites distributed by amenity type*

	<b>Normal scenario</b>	<b>Removed / Inactive</b>	<b>Flooded scenario</b>
<b>Number of hospitals</b>	195	30	165
<b>Number of clinics</b>	1,380	349	1,031
<b>Σ</b>	1,575	379	1,196

### 5.2.1 Distribution of Healthcare Supply

The spatial distribution of available healthcare supply per square kilometre, referring to the existence of health sites, were identified by the location of each facility and visualized in figure 15. It must be noted that not all cells within the grid have a size of one square kilometre. The ones located at the city border are truncated and are consequently smaller. The left map shows the situation for a normal and daily situation, whereas the right map gives insights about the changing and decreasing supply during the flood in 2013.

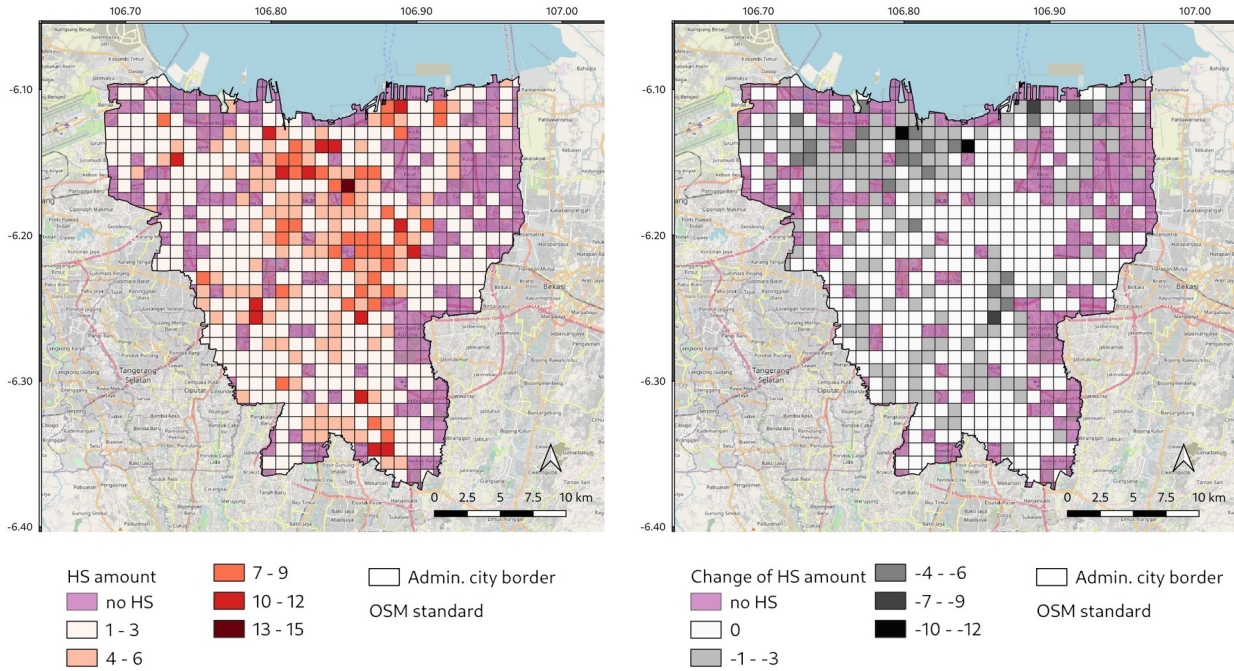


Figure 15: Spatial density of health site locations: (left) amount of health sites (HS) per square kilometre in the normal scenario, (right) 2013 flood impact on amount of HS per square kilometre

Note: Flood impact were identified by the cell difference between the flooded and the normal scenario. Negative values indicate the decreasing number of available health sites per square kilometre. The city centre, but also the western and southern region of the city have areas with high concentrations of facilities within the normal scenario. No or hardly any facilities characterise the western part of the city. Particularly affected by the flood is the northern part of the city, whereas the centre experiences little or no losses. The maps are projected in WGS 84, EPSG: 4326.

Within the normal scenario a cluster of health sites exists, within the northern area and the city centre, covering a large spatial area and offering spots with a high healthcare density, including a maximum density of 13 to 15 health facilities per square kilometre. Additional hotspots with 10 to 12 amenities are scattered over the complete area, in particular in the southern and in the western districts. In comparison to the described high density, a large part of the urban area does not have the direct offer of health capacities. One third of the existing grid cells are counted to that group and are distributed over the complete city centre, where the areas close to the city border and in particular the eastern regions are affected by this situation.

Within the flooded scenario, only the areas directly affected by the disaster experienced a decreasing degree of facilities. As a result, the north-western region was most affected, including two locations near the coast with the highest rate of change. Furthermore, the city centre and in particular the eastern part of this region were not or not strongly affected as well as the amenity hotspots located in the south of Jakarta.

To receive deeper insights about the existing healthcare supply, the density of the available bed capacity within the city of Jakarta was examined and presented in figure 16, considering the same grid overlay layer as in figure 15. Each hospital and clinic offer an individual number of beds, which was summed up for each square kilometre. The left map shows the situation for the normal scenario, whereas the right map shows the direct flood impact and consequently the decreasing amount of available beds per square kilometre.

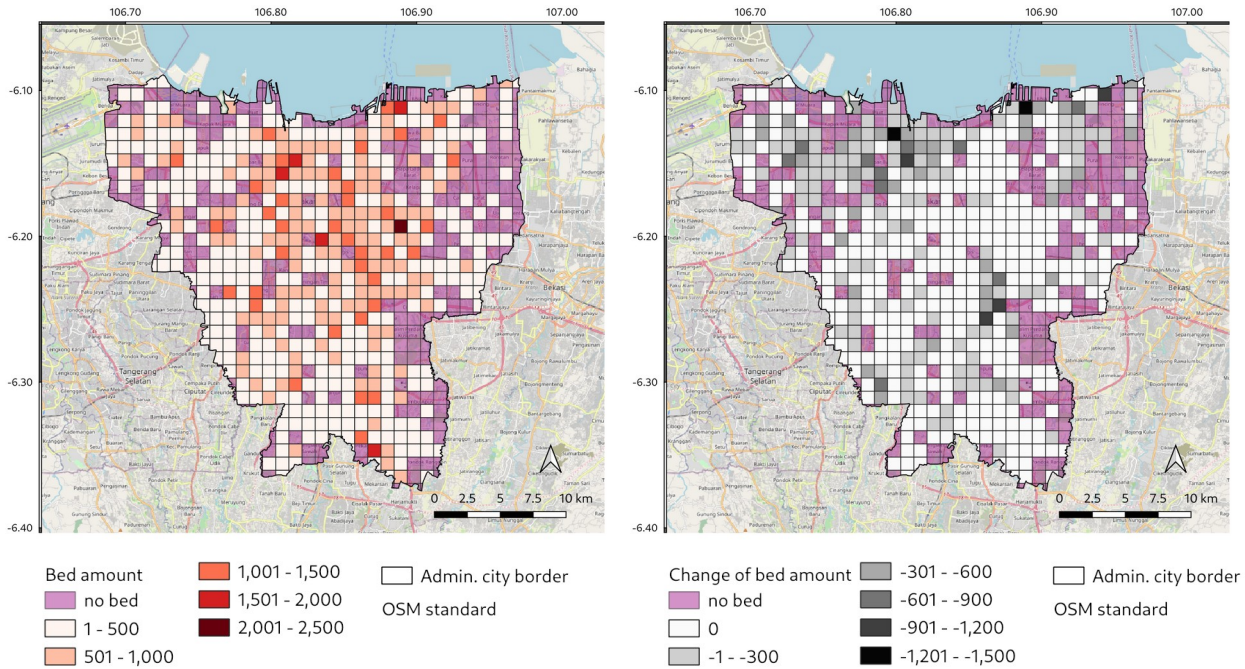


Figure 16: Spatial density of available bed capacity: (left) amount of beds per square kilometre in the normal scenario, (right) flood impact on number of beds per square kilometre

*Note: Flood impact was identified by the cell difference between the flooded and the normal scenario. Negative values indicate the decreasing number of available beds per square kilometre. Within the normal scenario the city centre region is characterized by a high amount of care beds per square kilometre. Like the results in figure 15, no or hardly any beds are available in the western part of the city. The north of the city and parts of the south are particularly affected by a loss of beds due to the flood, while the centre has little or no losses. The maps are projected in WGS 84, EPSG: 4326.*

More than 40 percent of the existing grid cells, within the normal scenario, offered one to 500 beds, which are distributed over the entire area, but in particular in the region close to the western city border. The city centre is characterized by a comparatively high capacity density with hotspots providing up to 2,001 to 2,500 beds per square kilometre. Equal to figure 15 and the results of the health site distribution, the same areas which do not have a local health amenity have neither available hospital nor clinic beds.

The flood impacted the area of almost a quarter of the grid cells, whereas 308 of 733 cells were not affected and a third of the cells already offered no bed capacity under normal conditions. There are two spots, which experienced a stronger impact, with a

decreasing amount of 1,201 to 1,500 beds, located in the north, close to the coast. Four additional spatial points, located close to the sea and in the southern, centrally located region suffered a change of -901 to -1,200 compared to the normal situation. Both, the city centre and the southern part of the city, were not affected or only up to a loss of 300 beds per square kilometre. The north-western region of the city, which was the area most affected by the flood, experienced in large parts a reduction of only one to 300 beds per square kilometre.

### 5.2.2 Mobility-based Accessibility

The mobility-based accessibility to the nearest healthcare facility was differentiated in terms of the type of facility. Figure 17 and 18 show the isochrone results, based on the locations of the hospitals and clinics, for the normal scenario and the direct and indirect flood impact on it.

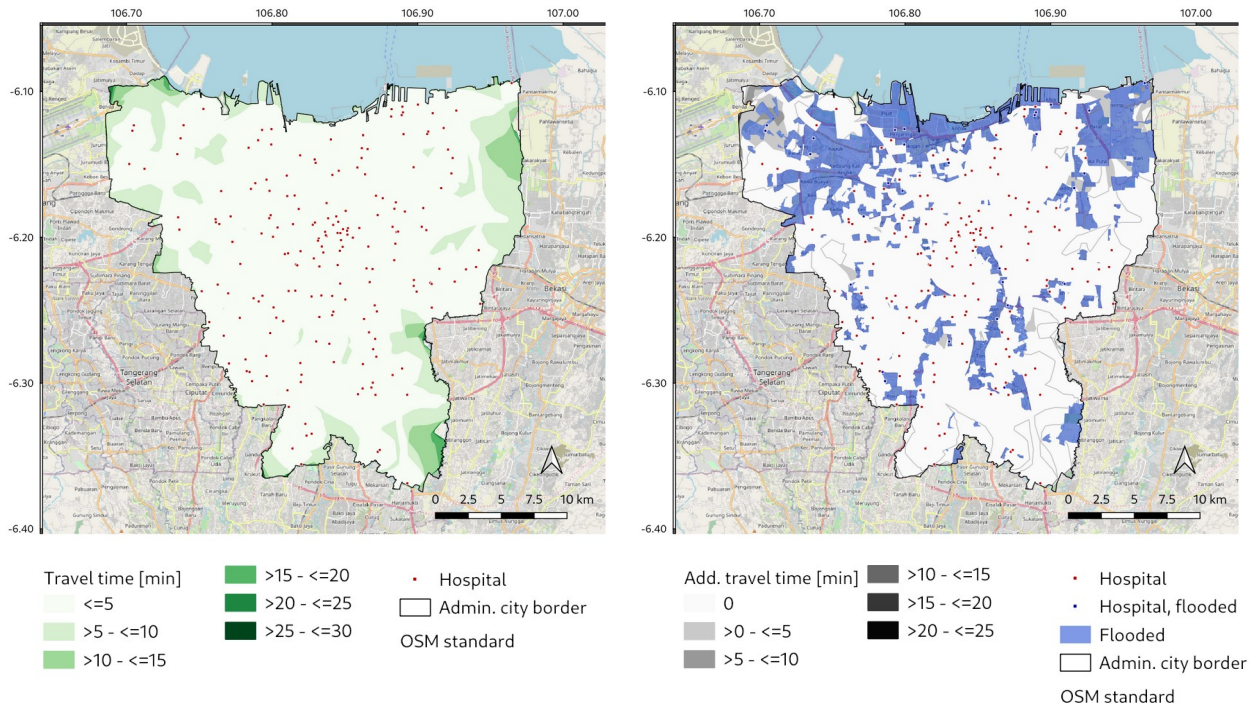


*Figure 17: Minimum needed journey time based on car driving shortest routing profile to at least one hospital: (left) within normal scenario, (right) additional needed journey time due to 2013 flood impact*

*Note: Flood impact results were received by the spatial difference of each isochrone between the flooded and the normal scenario. Higher values indicate a higher amount of additional needed journey time to at least one hospital. Most of the city area has access to at least one hospital within a 5-minute drive within the normal scenario. This access is combined with a longer car journey near the city border. The access is maintained for most parts during the flood. Apart from the directly flooded areas, mainly areas in the north are in need of additional travel time. The maps are projected in WGS 84, EPSG: 4326.*

Accessibility to hospital care, shown in figure 17, was defined by the required travel time to the nearest facility, which within the normal scenario was divided into a 5- to 30-minute range with a 5-minute interval. The left map within figure 17 shows that almost the entire area of the city of Jakarta have access to at least one hospital within a 25-minute car drive. Exceptions are small areas at the city border, which represent parks or areas which have not been included in the routing calculations due to privatised access. The majority of the urban space have access within five minutes, whereby the spatial density of available hospitals has an influence on local accessibility. The number of facilities decrease towards the outskirts of the city, why in this region areas exist with a higher required travel time. This is largely limited to up to ten minutes, but areas directly next to the city border are partly affected by a travel time of up to 25 minutes. A longer travel time is not required within the city.

The flooding had direct as well as indirect impact on the described accessibility. Directly affected were those areas which were actively flooded and therefore no longer passable, shown within the right-hand map of figure 17. Indirectly affected were those areas which still have access during a disaster compared to the normal scenario, but which require a longer journey time to the nearest hospital. It is noticeable, that in terms of indirect impact, small areas within the city area are affected with an additional travel time of up to five minutes. In the north-western region of the city, north of the area most affected by the flood, an additional travel time of up to ten minutes partly must be considered. Areas which are close to the city border and are affected by an additional travel time load have in part no access of less than five minutes even under normal conditions. Small spatial fragments close to the city border are subject to an additional travel time of more than ten minutes.

The results regarding the accessibility to the clinics and the spatial supply of these within the city as well as the flood impact on it are shown in figure 18. The required travel time within the normal scenario is illustrated in the left map. Basically, it is noticeable that almost the entire city area has access to one clinic within less than five minutes by car. Similar to the context of accessibility to hospitals, the need for travel time to a clinic on the outskirts of the city increases. It should also be noted that only small spatial fragments, which are in this area, require a larger time frame of more than 15 minutes.

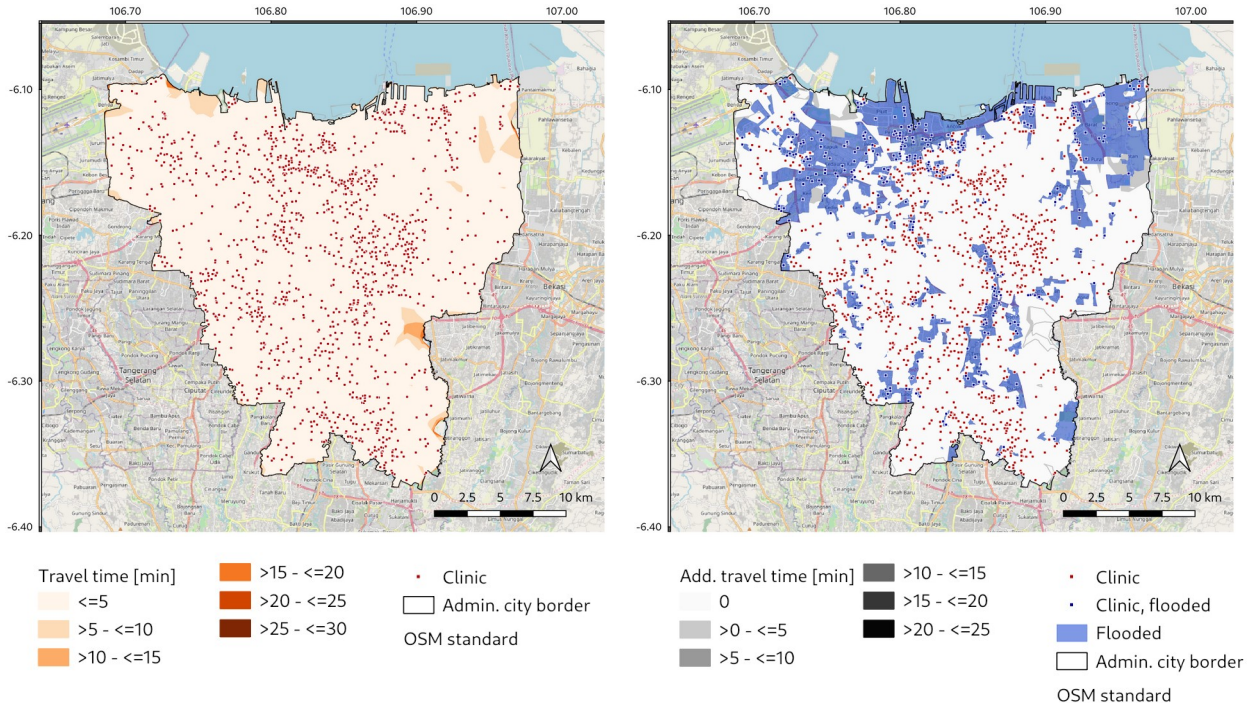


Figure 18: Minimum needed journey time based on car driving shortest routing profile to at least one clinic: (left) within the normal scenario, (right) additional needed journey time due to 2013 flood impact

Note: Flood impact results were received by the spatial difference of each isochrone between the flooded and the normal scenario. Higher values indicate a higher amount of additional needed journey time to at least one clinic. Most of the city has access to at least one clinic within a 5-minute car drive within the normal scenario. The duration of the required travel time increases near the city border due to the flood, but much less than in the context of the hospitals. In case of flooding, access to at least one facility can be maintained, except for small areas in the north of the city. The maps are projected in WGS 84, EPSG: 4326.

The indirect flood impact on the spatial access to one clinic is visualized in the right-hand map in figure 18, whereby the additional time required within the flooded scenario is presented. Apart from the direct restriction by the flood, the mobility-based spatial access to the clinics are largely maintained by the usual travel time. Almost the entire city area experienced an unchanged need of travel time to at least one clinic. In the northern part of the city, in the spatial surroundings of the flood areas, the additional number of minutes increased to a maximum of five. Spatial fragments representing an additional duration of up to 15 minutes are present at the outskirts of the city, whereas no areas within the flood scenario experienced an additional travel time of more than 15 minutes.

The results regarding accessibility to hospitals and clinics were clarified in figure 19. It gives insights about the size of the city area that has access within the respective time span and how this area size changed in the event of flooding. The left histogram shows the

results in the context of hospitals, whereas the right histogram of figure 19 shows the results for the clinic context.

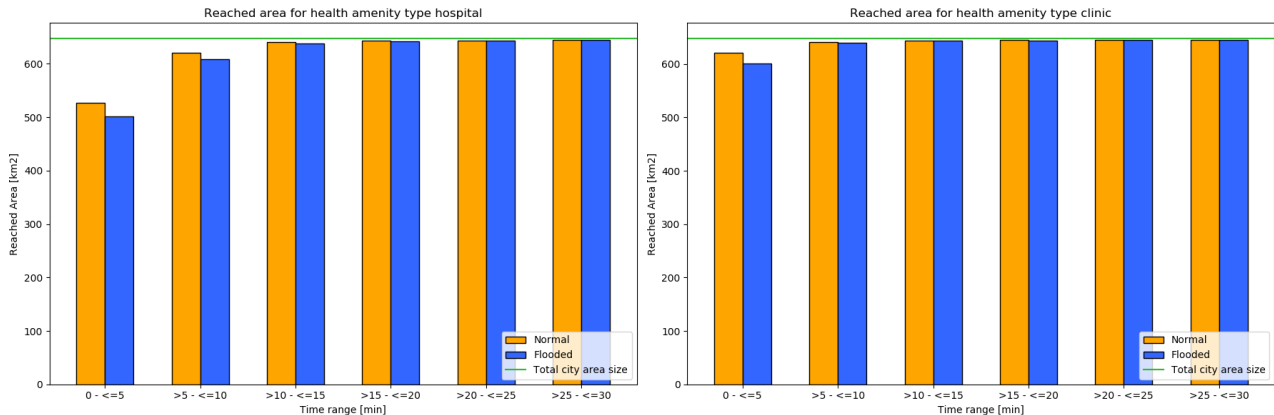


Figure 19: Accessible area size for specific travel time: (left) access to at least one hospital, (right) access to at least one clinic

Note: The size of the accessed area, for the normal respectively the flooded scenario, were calculated by summing up the size of isochrones for each time interval. Available access to one hospital exists for almost the entire urban area within the normal and flooded scenario in less than 20 minutes travel time and to a clinic in less than 15 minutes.

The area of the city of Jakarta is represented by a size of 661.5 square kilometre. In addition to the results already presented, it can be seen, that the maximum required travel time of ten minutes to one hospital was affected by the flood. Access exists and can be maintained in the entire urban area within less than 20 minutes in the normal and flooded scenario. Furthermore, the maintenance of the healthcare aspect is particularly evident when looking at the results in terms of access to clinics. Here, only a noteworthy reduction in area size within the time span of less than ten minutes exists, whereas no change emerged, considering a longer journey time.

Considering the population with access to hospitals and clinics within the needed travel time, as shown in figure 20 access to healthcare facilities and the maintenance of such access is emphasized. The total urban population of Jakarta amounts to 10.7 million. The histogram results of figure 19 and 20 are very similar in their appearance. Consequently, almost the entire population has access to one hospital in less than 15 minutes and to at least one clinic in less than ten minutes in both the normal and the flooded scenario.

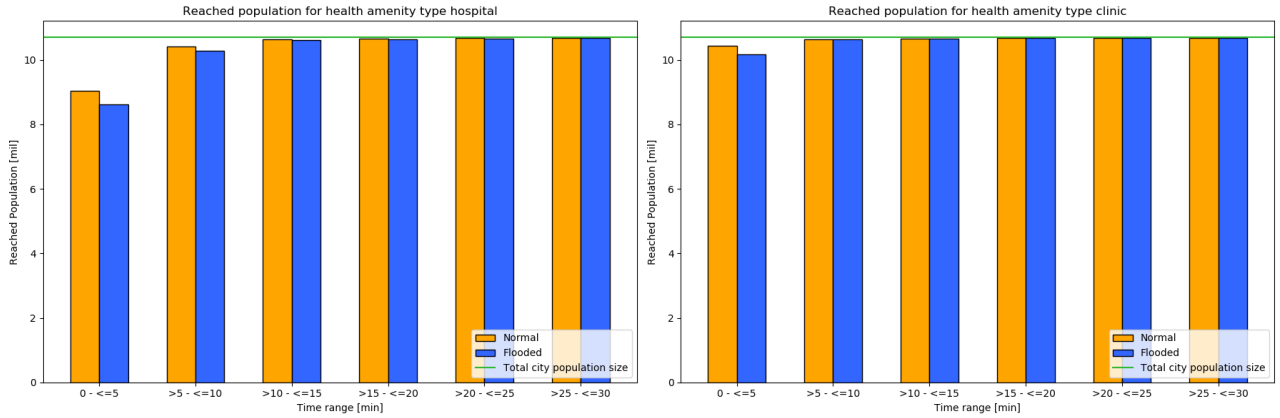


Figure 20: Amount of city population with healthcare access within specific time range: (left) access to at least one hospital, (right) access to at least one clinic

Note: The population with access were calculated by summing up the number of residents living within the specific isochrones. The flood decreased the population amount with a maximum 5-minute access to one hospital from 84 to 80 percent. However, 100 percent of the population has access to one hospital within less than 15 minutes by car. In contrast, access to one clinic within less than ten minutes is available to the entire population within the normal and the flooded scenario.

### 5.2.3 Supply and Demand related Access

Persons who are resident within the calculated hospital isochrones respectively catchment areas have access to one hospital and therefore to the number of beds available. If there is a higher density of hospitals, the person can choose between several facilities within the same travel time frame, which means that a higher bed capacity is available. This cumulative bed capacity is shown in figure 21. A high bed capacity exists especially in the city centre, providing a higher density of hospitals, and along the main roads, which offer a high speed limit for cars. The main roads near the city centre have access values of up to 10,000 beds within a 5-minute car drive. By contrast, areas close to the city border and small districts located close to the centre show values of 45 to 2,000 beds. In addition, areas exist, which do not offer access to a hospital and therefore to a bed within a 5-minute drive at all. These areas are located near the border of the city.

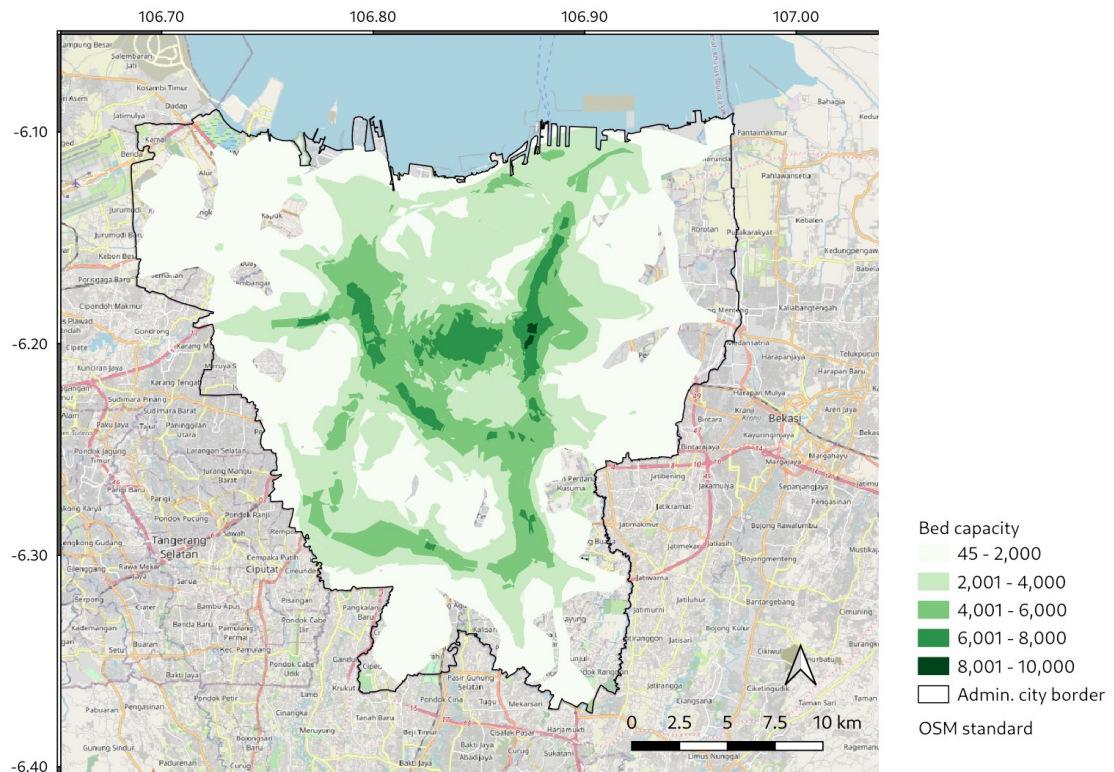


Figure 21: Cumulative amount of available hospital beds, accessible within a 5-minute car drive

Note: Calculated following the process, shown in figure 6. Overlapping isochrone areas, in connection with the respective number of beds, offer a quantitative higher access to health facilities within the defined time range. The city centre as well as the main roads offer high access due to, *inter alia*, the higher density of health facilities within the city centre and better mobility-based accessibility along the main roads. The map is projected in WGS 84, EPSG: 4326.

In the context of this calculation, the demand for healthcare was defined by the resident population density. Figure 22 shows the density per 5-minute isochrone respectively catchment area fragment, with a higher population density particularly in the north-western part of the city. In this region, areas exist with more than 25,000 residents per square kilometre, whereas north of this area and close to the coast, districts subsist with the lowest values of 0 to 5,000 people per square kilometre. In addition, some smaller areas in the central and eastern parts of the city show values of around 20,000 people per square kilometre.

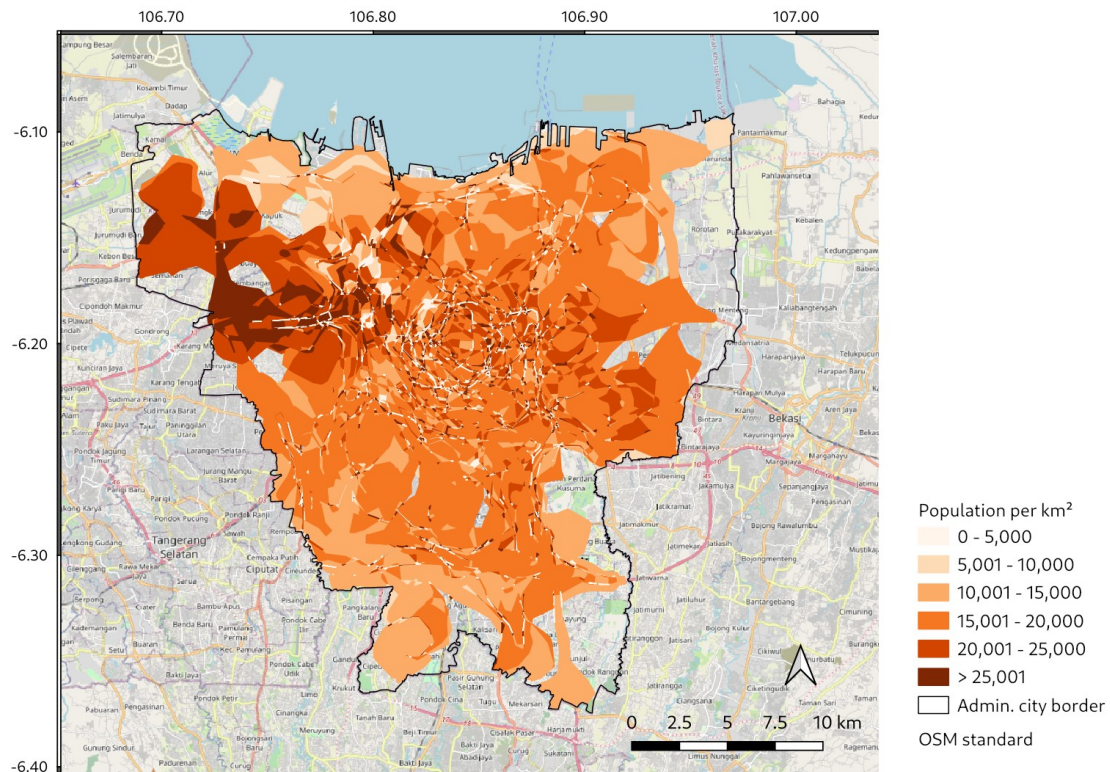


Figure 22: Population density for each 5-minute hospital isochrone fragment

*Note: Due to small spatial splitter fragments and even value gradations, the values of the 87th percentile can be found between 0 and 25,000, whereas the outliers are grouped in the value interval of >25,000. Isochrone boundaries were unioned and polygonized to generate all available isochrone fragments (see figure 6, middle, for generating process). The population density was calculated for each fragment. The north-western region of the city is characterized by the highest population density. The map is projected in WGS 84, EPSG: 4326.*

The results shown in figure 21 and 22 were set into relation to generate findings regarding the accessibility of one person per square kilometre to hospital beds within a 5-minute car drive. The left-hand map in figure 23 gives insights about this state within the normal scenario, whereas the right-hand map shows the results of how it changed in the event of flooding.

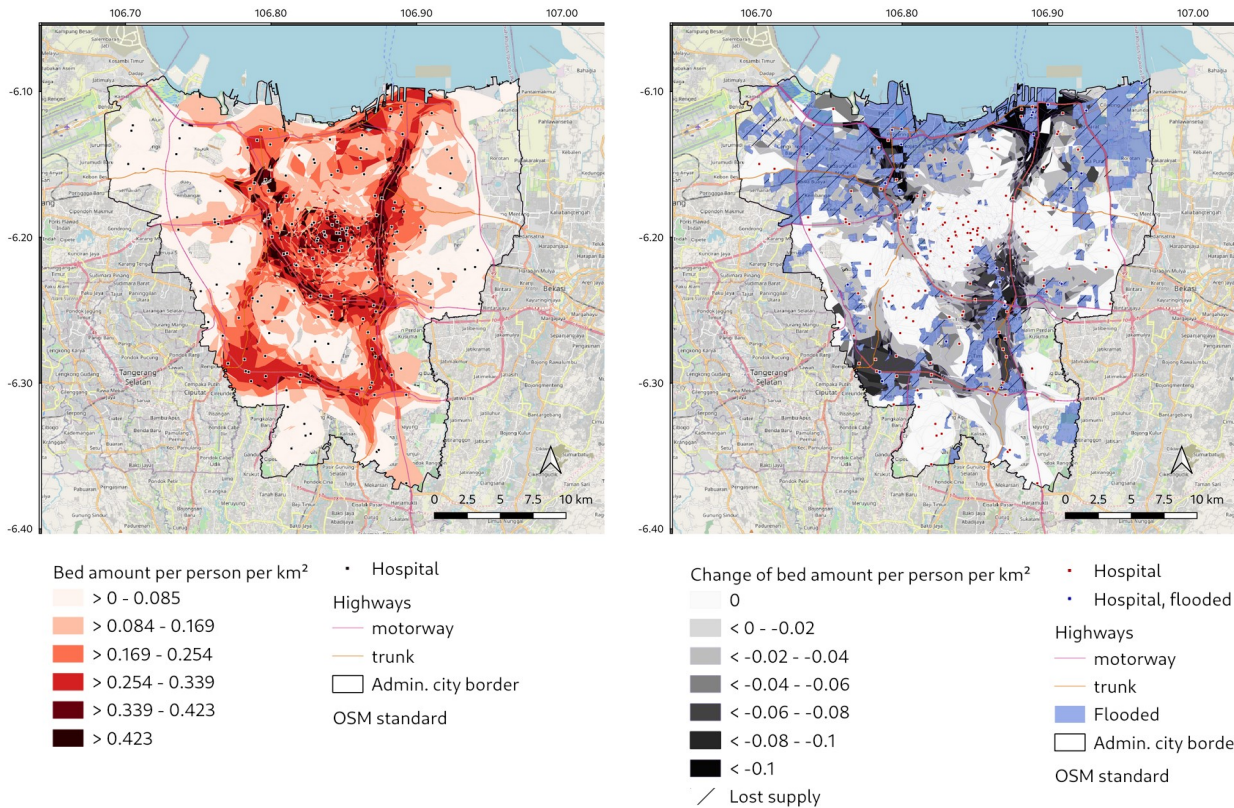


Figure 23: Cumulative amount of available hospital beds per person per square kilometre accessible within a 5-minute car drive: (left) normal scenario, (right) 2013 flood impact

Note visualization: (left) values of the 95th percentile can be found between 0 and 0.423, whereas the outliers are grouped in the value interval of > 0.423, (right) visualization of unchanged and negatively changed values, whereby outliers of top 5th percentile are grouped in the value interval of < -0.1. The maps are projected in WGS 84, EPSG: 4326.

Note calculation: Isochrone boundaries were unioned and polygonized to generate all available isochrone fragments (see figure 6 for generating process). The cumulative bed capacity of each fragment was set in relation to the respective population density, applying the supply-to-population ratio. The flood impact was received by calculating the spatial difference of each valued isochrone between the flooded and the normal scenario. Negative values indicate the loss of available beds per person per square kilometre.

Within the normal scenario, a high supply per population demand exists in the city centre and along the main roads connecting the northern and the southern area. The supply can be maintained in the city centre during the flood, whereas the northern and southern parts along the main roads are strongly negatively affected.

When looking at the results of the normal scenario, striking regional differences in values can be identified. On the one hand, the city centre, as well as the areas along most main roads, are highly valued. With more than 0.423 beds per person per square kilometre, small area segments, in the city centre and in areas close to the city centre, were evaluated. The main road that circles the city centre and the connecting roads from north to south close to the city centre are particularly prominent, with values ranging from

0.169 to more than 0.423. Furthermore, the area along the south-bound east-west connection was marked with 0.254 to 0.339 accessible beds per person per square kilometre. In contrast, the main roads near the city border in the east and west were rated low with less than 0.085, which means, that the available care access in this area is rather bad.

Within the right-hand map of figure 23, the flood impact and the change in bed capacity per person per square kilometre can be observed. Areas with an unchanged capacity offer can be found in the centre of the city and in districts areas close to the city border. However, the north of the city was particularly affected by the change, as was the area south of the city centre. The areas that were mainly affected by the decreasing supply and access to it are those which were actively flooded and consequently experienced a failure of road network sections and hospitals. The flood, which was very pronounced in the north, leaded to a high degree of failure and loss of active supply. In addition, the areas along the main transport axes were more affected by the change than the city centre or smaller districts. The area east of the city centre along the north-south main road experienced a reduction in the northern region by more than 0.1 beds per person per square kilometre. In the southern section, the flood caused changes of varying intensity. The area along the road junction, which connects the main roads running north-south and east-west, was predominantly affected by a change of -0.08 to more than -0.1 beds, whereas an increasing distance is associated with a lower decrease of -0.02 to -0.04 available hospital beds per person per square kilometre accessible within a 5-minute car drive. The area in the northern part of the city, between the directly flood affected areas, and the bordering area in the south (-0.02 to -0.04) was heavily affected, too, with a decrease of partly more than -0.1. The fourth heavily impacted region is located in the southwest in the outskirts of the city, along the main road, with a decrease in bed capacity per person per square kilometre of around -0.06 to -0.1.

#### 5.2.4 Discussion

The results presented in the previous chapter were received by examining the RQ2, phrased in chapter 2.4. The following chapter is intended to interpret and discuss these results including the different aspects in order to provide an answer. Although, the analysis of this study was based on the 2013 flood, the identified results can be used as orientation for future floods, as they may have similar recurrent spatial expansions.

#### **Distribution of Healthcare Supply:**

The existence and demand-oriented spatial distribution of active health amenities is the base of a successful and effective healthcare. The results of figure 15 and 16, which

show the spatial distribution and availability of healthcare facilities and care beds, have similarities. The existing supply varies within the urban area, with a higher concentration of care facilities within the city centre and in the adjacent areas and a decreasing supply towards the city border. This may be explained, among other things, by urban infrastructure planning, as there are often residential areas in the outer regions and services more available in the inner city. As a result, supply within the city also shows local quantitative differences. One advantage of a more central intensive supply is the shortest travel time required on average for all districts. Furthermore, the individual regional hotspots, within the outer areas, point to local supply. The areas located in the east differ notably from the western districts. The eastern area close to the centre has the highest density of healthcare facilities and, with up to 2,500, the highest density of available beds per square kilometre. In contrast to this, a large area with no direct and local care is available. In terms of population distribution, this situation can be explained by the fact that the eastern districts have the lowest population numbers and that the supply is generally decreasing near the city border.

For a stable and crisis-proof supply, a spatially even distribution of the facilities is useful. As the city centre was only slightly affected by the flood, the direct impact on the location of the utilities was minimal. This had the advantage that the highest density of healthcare facilities and nursing beds were available at this location and that they had the chance to continue to operate actively. On the other hand, the situation was particularly problematic in the north-western region of the city, where up to 12 facilities per square kilometre with up to 1,500 beds per square kilometre were lost in some cases. Apart from this severe local restriction, this area was also affected on a large scale. Although the failure of 300 beds per square kilometre was relatively low in comparison and therefore manageable, the large-scale failure caused an accumulation of problems.

### **Mobility-based Accessibility:**

In addition to the consideration of spatial distribution, mobility-based accessibility also has an influence on healthcare. The analysis revealed that the major part of the urban area have access to healthcare facilities within a 5-minute car drive. This is partly due to the location of the health sites, which, although spatially not evenly distributed, are spread over most of the urban area. Figure 15 and 16 show the density per square kilometre, whereas figure 17 and 18 show the actual locations of the amenities. Although there are areas with a conspicuous low or no concentration of supply locations, in most cases successful access can be achieved within a very short journey time. With reference to the hospitals, this access decreases more clearly in the area near the city border than in the context of the clinics. This is mainly due to the lower number of hospitals, 195 compared to 1,380 existing clinics (see table 3). Nevertheless, the access is good in terms of area size, and due to the high density of health sites in some cases, it is even possible to choose between several care centres within the same travel time frame. Haynes et al. (2003) found

out that some patients, registered in Eastern England, are willing to accept a longer travel time instead of the nearest health facility. This willingness could have the advantage of choosing specific facilities for the necessary treatment, thus providing more efficient and effective care.

In terms of travel time, access to health facilities remained the same in most parts of the city, in case of the 2013 flood scenario (see right-hand maps in figure 17 and 18). This is partly due to the given spatial distribution of facilities and partly due to the available choice of amenities. The areas that had to consider additional travel time were mostly located in the immediate vicinity of the flood. The direct flood impact was noticeable through the failure of supply points and roads. However, the indirect flood effects were identified, by the choice of alternative health locations and alternative routes in order to receive primary care, which could have health consequences for the person affected. The histograms in figure 19 and 20 reinforce the results of the efficient access to health facilities and the fact that most of this access could be maintained. As noted above, most of the urban area have access within a very short travel time within the normal and the 2013 flooded scenario. By considering the distribution of the population, this also applies to the residential areas with the highest population density.

### **Supply and Demand related Access:**

One aspect of the study highlighted in figure 16 was further investigated in figure 21 and, in addition to the spatial and cumulative distribution, the mobility-based access to hospital beds within a 5-minute car drive was analysed. The results revealed a strong quantitative difference about fast access to hospital beds. People in the city centre or in areas along the main roads have a significantly higher amount of beds available than those in small districts or in the outskirts. The distribution of population and consequently the general demand for care pronounce these differences even more. The ratio of supply and demand to hospital beds within a 5-minute drive, as shown in figure 23, indicates the striking lower supply within the districts close to the city border. As this study did not calculate the usual bed per person ratio, the results are difficult or impossible to compare with those of other countries and other studies. Consequently, the results cannot be used to assess whether an area has an under- or oversupply for the population, but rather what quantitative differences exist in supply within the city.

The high concentration of hospitals within the city centre have the already mentioned advantages of being the quickest to access on average for all and the most time efficient to supply all urban areas from this location. The disadvantage, however, is that the areas with a high population density have a comparatively low supply density, see north-western region of figure 23 (left). Furthermore, local low speed limits exist, which result in smaller catchment and accessibility areas within the defined time frame and consequently a lower quantitative supply offer. In contrast to this, a high supply per population density is

evident in the districts along the main roads, where the population amount per square kilometre is in line with the urban average. This is evidence of the great importance of these roads and of the main transport axes, which have traffic-promoting characteristics such as high traffic capacity and high speed limits. An efficient and effective supply is therefore strengthened based on a 5-minute car journey.

In addition to the areas, which were directly flooded, the effects of the disaster also affected adjacent areas. In some cases, this led to significant losses of supply. The bed supply in the north-western part of the city is rather poor during a normal, daily situation compared to other urban areas. In the event of the 2013 flooding, a large part of this area was completely cut off and isolated, and for other parts the supply deteriorated considerably. This led to notable supply shortages in the directly adjacent areas. The situation was different in the other three areas, which experienced strong negative effects on supply due to the flood. In the normal scenario these areas have a comparatively good to very good supply. Although the decline had an impact on local healthcare, including additional capacity required due to the flood, the situation in these areas was not as delicate as in the north-western region of the city.

### **Limitations and Improvements:**

If a health facility is spatially cut off and isolated from the major part of the city by the flood, this location is still accessible from the immediate surrounding and non-flooded area. Consequently, this area has access to active healthcare based on the results of the flood. However, the amenities with the available beds can only provide successful care if staff, such as doctors and nurses, have access to the site. If these groups of people live outside the isolated area, they are not able to access the area in the usual way and therefore to carry out the needed care activities. This was the case in areas in the north-western part of the city where the 2013 flooding was at its worst. In addition, the bed-nursing staff ratio is important for the supply of the entire city area. Doctors and nursing staff have limited supply capacities, and an oversupply of beds and patients can lead to overwork and excessive demand.

The need for healthcare was defined in this thesis context, by the amount of population, in order to determine the relation between supply and demand. Alternatively, if data access is available, data from, for example, insurance companies can be used to specify the results. In case of a flood, the need for treatment is likely to increase, since in addition to the existing patients and the daily needs, the facilities are additionally burdened by the people affected by the flood. The problem here is that the supply decreases due to the direct and indirect flood impacts. Amenities, located within the flood area, can neither be reached by the population nor provide care. This reduction in supply creates an additional burden on the still existing hospitals and clinics. In addition to the evacuated patients of the inactive facilities, the people who would have sought access to another

hospital or clinic if the amenity had been maintained must also be cared for. One way to reduce the lack of care sites and the resulting additional burden may be to take over unusual treatment tasks from, for example, doctors' surgeries. Furthermore, the additional demand may be met by short-term emergency accommodation and emergency facilities in order to carry out smaller treatments in addition to any initial care.

With the focus on spatial distribution and mobility-based access to healthcare, the individual acceptance and affordability of care services was not included in this thesis. Consequently, when analysing the results, it must be kept in mind that various aspects such as gender and age, costs as well as ethnic and religious backgrounds also have an influence (Penchansky and Thomas, 1981; Jalil et al., 2018). Healthcare in Indonesia, in particular based on "out-of-pocket" financing (World Health Organization; 2017), can lead to limited access for certain groups of people. In the event of a disaster, however, restricted public and private care may decrease, resulting in general emergency care for all affected people. Financial resources from NGOs, international and national institutions may also help to cover the costs necessary to ensure the provision of care.

The mobility-based accessibility was calculated within this thesis based on the routing profile '*driving-car*'. Consequently, it was assumed that everyone has a car at their disposal and is willing to use it in case of an emergency. Persons without the ability to drive a car and those who do not own a car were therefore disregarded in this context, which may make actual access for this population group notable worse. However, the results of the isochrone calculations, whereby the locations of the facilities were used as the centre, may be considered bilaterally in this context. On the one hand, only the people living in these catchment areas have access to the facilities within the defined car-related travel time. On the other hand, it is also possible to send emergency care by ambulance from the health site to the area in order to provide first aid. In such a case, there is no restricted speed limit for the rescue transport, so that the mobility-based access only depends on the existing traffic.

## 6 Conclusion

This work examined the road network and the access to healthcare in the city of Jakarta, Indonesia as well as the impact of the 2013 flood on it. This included the identification of road segments suitable for fast routing and as quickly accessible supply points (RQ1). It became clear that the city centre and the main roads are particularly important and that their functions were able to be maintained to a large extent during the named flooding. Furthermore, the area was examined regarding various aspects of healthcare provision, as well as the change in this provision due to the effects of the flood, whereby the presence of and spatial access to this supply has an influence (RQ2). It was found that care exists for most people, regarding short access to at least one amenity, but that there are great spatial differences related to demand and available access to existing care capacities. A high supply of healthcare facilities was found in the city centre and along the main roads, similar to the investigation of the road network. The city centre was able to maintain this supply even within the flooded scenario. Therefore, the city centre serves as a hub for time-efficient mobility and rapid healthcare.

Although, this thesis investigated the impacts of the 2013 flood, the received results may also be valid for other flood scenarios, as the occurring floods are possible to have similar recurring spatial expansions. In order to further classify the results regarding their reliability, it may be useful to examine and compare the impacts of the extreme floods of the past years within further research studies. On the one hand, recurring patterns, with a special focus on the city centre and the main roads, and on the other hand, flood-related changing behavioural traits can occur. Such insights can provide a base for better handling with future floods and disasters.

The maintenance of the road network functions depends on several road segments. Motorway junctions and bridges may be particularly relevant and holding a higher importance for the resilience of the functionality. A determination of the influence of the individual segments on the maintenance of the overall functions and the effects of a failure of these can provide further insights into the behaviour of the network in the context of an internal or external disturbance (Porta et al., 2006). Additional recording of the individual importance may therefore lead to more effective protection of relevant road segments and a higher resilience towards future disasters.

The route suggestions, with the focus on the shortest travel time, based on the given characteristics of the road network, do not necessarily represent the actual, reality-based fastest routes. The changing traffic volume and occurring traffic jams have an influence on the travel time. A further investigation of the road network with, e.g., daily

changing traffic volume may give insights into alternative routes. Additional examinations would therefore be useful and beneficial.

Furthermore, successful access to health facilities depends on several different aspects, both objective and subjective. In addition to the spatial availability and accessibility of the facilities, *inter alia*, cultural and financial aspects are relevant (Penchansky and Thomas, 1981). A subsequent study with a differentiation of the facilities into private and government supply as well as an identification of possible religious orientations offers potential.

In the context of increasingly anthropogenic actions and progressive climate change, it is essential to deal with the problem and to develop effective protection measures on a large scale. The Master Plan for National Capital Integrated Coastal Development (NCICD) (van der Wulp et al. 2016; Van Dijk, 2016) and the consideration of relocation of the city (Dinata 2020; Van de Vuurst and Escobar, 2020) are the current answers chosen in Jakarta.

## References

- Abidin, Hasanuddin Z., Heri Andreas, Irwan Gumilar, Yoichi Fukuda, Yusuf E. Pohan, and T. Deguchi. 2011. "Land Subsidence of Jakarta (Indonesia) and Its Relation with Urban Development." *Natural Hazards* 59 (3): 1753–71. <https://doi.org/10.1007/s11069-011-9866-9>.
- Abshirini, Ehsan, and Daniel Koch. 2017. "Resilience, Space Syntax and Spatial Interfaces: The Case of River Cities." *A/Z : ITU Journal of Faculty of Architecture* 14 (1): 25–41. <https://doi.org/10.5505/itujfa.2017.65265>.
- Abshirini, Ehsan, Daniel Koch, and Ann Legeby. 2017. "FLOOD HAZARD AND ITS IMPACT ON THE RESILIENCE OF CITIES: An Accessibility-Based Approach to Amenities in the City of Gothenburg, Sweden," July, 15.
- AHA Centre. 2020. "Situation Updates No. 3: Massive Floods in Greater Jakarta Area - Indonesia." October 1, 2020. [https://reliefweb.int/sites/reliefweb.int/files/resources/AHA\\_Situation\\_Updates\\_No3\\_Greater\\_Jakarta\\_Floods\\_FINAL.pdf](https://reliefweb.int/sites/reliefweb.int/files/resources/AHA_Situation_Updates_No3_Greater_Jakarta_Floods_FINAL.pdf).
- Ahmadzai, Farhad, K.M.Lakshmana Rao, and Shahzada Ulfat. 2019. "Assessment and Modelling of Urban Road Networks Using Integrated Graph of Natural Road Network (a GIS-Based Approach)." 2019. <https://doi.org/10.1016/j.jum.2018.11.001>.
- Albano, R., A. Sole, J. Adamowski, and L. Mancusi. 2014. "A GIS-Based Model to Estimate Flood Consequences and the Degree of Accessibility and Operability of Strategic Emergency Response Structures in Urban Areas." *Natural Hazards and Earth System Sciences* 14 (11): 2847–65. <https://doi.org/10.5194/nhess-14-2847-2014>.
- Alderman, Katarzyna, Lyle R. Turner, and Shilu Tong. 2012. "Floods and Human Health: A Systematic Review." *Environment International* 47 (October): 37–47. <https://doi.org/10.1016/j.envint.2012.06.003>.
- Anderson, Jennings, Dipto Sarkar, and Leysia Palen. 2019. "Corporate Editors in the Evolving Landscape of OpenStreetMap." *ISPRS International Journal of Geo-Information* 8 (5): 232. <https://doi.org/10.3390/ijgi8050232>.
- Arrighi, C., M. Pregnolato, R.J. Dawson, and F. Castelli. 2019. "Preparedness against Mobility Disruption by Floods." *Science of The Total Environment* 654 (March): 1010–22. <https://doi.org/10.1016/j.scitotenv.2018.11.191>.
- Baker, Judy L. 2012. "Climate Change, Disaster Risk, and the Urban Poor - Cities Building Resilience for a Changing World." 2012. <http://documents1.worldbank.org/curated/en/644301468338976600/pdf/683580PUB0EPI0067869B09780821388457.pdf>.
- Barthélemy, Marc. 2011. "Spatial Networks." *Physics Reports* 499 (1–3): 1–101. <https://doi.org/10.1016/j.physrep.2010.11.002>.
- Baum, Moritz, Valentin Buchhold, and Julian Dibbelt. 2015. "Fast Computation of Isochrones in Road Networks," December, 27. <https://arxiv.org/abs/1512.09090v1>.
- Bavelas, Alex. 1948. "A Mathematical Model for Group Structures." *Human Organization* 7 (3): 16–30. <https://doi.org/10.17730/humo.7.3.f4033344851gl053>.
- Beauchamp, Murray A. 1965. "An Improved Index of Centralit." <https://doi.org/10.1002/bs.3830100205>.
- Bégin, D., R. Devillers, and S. Roche. 2013. "ASSESSING VOLUNTEERED GEOGRAPHIC INFORMATION (VGI) QUALITY BASED ON CONTRIBUTORS' MAPPING BEHAVIOURS." *ISPRS - International Archives of the Photogrammetry, Remote Sensing and Spatial Information Sciences* XL-2/W1 (May): 149–54. <https://doi.org/10.5194/isprsarchives-XL-2-W1-149-2013>.

- Berche, B., C. von Ferber, T. Holovatch, and Yu. Holovatch. 2009. “Resilience of Public Transport Networks against Attacks.” *The European Physical Journal B* 71 (1): 125–37. <https://doi.org/10.1140/epjb/e2009-00291-3>.
- Bisenius et al. 2018. *2018 Proceedings of the Twentieth Workshop on Algorithm Engineering and Experiments (ALENEX)*. Edited by Rasmus Pagh and Suresh Venkatasubramanian. Philadelphia, PA: Society for Industrial and Applied Mathematics. <https://doi.org/10.1137/1.9781611975055>.
- Blackwood, Rosalind, and Claire Currie. (2009) 2016. “Measures of Supply and Demand.” Text. Health Knowledge. 2016. <https://www.healthknowledge.org.uk/public-health-textbook/research-methods/1c-health-care-evaluation-health-care-assessment/measures-supply-demand>.
- Boeing, Geoff. 2017. “OSMnx: New Methods for Acquiring, Constructing, Analyzing, and Visualizing Complex Street Networks | Elsevier Enhanced Reader.” 2017. <https://doi.org/10.1016/j.compenvurbsys.2017.05.004>.
- . 2018. “A Multi-Scale Analysis of 27,000 Urban Street Networks: Every US City, Town, Urbanized Area, and Zillow Neighborhood.” *Environment and Planning B: Urban Analytics and City Science*, August, 239980831878459. <https://doi.org/10.1177/2399808318784595>.
- Boldi, Paolo, and Sebastiano Vigna. 2013. “Axioms for Centrality.” *ArXiv:1308.2140 [Physics]*, November. <http://arxiv.org/abs/1308.2140>.
- Bondy, J. A., and U. S. R. Murty. 1976. “Graph Theory with Applications.” 1976. <https://www.zib.de/groetschel/teaching/WS1314/BondyMurtyGTWA.pdf>.
- Borowska-Stefańska, Marta, Michał Kowalski, and Szymon Wiśniewski. 2019. “The Measurement of Mobility-Based Accessibility—The Impact of Floods on Trips of Various Length and Motivation.” *ISPRS International Journal of Geo-Information* 8 (12): 534. <https://doi.org/10.3390/ijgi8120534>.
- Brandes, Ulrik. 2001. “A Faster Algorithm for Betweenness Centrality\*.” *The Journal of Mathematical Sociology* 25 (2): 163–77. <https://doi.org/10.1080/0022250X.2001.9990249>.
- BTS, Bureau of Transportation Statistics, and U.S. Department of Transportation. 1997. “Transportation Statistics Annual Report 1997.” 1997. [https://www.bts.gov/sites/bts.dot.gov/files/legacy/publications/transportation\\_statistics\\_annual\\_report/1997/pdf/report.pdf](https://www.bts.gov/sites/bts.dot.gov/files/legacy/publications/transportation_statistics_annual_report/1997/pdf/report.pdf).
- Caschili, Simone, and Andrea De Montis. 2013. “Accessibility and Complex Network Analysis of the U.S. Commuting System.” *Cities* 30 (February): 4–17. <https://doi.org/10.1016/j.cities.2012.04.007>.
- Cochrane, A L, A S St Leger, and F Moore. 1978. “Health Service ‘input’ and Mortality ‘Output’ in Developed Countries.” *Journal of Epidemiology & Community Health* 32 (3): 200–205. <https://doi.org/10.1136/jech.32.3.200>.
- Coles, Daniel, Dapeng Yu, Robert L. Wilby, Daniel Green, and Zara Herring. 2017. “Beyond ‘Flood Hotspots’: Modelling Emergency Service Accessibility during Flooding in York, UK.” *Journal of Hydrology* 546 (March): 419–36. <https://doi.org/10.1016/j.jhydrol.2016.12.013>.
- Crucitti, Paolo, Vito Latora, and Sergio Porta. 2006. “Centrality in Networks of Urban Streets.” *Chaos: An Interdisciplinary Journal of Nonlinear Science* 16 (1): 015113. <https://doi.org/10.1063/1.2150162>.
- Cutini, Valerio. 2013. “THE CITY, WHEN IT TREMBLES: Earthquake Destructions, Post-Earthquake Reconstructions and Grid Configuration.” In , 17. Seoul. [http://sss9sejong.or.kr/paperpdf/ussecp/SSS9\\_2013\\_REF102\\_P.pdf](http://sss9sejong.or.kr/paperpdf/ussecp/SSS9_2013_REF102_P.pdf).
- Demšar, Urška, Olga Špatenková, and Kirsi Virrantaus. 2008. “Identifying Critical Locations in a Spatial Network with Graph Theory.” *Transactions in GIS* 12 (1): 61–82. <https://doi.org/10.1111/j.1467-9671.2008.01086.x>.
- Desai, Kiran. 2008. “Isochrones: Analysis of Local Geographic Markets,” October, 7. <https://www.mayerbrown.com/files/Publication/7633e871-05b8-428f-bbcd-cf6d9163bab8/>

- Presentation/PublicationAttachment/c7b45b1f-d4f4-413c-b5aa-b0579c87049f/Isochrones-Desai\_Iss2\_1108.pdf.
- Dijkstra, E. W. 1959. "A Note on Two Problems in Connexion with Graphs," 3. <https://doi.org/10.1007/BF01386390>.
- Dinata, Ari Wirya. 2020. "Jakarta: Is Relocation the Answer?" The ASEAN Post. January 10, 2020. <https://theaseanpost.com/article/jakarta-relocation-answer>.
- Erkens, G., T. Bucx, R. Dam, G. de Lange, and J. Lambert. 2015. "Sinking Coastal Cities." *Proceedings of the International Association of Hydrological Sciences* 372 (November): 189–98. <https://doi.org/10.5194/piahs-372-189-2015>.
- Euler, Leonhard. 1741. "Solutio Problematis Ad Geometriam Situs Pertinentis," 15. <https://scholarlycommons.pacific.edu/cgi/viewcontent.cgi?article=1052&context=euler-works>.
- Freeman, Linton C. 1977. "A Set of Measures of Centrality Based on Betweenness." *Sociometry* 40 (1): 35. <https://doi.org/10.2307/3033543>.
- . 1978. "Centrality in Social Networks Conceptual Clarification." *Social Networks* 1 (3): 215–39. [https://doi.org/10.1016/0378-8733\(78\)90021-7](https://doi.org/10.1016/0378-8733(78)90021-7).
- Frith, Michael J., Shane D. Johnson, and Hannah M. Fry. 2017. "Role of the Street Network in Burglars' Spatial Decision-Making\*." *Criminology* 55 (2): 344–76. <https://doi.org/10.1111/1745-9125.12133>.
- Gauthier, Pauline, Angelo Furno, and Nour-Eddin El Faouzi. 2018. "Road Network Resilience: How to Identify Critical Links Subject to Day-to-Day Disruptions." *Transportation Research Record: Journal of the Transportation Research Board* 2672 (1): 54–65. <https://doi.org/10.1177/0361198118792115>.
- Geurs, Karst T., and Bert van Wee. 2004. "Accessibility Evaluation of Land-Use and Transport Strategies: Review and Research Directions." *Journal of Transport Geography* 12 (2): 127–40. <https://doi.org/10.1016/j.jtrangeo.2003.10.005>.
- Gil, J., and P. Steinbach. 2008. "From Flood Risk to Indirect Flood Impact: Evaluation of Street Network Performance for Effective Management, Response and Repair." In *Flood Recovery, Innovation and Response I*, I:335–44. London, England: WIT Press. <https://doi.org/10.2495/FRIAR080321>.
- Gil, Jorge. 2014. "Analyzing the Configuration of Multimodal Urban Networks." *Geographical Analysis* 46 (4): 368–91. <https://doi.org/10.1111/gean.12062>.
- Green, Daniel, Dapeng Yu, Ian Pattison, Robert Wilby, Lee Bosher, Ramila Patel, Philip Thompson, et al. 2017. "City-Scale Accessibility of Emergency Responders Operating during Flood Events." *Natural Hazards and Earth System Sciences* 17 (1): 1–16. <https://doi.org/10.5194/nhess-17-1-2017>.
- Gross, Jonathan L., Jay Yellen, and Ping Zhang. 2015. *Handbook of Graph Theory, Second Edition - Handbook of Graph Theory, 2nd Edition*. Boca Raton, FL 33487-2742: Taylor & Francis Group. <https://learning.oreilly.com/library/view/handbook-of-graph/9781439880197/cover.xhtml>.
- Guagliardo, Mark F. 2004. "Spatial Accessibility of Primary Care: Concepts, Methods and Challenges." *International Journal of Health Geographics*, 13. <https://doi.org/10.1186/1476-072X-3-3>.
- Haynes, Robin, Andrew Lovett, and Gisela Sünnenberg. 2003. "Potential Accessibility, Travel Time, and Consumer Choice: Geographical Variations in General Medical Practice Registrations in Eastern England." *Environment and Planning A: Economy and Space* 35 (10): 1733–50. <https://doi.org/10.1068/a35165>.
- HeiGIT gGmbH. (2018) 2020. *GIScience/Openrouteservice-Py*. Python. GIScience Research Group. <https://github.com/GIScience/openrouteservice-py>.

- . (2017) 2020. *GIScience/Openrouteservice*. Java. GIScience Research Group. <https://github.com/GIScience/openrouteservice>.
- Heron, Michael J., Vicki L. Hanson, and Ian Ricketts. 2013. “Open Source and Accessibility: Advantages and Limitations.” *Journal of Interaction Science* 1 (1): 2. <https://doi.org/10.1186/2194-0827-1-2>.
- Hillier, Bill, and Julianne Hanson. 1984. In *The Social Logic of Space*. Cambridge University Press. <https://doi.org/10.1017/CBO9780511597237>.
- Hillier, Bill, Tao Yang, and Alasdair Turner. 2012. “Normalising Least Angle Choice in Depthmap and How It Opens New Perspectives on the Global and Local Analysis of City Space.” <http://joss.bartlett.ucl.ac.uk/journal/index.php/joss/article/download/141/pdf>.
- Holling, C. S. 1996. “Engineering Resilience versus Ecological Resilience,” 13. <https://www.nap.edu/read/4919/chapter/4>.
- HOT. 2018. “Humanitarian OpenStreetMap Team | Disaster Early Warning And Capacity Building: InAWARE.” 2018. <https://www.hotosm.org/projects/disaster-early-warning-and-capacity-building-inaware>.
- . n.d. “Humanitarian OpenStreetMap Team | What We Do.” Accessed July 28, 2020. <https://www.hotosm.org/what-we-do>.
- Iyer, Swami, Timothy Killingback, Bala Sundaram, and Zhen Wang. 2013. “Attack Robustness and Centrality of Complex Networks.” Edited by Satoru Hayasaka. *PLoS ONE* 8 (4): e59613. <https://doi.org/10.1371/journal.pone.0059613>.
- Jalil, Ilham Abd, Abdul Rauf Abdul Rasam, Nor Aizam Adnan, Noraain Mohamed Saraf, and Ahmad Norhisyam Idris. 2018. “Geospatial Network Analysis for Healthcare Facilities Accessibility in Semi-Urban Areas.” In *2018 IEEE 14th International Colloquium on Signal Processing & Its Applications (CSPA)*, 255–60. Batu Ferringhi: IEEE. <https://doi.org/10.1109/CSPA.2018.8368722>.
- Jenelius, Erik, and Lars-Göran Mattsson. 2015. “Road Network Vulnerability Analysis: Conceptualization, Implementation and Application.” *Computers, Environment and Urban Systems* 49 (January): 136–47. <https://doi.org/10.1016/j.comenvurbssys.2014.02.003>.
- Joseph, Alun E., and David R. Phillips. 1984. *Accessibility and Utilization: Geographical Perspectives on Health Care Delivery*. SAGE. <https://www.jstor.org/stable/622077>.
- Jungnickel, D. 2008. *Graphs, Networks, and Algorithms*. 3rd ed. Algorithms and Computation in Mathematics, v. 5. Berlin ; New York: Springer.
- Kanuganti, Shalini, A.K. Sarkar, and Ajit Pratap Singh. 2016. “Quantifying Accessibility to Health Care Using Two-Step Floating Catchment Area Method (2SFCA): A Case Study in Rajasthan.” *Transportation Research Procedia* 17: 391–99. <https://doi.org/10.1016/j.trpro.2016.11.080>.
- Khan, Abdullah A. 1992. “An Integrated Approach to Measuring Potential Spatial Access to Health Care Services.” *Socio-Economic Planning Sciences* 26 (4): 275–87. [https://doi.org/10.1016/0038-0121\(92\)90004-O](https://doi.org/10.1016/0038-0121(92)90004-O).
- Kim, Yeeun, Young-Ji Byon, and Hwasoo Yeo. 2018. “Enhancing Healthcare Accessibility Measurements Using GIS: A Case Study in Seoul, Korea.” Edited by Tayyab Ikram Shah. *PLOS ONE* 13 (2): e0193013. <https://doi.org/10.1371/journal.pone.0193013>.
- King, David, Aya Aboudina, and Amer Shalaby. 2020. “Evaluating Transit Network Resilience through Graph Theory and Demand-Elastic Measures: Case Study of the Toronto Transit System.” *Journal of Transportation Safety & Security* 12 (7): 924–44. <https://doi.org/10.1080/19439962.2018.1556229>.
- Kirkley, Alec, Hugo Barbosa, Marc Barthelemy, and Gourab Ghoshal. 2018. “From the Betweenness Centrality in Street Networks to Structural Invariants in Random Planar Graphs.” *Nature Communications* 9 (1): 1–12. <https://doi.org/10.1038/s41467-018-04978-z>.

- Lawal, Olanrewaju, and Felix E. Anyiam. 2019. "Modelling Geographic Accessibility to Primary Health Care Facilities: Combining Open Data and Geospatial Analysis." *Geo-Spatial Information Science* 22 (3): 174–84. <https://doi.org/10.1080/10095020.2019.1645508>.
- Luo, Wei. 2004. "Using a GIS-Based Floating Catchment Method to Assess Areas with Shortage of Physicians." *Health & Place* 10 (1): 1–11. [https://doi.org/10.1016/S1353-8292\(02\)00067-9](https://doi.org/10.1016/S1353-8292(02)00067-9).
- Luo, Wei, and Yi Qi. 2009. "An Enhanced Two-Step Floating Catchment Area (E2SFCA) Method for Measuring Spatial Accessibility to Primary Care Physicians." *Health & Place* 15 (4): 1100–1107. <https://doi.org/10.1016/j.healthplace.2009.06.002>.
- Luo, Wei, and Fahui Wang. 2003. "Measures of Spatial Accessibility to Health Care in a GIS Environment: Synthesis and a Case Study in the Chicago Region." *Environment and Planning B: Planning and Design* 30 (6): 865–84. <https://doi.org/10.1068/b29120>.
- Lyons, Stephanie. 2015. "The Jakarta Floods of Early 2014: Rising Risks in One of the World's Fastest Sinking Cities," 18. <http://labos.ulg.ac.be/hugo/wp-content/uploads/sites/38/2017/11/The-State-of-Environmental-Migration-2015-103-120.pdf>.
- Mirbabaie, Milad, Stefan Stieglitz, and Stephan Volkeri. 2016. "Volunteered Geographic Information and Its Implications for Disaster Management." In *2016 49th Hawaii International Conference on System Sciences (HICSS)*, 207–16. Koloa, HI, USA: IEEE. <https://doi.org/10.1109/HICSS.2016.33>.
- Neis, Pascal, and Dennis Zielstra. 2014. "Recent Developments and Future Trends in Volunteered Geographic Information Research: The Case of OpenStreetMap." *Future Internet* 6 (1): 76–106. <https://doi.org/10.3390/fi6010076>.
- Octavianti, Thanti, and Katrina Charles. 2019. "The Evolution of Jakarta's Flood Policy over the Past 400 Years: The Lock-in of Infrastructural Solutions." *Environment and Planning C: Politics and Space* 37 (6): 1102–25. <https://doi.org/10.1177/2399654418813578>.
- OpenStreetMap contributors. 2018. "HOT - PDC InAware Indonesia Mapping Project - OpenStreetMap Wiki." 2018. [https://wiki.openstreetmap.org/wiki/HOT\\_-\\_PDC\\_InAware\\_Indonesia\\_Mapping\\_Project](https://wiki.openstreetmap.org/wiki/HOT_-_PDC_InAware_Indonesia_Mapping_Project).
- . 2020a. "Elements - OpenStreetMap Wiki." 2020. <https://wiki.openstreetmap.org/wiki/Elements>.
- . 2020b. "OpenStreetMap." OpenStreetMap. 2020. <https://www.openstreetmap.org/>.
- . 2020c. "PBF Format - OpenStreetMap Wiki." August 29, 2020. [https://wiki.openstreetmap.org/wiki/PBF\\_Format](https://wiki.openstreetmap.org/wiki/PBF_Format).
- . n.d. "OpenStreetMap." OpenStreetMap. Accessed July 28, 2020. <https://www.openstreetmap.org/about>.
- OpenStreetMap Indonesia. 2020. "Fasilitas Kesehatan – Google Drive." 2020. <https://drive.google.com/drive/folders/1azUAetAfVKHmkh8MdBnZv6owD-jzvBkd>.
- Opsahl, Tore, Filip Agneessens, and John Skvoretz. 2010. "Node Centrality in Weighted Networks: Generalizing Degree and Shortest Paths." *Social Networks* 32 (3): 245–51. <https://doi.org/10.1016/j.socnet.2010.03.006>.
- O'Sullivan, David, Alastair Morrison, and John Shearer. 2000. "Using Desktop GIS for the Investigation of Accessibility by Public Transport: An Isochrone Approach." *International Journal of Geographical Information Science* 14 (1): 85–104. <https://doi.org/10.1080/136588100240976>.
- Panig, Stefan. 2019. "Implementierung eines Algorithmus zur schnellen Berechnung metrik-affiner Isochronen in einem Straßennetzwerk."
- Penchansky, Roy, and J. William Thomas. 1981. "The Concept of Access: Definition and Relationship to Consumer Satisfaction." <https://doi.org/10.2307/3764310>.
- Porta, Sergio, Paolo Crucitti, and Vito Latora. 2006. "The Network Analysis of Urban Streets: A Primal Approach." *Environment and Planning B: Planning and Design* 33 (5): 705–25. <https://doi.org/10.1068/b32045>.

- \_\_\_\_\_. 2008. "Multiple Centrality Assessment in Parma: A Network Analysis of Paths and Open Spaces." *URBAN DESIGN International* 13 (1): 41–50. <https://doi.org/10.1057/udi.2008.1>.
- Porta, Sergio, Paolo Pasino, Ombretta Romice, and Emanuele Strano. 2013. "Multiple Centrality Assessment. Sergio Porta and His Colleagues Apply a Computer Based Methodology to Mixed Use Streets." *Journal of Urban Design*, no. 125 (January). <https://www.researchgate.net/publication/271515613>.
- Prasetyanti, Retnayu. 2015. "Slum Kampong Tourism 'Jakarta Hidden Tour': Designing Eco-Cultural Based Pro-Poor Tourism." *European Journal of Interdisciplinary Studies* 1 (3): 11.
- Python Software Foundation. 2020. "Download Python." Python.Org. 2020. <https://www.python.org/downloads/>.
- QGIS Development Team. 2020. "Discover QGIS." 2020. <https://www.qgis.org/en/site/about/index.html>.
- Radke, John, and Lan Mu. 2000. "Spatial Decompositions, Modeling and Mapping Service Regions to Predict Access to Social Programs." *Annals of GIS* 6 (2): 105–12. <https://doi.org/10.1080/10824000009480538>.
- Raifer, Martin. 2014. "Der TURBO für die Overpass-API | OSMBlog." January 31, 2014. <https://blog.openstreetmap.de/blog/2014/01/der-turbo-fuer-die-overpass-api/>.
- Rekha, R. Shanmathi, Shayesta Wajid, Nisha Radhakrishnan, and Samson Mathew. 2017. "Accessibility Analysis of Health Care Facility Using Geospatial Techniques." *Transportation Research Procedia* 27: 1163–70. <https://doi.org/10.1016/j.trpro.2017.12.078>.
- Rochat, Yannick. 2009. "Closeness Centrality Extended To Unconnected Graphs : The Harmonic Centrality Index," 15. infoscience.epfl.ch/record/200525/files/%5bEN%5dASNA09.pdf.
- Sabidussi, Gert. 1966. "The Centrality Index of a Graph," 23. <https://doi.org/10.1007/BF02289527>.
- Senaratne, Hansi, Amin Mobasher, Ahmed Loai Ali, Cristina Capineri, and Mordechai (Muki) Haklay. 2017. "A Review of Volunteered Geographic Information Quality Assessment Methods." *International Journal of Geographical Information Science* 31 (1): 139–67. <https://doi.org/10.1080/13658816.2016.1189556>.
- Singh, Prasoon, Vinay Shankar Prasad Sinha, Ayushi Vijhani, and Neha Pahuja. 2018. "Vulnerability Assessment of Urban Road Network from Urban Flood." *International Journal of Disaster Risk Reduction* 28 (June): 237–50. <https://doi.org/10.1016/j.ijdrr.2018.03.017>.
- Siswanto, Siswanto, Geert Jan van Oldenborgh, Gerard van der Schrier, Rudmer Jilderda, and Bart van den Hurk. 2016. "Temperature, Extreme Precipitation, and Diurnal Rainfall Changes in the Urbanized Jakarta City during the Past 130 Years: PRECIPITATION CHARACTERISTICS CHANGES IN THE URBANIZED CITY." *International Journal of Climatology* 36 (9): 3207–25. <https://doi.org/10.1002/joc.4548>.
- Sohn, Jungyul. 2006. "Evaluating the Significance of Highway Network Links under the Flood Damage: An Accessibility Approach." *Transportation Research Part A: Policy and Practice* 40 (6): 491–506. <https://doi.org/10.1016/j.tra.2005.08.006>.
- Staudt, Christian L, Aleksejs Sazonovs, and Henning Meyerhenke. 2014a. "NetworKit: An Interactive Tool Suite for High-Performance Network Analysis," 24. <https://www.linkgroup.hu/docs/Networkkit-analysis-tool.pdf>.
- \_\_\_\_\_. 2014b. "NetworKit: An Interactive Tool Suite for High-Performance Network Analysis," 15. <https://www.researchgate.net/publication/260756093>.
- Staudt, Christian L., Aleksejs Sazonovs, and Henning Meyerhenke. 2015. "NetworKit: A Tool Suite for Large-Scale Complex Network Analysis." *ArXiv:1403.3005 [Physics]*, November. <http://arxiv.org/abs/1403.3005>.
- The World Bank Group. 2016. "Indonesia's Urban Story." Text/HTML. World Bank. 2016. <https://www.worldbank.org/en/news/feature/2016/06/14/indonesia-urban-story>.

- \_\_\_\_\_. 2020a. "GDP per Capita (Current US\$) - Indonesia | Data." 2020. <https://data.worldbank.org/indicator/NY.GDP.PCAP.CD?locations=ID>.
- \_\_\_\_\_. 2020b. "Overview." Text/HTML. World Bank. 2020. <https://www.worldbank.org/en/country/indonesia/overview>.
- UNISDR. 2009. "2009 UNISDR Terminology on Disaster Risk Reduction." 2009. [https://www.unisdr.org/files/7817\\_UNISDRTerminologyEnglish.pdf](https://www.unisdr.org/files/7817_UNISDRTerminologyEnglish.pdf).
- United Nations. 2020. *World Population Prospects 2019 - Volume II: Demographic Profiles*. UN. <https://doi.org/10.18356/7707d011-en>.
- United Nations, Department of Economic and Social Affairs, and Population Division. 2019. *World Urbanization Prospects: The 2018 Revision (ST/ESA/SER.A/420)*. New York: United Nations.
- Van de Vuurst, Paige, and Luis E. Escobar. 2020. "Perspective: Climate Change and the Relocation of Indonesia's Capital to Borneo." *Frontiers in Earth Science* 8 (January): 5. <https://doi.org/10.3389/feart.2020.00005>.
- Van Dijk, Meine Pieter. 2016. "Financing the National Capital Integrated Coastal Development (NCICD) Project in Jakarta (Indonesia) with the Private Sector." *Journal of Coastal Zone Management* 19 (4). <https://doi.org/10.4172/2473-3350.1000435>.
- Vargas, John, Shivangi Srivastava, Devis Tuia, and Alexandre Falcao. 2020. "OpenStreetMap: Challenges and Opportunities in Machine Learning and Remote Sensing." *IEEE Geoscience and Remote Sensing Magazine*, 0–0. <https://doi.org/10.1109/MGRS.2020.2994107>.
- Wang, Juan. 2018. "Improved Centrality Indicators to Characterize the Nodal Spreading Capability in Complex Networks." *Applied Mathematics and Computation* 334: 13. <https://doi.org/10.1016/j.amc.2018.04.028>.
- World Health Organization, ed. 2000. *The World Health Report 2000: Health Systems: Improving Performance*. Geneva: WHO. [https://www.who.int/whr/2000/en/whr00\\_en.pdf?ua=1](https://www.who.int/whr/2000/en/whr00_en.pdf?ua=1).
- \_\_\_\_\_. 2017. "The Republic of Indonesia Health System Review." 2017. <https://apps.who.int/iris/bitstream/handle/10665/254716/9789290225164-eng.pdf;sequence=1>.
- WorldPop. 2020a. "Indonesia - Population Counts - Humanitarian Data Exchange." 2020. <https://data.humdata.org/dataset/worldpop-population-counts-for-indonesia>.
- \_\_\_\_\_. 2020b. "WorldPop." 2020. <https://www.worldpop.org/>.
- Wulp, Simon A. van der, Larissa Dsikowitzky, Karl Jürgen Hesse, and Jan Schwarzbauer. 2016. "Master Plan Jakarta, Indonesia: The Giant Seawall and the Need for Structural Treatment of Municipal Waste Water." *Marine Pollution Bulletin* 110 (2): 686–93. <https://doi.org/10.1016/j.marpolbul.2016.05.048>.
- Zhang, Yuanyuan, Xuesong Wang, Peng Zeng, and Xiaohong Chen. 2011. "Centrality Characteristics of Road Network Patterns of Traffic Analysis Zones." *Transportation Research Record: Journal of the Transportation Research Board* 2256 (1): 16–24. <https://doi.org/10.3141/2256-03>.
- Zhong, Chen, Stefan Müller Arisona, Xianfeng Huang, Michael Batty, and Gerhard Schmitt. 2014. "Detecting the Dynamics of Urban Structure through Spatial Network Analysis." *International Journal of Geographical Information Science* 28 (11): 2178–99. <https://doi.org/10.1080/13658816.2014.914521>.

## **Acknowledgement**

I want to thank my supervisors Dr. Sven Lautenbach and Prof. Dr. Alexander Zipf for their support and feedback throughout my work. In addition, I want to thank the HeiGIT team, especially Benjamin Herfort and Melanie Eckle, for their input, and of course, everyone who kept motivating me.

Furthermore, I want to thank the Humanitarian OpenStreetMap Team Indonesia for their work and for providing their data.

## **Affidavit**

Hiermit versichere ich, dass ich die vorliegende Masterarbeit ohne Hilfe Dritter und ohne Benutzung anderer als der angegebenen Quellen und Hilfsmittel angefertigt und die den benutzten Quellen wörtlich oder inhaltlich entnommenen Stellen als solche kenntlich gemacht wurden. Diese Arbeit hat in gleicher oder ähnlicher Form noch keiner Prüfungsbehörde vorgelegen.

Heidelberg, 21. Oktober 2020

.....  
Isabell Greta Klipper